

UNIVERSITÉ DU QUÉBEC À TROIS-RIVIÈRES

SYNTHÈSE DE BIOCHARBON PAR PYROLYSE ASSISTÉE AUX ULTRASONNS ET  
LEURS APPLICATIONS DANS LE TRAITEMENT DES EAUX

*SYNTHESIS OF BIOCHARS FROM ULTRASOUND ENHANCED PYROLYSIS  
AND THEIR APPLICATION IN WATER TREATMENT*

THÈSE PRÉSENTÉE  
COMME EXIGENCE PARTIELLE DU  
DOCTORAT EN SCIENCES DE L'ÉNERGIE ET DES MATÉRIAUX

PAR  
ANEESHMA PETER

JUILLET 2021

Université du Québec à Trois-Rivières

Service de la bibliothèque

Avertissement

L'auteur de ce mémoire ou de cette thèse a autorisé l'Université du Québec à Trois-Rivières à diffuser, à des fins non lucratives, une copie de son mémoire ou de sa thèse.

Cette diffusion n'entraîne pas une renonciation de la part de l'auteur à ses droits de propriété intellectuelle, incluant le droit d'auteur, sur ce mémoire ou cette thèse. Notamment, la reproduction ou la publication de la totalité ou d'une partie importante de ce mémoire ou de cette thèse requiert son autorisation.

UNIVERSITÉ DU QUÉBEC À TROIS-RIVIÈRES

DOCTORAT EN SCIENCES DE L'ÉNERGIE ET DES MATÉRIAUX (PH. D.)

**Direction de recherche :**

---

Éric Loranger Directeur de recherche

---

Bruno Chabot Codirecteur de recherche

**Jury d'évaluation**

---

Éric Loranger Directeur de recherche

---

Bruno Chabot Codirecteur de recherche

---

Simon Barnabé Président de jury

---

André Lajeunesse Évaluateur interne

---

Ahmed Koubaa Évaluateur externe

Thèse soutenue le 13 mai 2021

**“Be the change you want to see in the world”**

**- Mahatma Gandhi**

## Acknowledgements

I am dedicating this work to God almighty for all the blessing and my parents for being a great support during my good and tough times.

I express my deep sense of gratitude and profound feeling of admiration to my research director Prof. Eric Loranger and my co-director Prof. Bruno Chabot for their advices, expert guidance, valuable suggestions, discussions and constant encouragement even during the good and bad phases of my Ph.D. Working with them has taught me how to be a good leader and how to deal obstacles with patience and positive attitude, let it be in career or life. Words are not enough to thank them for believing me and never let me feel low in this endeavour.

I am grateful for the defence committee for their valuable time and suggestions. Also, I am thankful to my doctoral exam committee members Prof. Simon Barnabe and Prof. André Lajeunesse for all the suggestions they have provided during my initial stages of research.

I take this opportunity to express my sincere thanks to all the members of Institut d'Innovations en Écomatériaux, Écoproduits et Écoénergies à base de biomasse (I2E3), especially Isabelle Boulan, Agnès Lejeune and Céline Leduc for their extreme help and support during the entire period. I thank all the members of Département de chimie, biochimie et physique (DCBP), and Institut de Recherche sur l'hydrogène (IRH) for providing me with the facilities to carry out my research. Also, I am thankful to the technicians at the Université de Montréal and the Université de Laval for the help to carry out the experiments. I am thankful to all my current and past lab mates for their all kind of help and support in the laboratory and for being a wonderful team. Special thanks to internship students Floriane Preyssler and Loic Espin for their help during experiments.

I owe greatly to the Queen Elizabeth II Diamond Jubilee Scholarship for the financial support and for all other immense supports. The leadership and community activities with QES family was a great experience and opportunity.

I am also thankful to my brother, sisters and all beloved friends and family in India and Canada for their love and support throughout. Sincere thanks to my friends Vishnu Nair Gopalakrishnan and Tara George for their extreme help during thesis writing. My time in Trois-Rivières is memorable because of the people I got here, friends that became a part of life. I owe them greatly for keeping me happy and motivated especially my husband Dr. Midhun Mohan who has been a great support through the sacrifices I made for this journey.

Special dedication to my nephew Jordan, who is always my reason to move on in life with a smile.

June 2021

## **Abstract**

With expected growth of the population and urbanization, combined with climate change and its unpredictable consequences, the demand for fresh water will be increasing in the next few decades. To ensure sustainability of water resources, major efforts must be made by key stakeholders, particularly governments, industries, companies, development organizations and the civil society.

Wastewater recycling is a potential avenue to reduce fresh-water demand by industries generating large volume of contaminated effluents. Most of the organic pollutants are biodegradable while inorganic pollutants, mainly heavy metals, are non-biodegradable which can easily enter the food chain through bioaccumulation and can cause severe health hazards. Researches have been carried on designing and developing materials that can remove these pollutants from water thereby making water recycling more efficient. There are many conventional techniques for wastewater treatments, a few of them namely, ion exchange, precipitation, electrocoagulation, activated carbon adsorption and packed bed filtration. However, most of these techniques are expensive which demands us to develop more cost-effective technologies with low-cost adsorbents.

In recent decades, biochar emerged as a substituent to charcoal or other activated carbon materials and has motivated many researchers to investigate and facilitate the properties due to its multifunctionality and effective properties. Biochar is a promising candidate for wastewater treatment, which is obtained from thermal degradation of carbon-rich biomass in an oxygen-limited environment. Recent studies have proved their excellent ability to immobilize organic and inorganic pollutants in soil and water systems. Unique properties of biochar including large specific surface area, porosity, enriched surface functional groups, mineral components and ion exchange property make it possible to be used as potential adsorbent to remove pollutants from aqueous solutions.

Physicochemical properties of biochar are depending on a few important factors such as type of feedstock, pyrolysis conditions and post and pre-processing of feedstocks.

Proper understanding about the influence of these factors on properties can be helpful to engineer the material structure for intended application. Power ultrasound on biomass applications is a recently developed technique which has potentially proved its efficiency in improving material properties. The application of ultrasound is based on the concept of cavitation. Formation of microjets during the implosion of cavitation bubbles disrupts the solid surface which is in contact and provides a unique physiochemical environment to the materials. The mechanical and sonochemical effect of ultrasound can make significant changes in surface as well as adsorption properties of biochar.

With the assistance of a thorough literature survey on wastewater treatment, relevant materials for heavy metal adsorption, different adsorption techniques, and synthesis and properties of biochars, the methodology begun with the ultrasonic pre-treatments on softwood chips. Post-consumer feedstock from paper industry was chosen as feedstock because of its easy availability, low-cost and processability. Ultrasonic pre-treatments were performed using different equipment configurations enabling power, frequency, and treatment time variations. The biochar was produced from lab-scale pyrolysis and the material was characterized using different characterisation techniques, including Fourier Transform- Infrared (FT-IR) Spectroscopy, Elemental Analysis (EA), Scanning Electron Microscopy (SEM), Energy Dispersive X-Ray Spectroscopy (EDX), Thermogravimetric Analysis (TGA) and Brunauer Emmet Teller (BET) isotherm studies etc. Results revealed that chemical characteristics of biochar derived from ultrasonic pre-treated wood remained the same as the untreated one, but the surface morphology and adsorption properties were enhanced. For the detailed understanding on the effect of each ultrasonic pre-treatments on adsorption properties of the biochar synthesized, batch adsorption studies were carried out using copper as a model metal contaminant. Adsorption kinetics, equilibrium adsorption isotherms and thermodynamic parameters (i.e., Gibbs free energy, entropy, enthalpy, activation energy) were studied using standardised protocols in different conditions of pH, temperature, concentration, etc.

Interesting results were obtained, confirming the influence of ultrasound frequencies, the power combined to the bath temperature and the exposure time against the adsorption capacity of the biochar produced. The 40 kHz pre-treated samples exhibited around 0.3 to

0.65 mg/g increase in equilibrium adsorption capacity ( $Q_e$ ). Though low frequency ultrasounds enhanced the equilibrium adsorption capacity, adsorption per unit surface area was higher for high frequency pre-treated samples. These results further have motivated us to investigate the effect of ultrasonic pre-treatment on alkali activation of biochar to have biochar with enhanced adsorption capacities. Two-step activation using sodium hydroxide had demonstrated improved adsorption properties and 170 kHz pre-treated sample exhibited an equilibrium adsorption capacity of 19.99 mg/g which is almost 22 times higher than that of corresponding non-activated sample. In multimetal solution of Cu (II), Ni (II) and Pb (II), the activated biochars exhibited selective adsorption towards copper metal. However, this adsorption capacity was approximately 20 percent less as compared to the single component system. The ability of ultrasonic pre-treatments to enhance surface modification has inspired us to study the iron impregnation efficiency of ultrasound pre-treated biochars as a satellite project. The lab-scale pyrolysis system could produce engineered biochars better yield exhibited after Fe impregnation. post-pyrolysis method demonstrated better surface morphology with higher frequency samples and exhibited better impregnation results compared to low frequency samples. The improved thermal stability and characteristics of the synthesized biochars introduces an efficient, low-cost alternative of biomass catalyst for applications such as bio-oil upgradation, hydrogen production etc.

The synthesized biochar in this project can be a potential candidate in the field of heavy metal removal from industrial wastewater and can selectively adsorb heavy metals with a better efficiency. This project is a successful example for implementing ultrasonication as a tool to enhance the physical properties of the processed wood feedstocks and the biochar derived from it, thus expanding its application in industrial level.

June 2021

### **Keywords**

Softwood chips, biochar, ultrasound pre-treatments, physicochemical properties, heavy metal adsorption, surface modifications

## Résumé

Considérant la croissance attendue de la population et de l'urbanisation, combinée au changement climatique aux conséquences imprévisibles, la demande d'eau douce augmentera constamment au cours des prochaines décennies. Pour assurer la pérennité des ressources en eau, des efforts importants doivent être consentis par les principaux partis prenants, en particulier les gouvernements, les industries, les entreprises, les organisations de développement et la société en général.

Le recyclage des eaux usées est une avenue potentielle pour réduire la demande en eau douce des industries générant un grand volume d'effluents contaminés. La plupart des polluants organiques sont biodégradables tandis que les polluants inorganiques, principalement les métaux lourds, ne le sont pas et peuvent facilement entrer dans la chaîne alimentaire par bioaccumulation et ainsi, potentiellement entraîner de graves risques pour la santé. Par conséquent, des recherches ont été menées sur la conception et le développement de matériaux capables d'éliminer ces polluants de l'eau, rendant ainsi le recyclage de l'eau possible et plus efficace. Il existe de nombreuses techniques classiques pour le traitement des eaux usées, dont notamment, l'échange d'ions, la précipitation, l'électrocoagulation, l'adsorption sur charbon actif et la filtration sur lit garni. Cependant, la plupart de ces techniques sont coûteuses, ce qui oblige le développement de technologies plus rentables avec des adsorbants bon marché.

Au cours des dernières décennies, le biochar est apparu comme un substituant au charbon de bois, ou à d'autres matériaux de charbon actif, et a motivé de nombreux chercheurs à l'étudier. Ce matériel est prometteur à cause de ses propriétés, de sa multifonctionnalité et de son potentiel d'efficacité. Le biochar est obtenu à partir de la dégradation thermique de biomasses riches en carbone dans un environnement limité ou sans oxygène. Des études récentes ont prouvé leur excellente capacité à immobiliser les polluants organiques et inorganiques dans les sols et les eaux. Les propriétés uniques du biochar (c.-à-d. sa grande surface spécifique et porosité, son enrichissement en groupements fonctionnels de surface, la présence de composants minéraux et une excellente capacité d'échange d'ions) lui

permettent d'être utilisé comme adsorbant potentiel pour éliminer les polluants en solutions aqueuses.

Les propriétés physico-chimiques du biochar dépendent de quelques facteurs importants tels que le type de matière première, les conditions de pyrolyse et le post et/ou prétraitement des matières premières. Une bonne compréhension de l'influence de ces facteurs sur les propriétés finales du matériau est nécessaire pour concevoir et ajuster la structure de celui-ci pour l'application prévue. L'utilisation d'ultrasons pour des applications avec biomasse est une technique récemment développée qui a potentiellement prouvé son efficacité dans l'amélioration de certaines propriétés des matériaux résultants. L'effet des ultrasons sur un matériau est basé sur le concept de cavitation. La formation de microjets lors de l'implosion de bulles de cavitation perturbe et attaque physiquement la surface solide en contact avec le jet en plus de fournir un environnement d'attaque chimique (sonochimique). Les effets mécanique et sonochimique des ultrasons, et en fonction de la fréquence de ceux-ci peuvent modifier considérablement la surface ainsi que les propriétés d'adsorption d'un biochar.

Suite à une étude approfondie de la littérature sur le traitement des eaux usées, les matériaux pertinents pour l'adsorption des métaux lourds, les différentes techniques d'adsorption et la synthèse et propriétés des biochars, une méthodologie de recherche par prétraitements ultrasoniques sur les copeaux de bois résineux a été amorcée. Des résidus de bois de l'industrie papetière ont été choisis comme matière première en raison de leur grande disponibilité, de leur faible coût et de leur potentiel de transformation. Des prétraitements par ultrasons ont été réalisés à l'aide de différentes configurations d'équipement permettant des variations de puissance, de fréquence et de temps de traitement. Par la suite, le biochar a été produit à partir d'une pyrolyse à échelle réduite au laboratoire. Le matériau a ensuite été caractérisé à l'aide de différentes techniques, notamment par spectroscopie Infrarouge à transformé de Fourier (FT-IR), l'analyse élémentaire (AE), par microscopie électronique à balayage (MEB), par spectroscopie de rayons X à dispersion d'énergie (EDX), par analyse thermogravimétrique (ATG) et par mesure de surface spécifique par la méthode de Brunauer, Emmet, Teller (BET). Les résultats ont révélé que les caractéristiques chimiques du biochar dérivé du bois prétraité aux ultrasons sont demeurées identiques à celles du bois non traité, mais que la surface spécifique et la capacité d'adsorption des métaux avaient été améliorées.

Afin de mieux comprendre l'effet de chaque prétraitement par ultrasons sur les propriétés d'adsorption du biochar synthétisé, des études d'adsorption par lots ont été réalisées en utilisant le cuivre comme contaminant métallique modèle. La cinétique d'adsorption, les isothermes d'adsorption à l'équilibre et les paramètres thermodynamiques (c.-à-d. énergie libre de Gibbs, entropie, enthalpie et énergie d'activation) ont été étudiés à l'aide de protocoles standardisés sous différentes conditions de pH, température, concentration, etc.

Des résultats intéressants ont été obtenus, confirmant l'influence de la fréquence des ultrasons, de la puissance combinée à la température du bain et au temps d'exposition sur la capacité d'adsorption du biochar produit. Les échantillons prétraités à 40 kHz présentaient une augmentation d'environ 0,3 à 0,65 mg/g de la capacité d'adsorption à l'équilibre ( $Q_e$ ). Bien que les ultrasons à basse fréquence aient amélioré la capacité d'adsorption à l'équilibre, l'adsorption par unité de surface fut plus élevée pour les échantillons prétraités à haute fréquence. Ces résultats nous ont entre autres motivé à étudier l'effet du prétraitement par ultrasons sur l'activation alcaline du biochar afin d'obtenir des capacités d'adsorption améliorées. L'activation en deux étapes à l'aide de l'hydroxyde de sodium a démontré des propriétés d'adsorption améliorées. L'échantillon prétraité à 170 kHz présentait une capacité d'adsorption à l'équilibre de 19,99 mg/g, ce qui est presque 22 fois supérieure à celle de l'échantillon non activé correspondant. Dans une solution multimétallique de Cu (II), Ni (II) et Pb (II), les biochars activés présentaient une adsorption sélective vers le cuivre. Cependant, cette capacité d'adsorption était d'environ 20 % inférieure à celle du système à un seul composant. La capacité des prétraitements par ultrasons ayant amélioré la modification de surface nous a ensuite inspiré pour étudier l'efficacité d'imprégnation du fer sur des biochars prétraités par ultrasons dans le cadre d'un projet satellite. Selon la littérature, le système de pyrolyse à l'échelle du laboratoire pourrait produire des biochars modifiés avec un meilleur rendement après imprégnation de Fer. La méthode de post-pyrolyse a démontré une meilleure morphologie de surface avec les échantillons de plus haute fréquence et a présenté de meilleurs résultats d'imprégnation par rapport aux échantillons de basse fréquence. La diffusion homogène améliorée de particules métalliques sur les échantillons de biochar prétraités par ultrasons a démontré une stabilité thermique et des caractéristiques améliorées des matériaux. À partir de biomasses, notre étude ouvre la porte à une alternative

de fabrication de catalyseur efficace et à faible coût pour des applications telles que la valorisation de l'huile biologique, la production d'hydrogène, etc.

Le biochar synthétisé dans ce projet est donc considéré comme un candidat potentiel dans le domaine de l'élimination des métaux lourds des eaux usées industrielles en adsorbant sélectivement les métaux lourds avec une meilleure efficacité. Ce projet est aussi un exemple de mise en œuvre de l'ultrasonication en tant qu'outil pour améliorer les propriétés physiques de matières premières du bois traité et du biochar qui en dérive, élargissant ainsi son potentiel d'application au niveau industriel.

Juin 2021

### **Mots-clés**

Copeaux résineux, biocharbon, prétraitements par ultrasons, propriétés physico-chimiques, adsorption de métaux lourds, modifications de surface

## Table of Contents

Acknowledgements .....	iv
Abstract.....	vi
Résumé .....	ix
List of Figures.....	xviii
List of Tables .....	xxi
List of Equations.....	xxii
List of Abbreviations .....	xxiv
Chapter 1 – Introduction.....	1
1.1 Fresh water demand and contamination problematic .....	1
1.2 Biomass research in Quebec, Canada.....	3
Chapter 2 – Thesis Overview .....	5
2.1 Objectives and Hypotheses.....	5
2.2 Experimental techniques.....	7
2.3 Safety Trainings.....	7
2.4 Waste Management .....	8
Chapter 3 – Literature Review .....	9
3.1 Biochar.....	9
3.1.1 Synthesis methods for biochar.....	10
3.1.1.1 Slow pyrolysis .....	10
3.1.1.2 Fast and flash pyrolysis .....	11
3.1.1.3 Hydrothermal carbonization .....	12
3.1.1.4 Torrefaction .....	12
3.1.1.5 Gasification.....	12
3.1.1.6 Type of pyrolysis used.....	13
3.1.2 Factors affecting biochar properties .....	13
3.1.3 Biochar for heavy metal adsorption.....	14

3.1.4	Modifications on biochar .....	16
3.1.4.1	Activation .....	17
3.1.4.2	Metal impregnation.....	19
3.1.4.3	Other Modifications.....	20
3.1.5	Wood biochar and its application on heavy metal removal.....	21
3.1.5.1	Components of wood and effect of slow pyrolysis .....	22
3.1.5.2	Heavy metal adsorption using wood biochars .....	25
3.2	Ultrasound .....	25
3.2.1	Types of ultrasound .....	26
3.2.1.1	Diagnostic Ultrasound .....	26
3.2.1.2	High Frequency Ultrasound.....	26
3.2.1.3	Power Ultrasound .....	27
3.2.2	Cavitation.....	27
3.2.2.1	Influence of frequency and power on cavitation .....	30
3.2.3	Power ultrasound on biomass applications.....	31
3.2.4	Power ultrasound on biochar .....	33
3.2.5	Other applications of power ultrasound.....	35
3.3	Theory of Adsorption .....	36
3.3.1	Factors affecting adsorption .....	36
3.3.2	Modes of adsorption and mechanism .....	38
3.3.2.1	Physisorption and Chemisorption.....	38
3.3.2.2	Kinetic models.....	39
3.3.3	Adsorption isotherms.....	42
3.3.3.1	Langmuir isotherm .....	42
3.3.3.2	Freundlich isotherm.....	44
3.3.3.3	Dubinin-Radushkevich (DR) isotherm.....	45
3.3.3.4	Redlich-Peterson isotherm.....	46
3.3.4	Thermodynamics of adsorption .....	46
Chapter 4 – Scientific Article 1: Synthesis and Characterisation of Ultrasound Pre-treated Softwood Biochar .....		48
4.1	Preface .....	48
4.2	Résumé .....	49
4.3	Abstract.....	50

4.4	Introduction .....	51
4.5	Materials and Methods .....	53
4.5.1	Biomass feedstock .....	53
4.5.2	Ultrasonic pre-treatments.....	53
4.5.3	Lab-scale pyrolysis .....	53
4.5.4	Chemical and physical characterisations .....	54
4.5.5	Adsorption of Cu using biochar.....	55
4.6	Results & Discussion.....	55
4.6.1	Chemical characterisation of biochar .....	55
4.6.2	Ultrasonic pre-treatment effects on surface morphology .....	58
4.7	Conclusions .....	60
4.8	Acknowledgment.....	60
4.9	References .....	61
4.10	Highlights .....	62
Chapter 5 – Scientific Article 2: Heavy Metal Adsorption using Synthesized Biochars.		63
5.1	Preface .....	63
5.2	Résumé .....	64
5.3	Abstract.....	65
5.4	Introduction .....	66
5.5	Materials and Methods .....	68
5.5.1	Biochar production and characterisation .....	68
5.5.2	Cu (II) adsorption experiments.....	69
5.6	Results and Discussions.....	73
5.6.1	Ultrasound pre-treatment effects on biochar .....	73
5.6.2	Effect of pH and surface zeta potential.....	74
5.6.3	Adsorption kinetics and statistical analysis .....	76
5.6.4	Isotherm models and thermodynamics studies .....	80
5.6.5	Comparison with Activated carbon .....	84
5.7	Conclusions .....	85
5.8	Acknowledgements .....	85
5.9	References .....	85
5.10	Highlights .....	91

Chapter 6 – Scientific Article 3: Alkali Activation and Influence of Ultrasonic Pre-treatments.....	92
6.1 Preface .....	92
6.2 Résumé .....	93
6.3 Abstract.....	94
6.4 Introduction .....	95
6.5 Materials & Methods.....	97
6.5.1 Biochar production .....	97
6.5.2 Base activation of as-synthesized biochar .....	98
6.5.3 Characterisation of biochar.....	99
6.5.4 Adsorption experiments.....	99
6.5.5 Multicomponent adsorption.....	100
6.5.6 Statistical regression for experimental data .....	101
6.6 Results and Discussion .....	101
6.6.1 Effect of alkali activation after ultrasound pre-treatment on surface morphology and chemical properties of biochar .....	101
6.6.2 Influence of ultrasound pre-treatment assisted activation on adsorption properties .....	104
6.6.3 Selectivity of heavy metals on modified biochars .....	110
6.7 Conclusions .....	111
6.8 Acknowledgement.....	112
6.9 References .....	112
6.10 Highlights .....	117
Chapter 7 – Scientific Article 4: Metal Impregnation on Ultrasound Pre-treated Wood Biochar.....	118
7.1 Preface .....	118
7.2 Résumé .....	119
7.3 Abstract.....	120
7.4 Introduction .....	121
7.5 Materials and Methods .....	123
7.5.1 Biomass feedstock and ultrasound pre-treatments .....	123
7.5.2 Lab-scale slow pyrolysis set up .....	124
7.5.3 Metal impregnation.....	125

7.5.4	Surface and chemical characterisations .....	126
7.6	Results and Discussion .....	127
7.6.1	Effect of iron impregnation on pyrolysis product yields .....	127
7.6.2	Ultrasound pre-treatment and pyrolysis effect on Fe-impregnation..	129
7.6.2.1	Effect of impregnation on biochar surface elemental composition .....	129
7.6.2.2	Effect of impregnation on biochar surface morphology .....	130
7.6.2.3	Effect of impregnation on biochar surface functional groups .....	132
7.6.2.4	Effect of iron impregnation on biochar thermal properties .	133
7.7	Conclusions .....	135
7.8	Conflicts of interest .....	135
7.9	Acknowledgement .....	135
7.10	References .....	136
7.11	Highlights .....	140
Chapter 8	– Conclusions and Future Perspectives .....	141
8.1	General conclusions.....	141
8.2	Future aspects .....	143
Appendix 1	– Supplementary Information of Article 2.....	145
Appendix 2	– Supplementary Information of Article 3.....	149
Chapter 9	– References.....	153

## List of Figures

Figure		Page
1.1	Effect of global population on freshwater demand .....	2
2.1	Organisation of research thesis .....	5
3.1	Biochar produced from softwood chips .....	9
3.2	Various thermal conversion methods for biomass feedstocks .....	10
3.3	Different surface interactions for heavy metal adsorption .....	15
3.4	Chemical structure of cellulose .....	23
3.5	An example for hemicellulose.....	23
3.6	Components of lignin .....	24
3.7	Type of sound waves and frequency range .....	26
3.8	Formation and growth of cavitation bubbles with wave cycle.....	28
3.9	Bubble collapse and microjet formation .....	29
3.10	Representation of adsorption and desorption on to a surface.....	36
3.11	(a) Representation of physisorption, and (b) rate of adsorption with increase in temperature (x is the amount of adsorbate, m is the amount of adsorbent and T is the temperature).....	38
3.12	(a) Representation of chemisorption, and (b) amount of adsorption with increase in temperature (x is the amount of adsorbate, m is the amount of adsorbent and T is the temperature) .....	39
4.1	a) Infrared spectra of feedstock and ultrasound pre-treated biochar. b) Thermogravimetric analysis of ultrasound untreated and pre-treated wood biochar .....	57
4.2	SEM images of biochar derived from ultrasound pre-treated wood chips. a) Untreated, b) UST 1, c) UST 2, d) UST 3, e) UST 4.....	58
4.3	Pseudo second order kinetic model for ultrasound pre-treated wood biochar UST-1 .....	59

5.1	Change in zeta potential with increase in pH of the metal solution .....	75
5.2	Adsorption capacity of biochar samples with increase in contact time. (a) Untreated biochar, (b) UST-3 (40 kHz, 1000 W, 80 °C for 2 h), (c) UST-6 (40 kHz, 250 W, 20 °C for 1 h), (d) UST-11 (170 kHz, 1000 W, 80 °C for 2 h), and (e) UST-14 (170 kHz, 250 W, 20 °C for 1 h).....	77
5.3	Statistical correlation of ultrasonic pre-treatment conditions on equilibrium adsorption capacity, $Q_e$ and rate constant $k$ : a) effect on $Q_e$ of 40 kHz samples, b) effect on $k$ of 40 kHz samples, c) effect on $Q_e$ of 170 kHz samples, and d) effect on $k$ of 170 kHz samples.....	79
5.4	Change in equilibrium adsorption capacity with concentration of metal at equilibrium: (a) Untreated biochar compared with UST-3 (40 kHz, 1000 W, 80 °C for 2 h) and UST- 11 (170 kHz, 1000 W, 80 °C for 2 h), (b) Untreated biochar compared with UST-6 (40 kHz, 250 W, 20 °C for 1 h) and UST-14 (170 kHz, 250 W, 20 °C for 1 h).....	80
5.5	Effect of temperature on equilibrium adsorption capacity of samples untreated, UST-3 (40 kHz, 1000 W, 80 °C for 2 h) and UST-11(170 kHz, 1000 W, 80 °C for 2 h).....	82
6.1	Scanning electron Microscope images with EDX mapping of: (a) Act-UST1 (40 kHz, 1000 W at 80 °C for 2 h), (b) Act-UST3 (170 kHz, 1000 W at 80 °C for 2 h) and Scanning electron microscope images of (c) Act-UST2 (40 kHz, 250 W at 20 °C for 1 h), (d) Act-UST4 (170 kHz, 250 W at 20 °C for 1 h) and (e) Act-Untreated at magnification at 250x magnification .....	102
6.2	Effect of contact time on adsorption capacity of biochar samples: (a) Activated biochar with 40 kHz ultrasound pre-treatment, (b) Activated biochar with 170 kHz ultrasound pre-treatment, (c) Activated biochar without ultrasound pre-treatment, and (d) FTIR comparison of Act-Untreated, Act-UST1 and Act-UST3 to confirm maximum carbonization .....	105
6.3	Comparison of competitive metal adsorption for Cu (II), Pb (II) and Ni (II) onto: (a) Act-UST1 (40 kHz, 1000 W at 80 °C for 2 h), (b) Act-UST2 (40 kHz, 250 W at 20 °C for 1 h), (c) Act-UST3 (170 kHz, 1000 W at 80 °C for 2 h), (d) Act-UST4 (170 kHz, 250 W at 20 °C for 1 h), and (e) Act-Untreated.....	111
7.1	Schematic representation of laboratory-scale pyrolysis set up to produce biochar.....	125
7.2	Schematic representation of Fe-impregnation methods .....	126
7.3	Pyrolysis product distribution of pre and post-pyrolysis methods: (a) product yield for pyrolysis without Fe-Impregnation, (b) product yield for pyrolysis after Fe-impregnation.....	128

7.4	Scanning Electron Microscope and EDX mapping images of different ultrasonic pre-treated samples: (a) and (b) Pre and post pyrolysis biochar of Fe- UST1 (c) and (d) Pre and post pyrolysis biochar of Fe- UST2 (e) and (f) Pre and post pyrolysis biochar of Fe- UST3 (g) and (h) Pre and post pyrolysis biochar of Fe- UST4 .....	131
7.5	Infrared spectra of Fe-impregnated biochars prepared from: (a) Pre-pyrolysis methods, (b) Post-pyrolysis method.....	132
7.6	Thermogravimetric analysis of Fe-impregnated biochars prepared using: (a) Pre-pyrolysis method, (b) Post-pyrolysis method.....	134

## List of Tables

Table		Page
4.1	List of pre-treatments performed on wood chips .....	53
4.2	Proximate and ultimate analysis of biochar .....	56
4.3	Surface charge nature of biochar .....	56
4.4	Adsorption kinetics of biochar .....	59
5.1	List of ultrasonic pre-treatments on wood chips .....	69
5.2	Proximate and Ultimate analyses of biochar and feedstock .....	73
5.3	Pseudo second order parameters for biochar samples .....	78
5.4	Parameters of linearized Freundlich and Langmuir isotherm models for Cu adsorption on biochar .....	81
5.5	Thermodynamic parameters of copper adsorption on biochar .....	83
5.6	Comparison on adsorption capacity with specific surface area .....	84
6.1	List of ultrasound pre-treatments on woodchips .....	98
6.2	Surface characteristics of biochar after base activation .....	103
6.3	Parameters of Pseudo second order kinetic models for Cu (II) adsorption on biochar samples .....	106
6.4	Comparison of BET surface area and copper adsorption capacities of wood-derived biochars from literature .....	107
6.5	Freundlich isotherm and thermodynamic parameters of biochar samples .....	109
7.1	Ultrasonic pre-treatment conditions applied to wood chips .....	124
7.2	Atomic percent of different elements present on biochar surface .....	129

## List of Equations

$Q = \frac{(C_{initial} - C_{final}) * V}{m}$	3.1 .....	40
$Q_t = Q_e(1 - e^{-k_1 t})$	3.2 .....	40
$Q_i = \frac{k_2 Q_e^2 t}{1 + k_2 Q_e t}$	3.3 .....	41
$Q_t = kt^{1/2} + C$	3.4 .....	41
$Q_t = \frac{1}{\beta} \text{Ln}(\alpha\beta) + \frac{1}{\beta} \text{Ln } t$	3.5 .....	42
$Q_e = \frac{(Q_{max} * b * C_e)}{(1 + b * C_e)}$	3.6 .....	43
$R_L = \frac{1}{(1 + bC_i)}$	3.7 .....	43
$Q_e = K_f C_e^{1/n}$	3.8 .....	44
$\text{Ln} Q_e = \text{Ln} Q_m - \beta * \varepsilon^2$	3.9 .....	45
$\varepsilon = RT * \text{Ln}(1 + \frac{1}{C_e})$	3.10 .....	45
$E = \frac{1}{\sqrt{2\beta}}$	3.11 .....	46
$Q_e = \frac{K_{RP} * C_e}{(1 + \alpha_{RP} * C_e^\beta)}$	3.12 .....	46
$K_e = \frac{Q_e}{C_e}$	3.13 .....	47
$\Delta G^0 = -RT \ln K_e$	3.14 .....	47
$\Delta G^0 = \Delta H^0 - T\Delta S^0$	3.15 .....	47

$\text{Ln}K_e = \frac{\Delta S^0}{R} - \frac{\Delta H^0}{RT}$	3.16 .....	47
$\text{Log}(Q_e - Q_t) = \log Q_e - \frac{k_1 * t}{2.303}$	5.1 .....	70
$\frac{1}{Q_t} = \frac{1}{k_2 * Q_e^2} + \frac{1}{Q_e}$	5.2 .....	70
$\text{Log}Q_e = \log K_f + \frac{1}{n} \log C_e$	5.3 .....	71
$\frac{C_e}{Q_e} = \frac{1}{b * Q_{\max}} + \frac{1}{Q_{\max}} C_e$	5.4 .....	71

## List of Abbreviations

<b>Abbreviation</b>	<b>Definition</b>
AC	Activated Carbon
As	Arsenic
At %	Atomic percent
BC	Biochar
BET	Brunauer Emmet Teller
C	Carbon
Cd	Cadmium
CO <sub>2</sub>	Carbon dioxide
Cr	Chromium
Cu	Copper
DBC	Digested biochar
EA	Elemental Analysis
EDTA	Ethylenediaminetetraacetic acid
EDX	Energy Dispersive X-Ray
FAO	Food & Agriculture Organisation
Fe	Iron
FeCl <sub>3</sub>	Iron (III) Chloride
FeNO <sub>3</sub>	Iron (III) Nitrate
FTIR	Fourier Transform Infra-Red
g	Gram
HCl	Hydrochloric acid
Hg	Mercury
H <sub>3</sub> PO <sub>4</sub>	Phosphoric acid
HTC	Hydrothermal Carbonisation
Hz	Hertz
J	Joule

K <sup>+</sup>	Potassium cation
KBr	Potassium bromide
kHz	Kilo hertz
KOH	Potassium hydroxide
L	Litre
MHz	Mega hertz
MgCl <sub>2</sub>	Magnesium (II) Chloride
MP-AES	Micro Plasma- Atomic Emission Spectroscopy
NaOH	Sodium hydroxide
NH <sub>4</sub>	Ammonium
Ni <sup>+</sup>	Nickel cation
Pb	Lead
PO <sub>4</sub>	Phosphate
PZC	Point Zero Charge
Q	Adsorption capacity
SEM	Scanning Electron Microscopy
T	Temperature
TEMPO	(2,2,6,6-tetra-methylpiperidine-1-yl) oxyl
TGA	Thermogravimetric Analysis
U	Uranium
UST	Ultrasound pre-treated
W	Watt
Wt %	Weight percent
Zn	Zinc
°C	Degree Celsius

## **Chapter 1 – Introduction**

### **1.1 Fresh water demand and contamination problematic**

Water is one of the most essential elements for our survival on earth, contributing to many aspects of human lives, ecosystem, climate, metabolic activities in living beings, etc. With the increase in world population and urbanization, combined with climate change and its unpredictable consequences, it is obvious that demand for fresh water will increase within the next few decades (Figure 1.1) [1-3]. This is particularly the case in developing and fast-growing countries where rapid industrialization significantly increases demand for freshwater, driving up the cost of water for industrial applications. Under such conditions, the supply of safe drinking water and access to adequate sanitation services for the population is a major concern. Water recycling and wastewater treatments are thus getting considerable attention to maintain the proper balance in the ecosystem [4,5]. Advanced wastewater treatment methodologies will be mandatory to allow reduction of freshwater consumption with minimum detrimental effects on plant operations and product quality.

Contamination of fresh water, especially due to non-biodegradable contaminants, have been an alarming issue mainly contributed by industrialization and other natural phenomena. As an example, the Yamuna River stretch in Delhi, India has been found to be contaminated with moderate to high levels of heavy metals at various sites by the untreated industrial discharge, lead battery-based industrial units, vehicular pollution, sewage discharge and surface run-off from contaminated areas [6]. Natural causes can also increase heavy metal pollution such as volcanic activity, metal corrosion, metal evaporation from soil and water and sediment re-suspension, soil erosion, geological weathering [7]. Heavy metals are particularly of concern due to their recalcitrance and persistence in the environment and thus should be strictly controlled to meet drinking water standards [8,9]. Although there is no specific definition for heavy metal, literature has defined it as a naturally occurring element having a high atomic weight and high density which is five times greater than that of water. Heavy metals are usually present in trace amounts in natural waters but many of them are toxic even at very low concentrations [10]. Metals such as arsenic, lead, cadmium, nickel,

mercury, chromium, cobalt, zinc and selenium are highly toxic even in trace quantities. They can enter the food chain through bioaccumulation and can cause severe health hazards such as kidney damage, liver damage, skin cancer, memory loss [11]. Major heavy metal disasters happened in Minamata (Mercury), Sandoz (Mercury) and Hinckley (Hexavalent chromium) are the awful examples of how these contaminants can be a greatest threat to environment and humanity [12]. Industries such as metal plating facilities, mining operations, fertilizer industries and leather tanning are among major contributors to heavy metal pollution due to the discharge of metal-contaminated wastewaters in the environment.

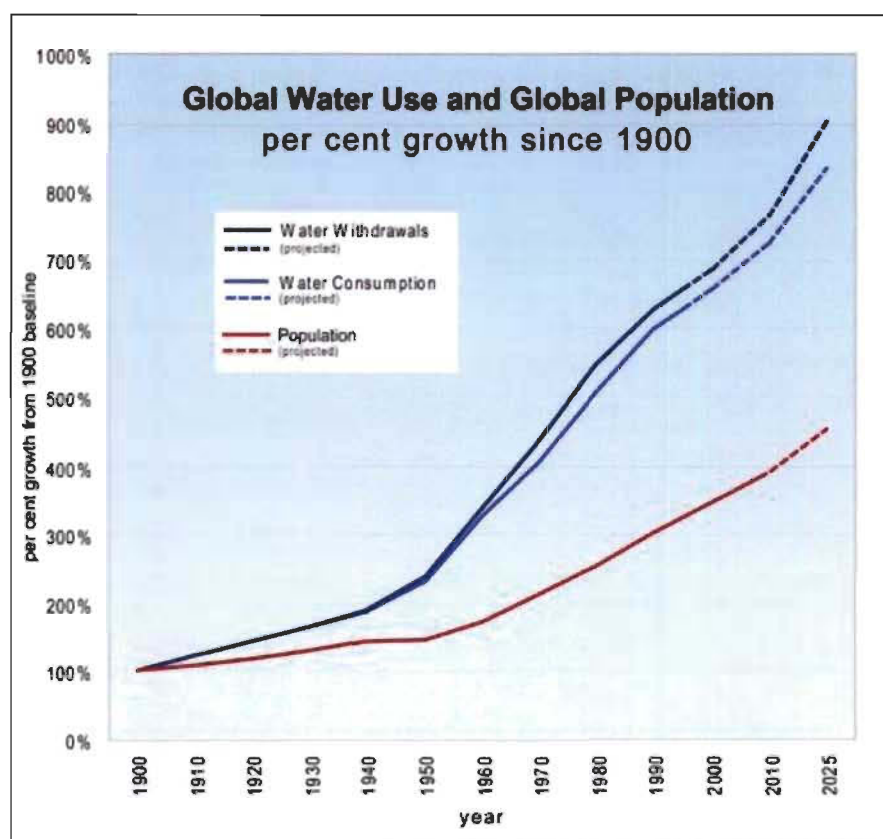


**Figure 1.1** Effect of global population on freshwater demand [3]

There are different techniques available to remove these toxic heavy metals from water such as precipitation, electrocoagulation, bio-sorption, membrane filtration, and ion exchange [13]. However, most of the conventional methods for water treatments are either expensive or limited in terms of efficiency for large scale production. The environmental risks associated to by-products (eg: toxic sludges in chemical precipitation, ion exchange resins,

saturated membranes after filtration) that are produced from processes themselves, extra operational costs for waste disposals, and high energy consumption makes them difficult to introduce in industrial level of water treatments [14, 15]. Therefore, intense research is going on to develop advanced and cost-effective technologies for water recycling.

Adsorption using biodegradable materials, especially activated carbons (ACs) attained much consideration in this scenario because of its exceptional adsorption capacity [16-17]. The main adsorption mechanism involved is the physical adsorption of guest molecules on the surface and pores of activated carbon. The higher specific surface area and micro pore volume has majorly contributed to the efficiency of these materials. ACs are widely used at the tertiary level of wastewater treatments to remove cationic as well as anionic contaminants. Nevertheless, their high cost, low selectivity and regeneration problems have limited their application to large scale [18-22]. Research interest into the production of alternative adsorbents to replace activated carbon has been extensive in recent years. Attention has been focused on various adsorbents having surface functionalities which can act as anchoring sites for the guest molecules.

## **1.2 Biomass research in Quebec, Canada**

Quebec, being rich in forest biomass availability, has made commitment in adopting research policies to make use of the biomass products in order to address challenges faced by environment. These policies are with particular objectives that focuses on reducing energy consumption, improving efficiency, developing green economy, and making full use of Quebec's natural resources efficiently (Quebec Energy Policy 2030) [23]. Converting traditional forestry feedstocks to create new high value-added bioproducts will be a significant footstep in Quebec's energy transition and bioeconomy. From traditional pulp and paper markets decline, thus increased availability, the processed feedstocks from different biomass industries are important to consider in this global perspective. Development of innovative technologies are needed to make sure that these post-consumer feedstocks are potentially used at higher efficiency and cost-effectively. Cost-effective thermochemical conversion techniques, invasive biomass processing machineries to improve material quality, chemical and physical modification on biomass derived products

and composites to have better physiochemical properties are example of such innovative ideas. Most of these methods can be implemented at various levels of biomass treatments with chemical treatments. Where as, we implement power ultrasonication as a physical pre-treatment in order to have modified material property even before the thermochemical conversion step.

Herein, we propose an efficient way to process post-consumer feedstock using power ultrasound to improve the material properties derived from these feedstocks and to potentially use them in treating inorganic contaminants from wastewater. We hope that the outcomes of this research will make a significant change in conventional methods of water recycling by providing better adsorbents, enhancing water sustainability and environmental protection.

## Chapter 2 – Thesis Overview

### 2.1 Objectives and Hypotheses

The main objective of this research project is to produce softwood derived biochar using ultrasound assisted lab-scale slow pyrolysis, study its adsorption behaviour towards the removal of heavy metals from water, and implement effective modification on biochar surface (activation & metal impregnation) to improve the physicochemical properties. The overview of the thesis is represented in Figure 2.1.

Ultrasound bath with different frequency, power, temperature, exposure time combinations has been utilized for optimizing the reaction conditions. The biochars derived from these ultrasound pre-treated woodchips were examined to understand the effect of each parameters towards metal adsorption properties. Different modifications on synthesized biochar surface like chemical activation and impregnation using metal were also examined and the ultrasonic effects on these processes were studied.

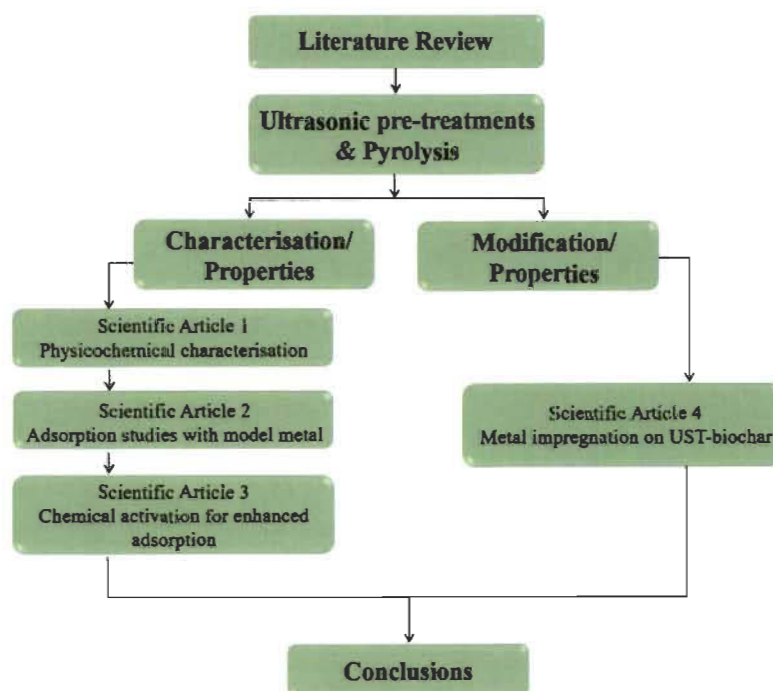


Figure 2.1 Organisation of research thesis

The major hypothesis of this research project is that the ultrasonic pre-treatments will have a significant effect on surface properties of biochars and physicochemical and adsorption properties of these biochar will be different with respect to each ultrasound pre-treatment conditions. This will lead towards enhanced adsorption behaviour of the material and this engineered biochar can be proposed as an efficient low-cost candidate to remove heavy metal contaminants from wastewater.

The objectives of the research project are given below.

- Detailed literature survey about biochar production, properties and application in the field of heavy metal removal, power ultrasound technique and its application in biomass processing and fundamentals of heavy metal adsorption and properties (Chapter 3)
- To synthesise biochar from ultrasound pre-treated wood chips using laboratory scale slow pyrolysis system and characterize the biochar to understand the physical and chemical effect of ultrasound on pyrolysis products yield and biochar structure (Scientific article 1 published in [IEEE-Explorer, IUS 2019](#), October 2019: Chapter 4)
- To study the adsorption properties of ultrasound pre-treated wood biochar using copper as a model metal (Scientific article 2 published in [Bioresource Technology Reports](#), May 2020: Chapter 5)
- To understand the ultrasound pre-treatment effects on alkali activation on biochar and study its heavy metal adsorption properties using single and multi-metal solution systems (Scientific article 3 published in [Journal of Environmental Management](#), April 2021: Chapter 6)
- To understand ultrasonic pre-treatment effects of iron impregnation and post and pre pyrolysis impregnation effects on ultrasound pre-treated biochars (Scientific article 4 published in [SN Applied Sciences](#), May 2021: Chapter 7)

## 2.2 Experimental techniques

All the prepared biochars were characterized using different characterization techniques such as American Society for Testing and Materials D1752-84, Fourier Transform Infrared Spectroscopy (FT-IR), Elemental Analysis (EA), Scanning Electron Microscopy (SEM), Energy dispersive X-ray spectroscopy (EDX), Thermogravimetric Analysis (TGA), Brunauer, Emmett and Teller (BET) surface area analysis, Nano-zetasizer, Micro Plasma-Atomic Emission Spectrometer (MP-AES). Batch adsorption tests were carried out using Copper (II) as model metal and the detailed investigation of kinetics, isotherm and thermodynamic properties were also performed. Multicomponent systems were studied using mix solutions of nickel, lead and copper. The detailed experimental conditions and instrument specifications are explained in materials and methodology section in each manuscript.

The change in adsorption capacity was measured using EDTA- Cu complexometric titration method suggested by Prasad and Raheem [24]. The complexing agent used is ethylenediaminetetraacetic acid (EDTA) in the form of its disodium dihydrate salt ( $\text{Na}_2\text{C}_{10}\text{H}_{18}\text{N}_2\text{O}_{10}$ ). Since EDTA forms complexes with many metal ions, this particular method can only be used in the absence of such ions as  $\text{Ca}^{2+}$ ,  $\text{Ni}^{2+}$ , etc. The complex dianion is formed with the release of two moles of  $\text{H}^+$  from EDTA, with the indicator being released from the copper ion. The indicator used for the titration is called murexide. This indicator is highly colored and will complex with the copper ion to give a different colored species. During the titration, the  $\text{EDTA}^{2-}$  forms a more stable complex and frees the indicator, which then displays its original color. The appearance of the free indicator means that all metal ions have been complexed by  $\text{EDTA}^{2-}$ , which signals the end point. By knowing the exact concentration and volume of EDTA titrated, the final concentration of Cu (II) can be calculated for known volume.

## 2.3 Safety Trainings

Safety inside as well as outside the laboratory has been the primary concern with at most consideration. Prior to the synthesis, all safety measures and safety trainings such as WHMIS, hydrogen safety training, liquid nitrogen safety training, fire safety training and

laboratory safety trainings were undertaken. Apart from these, a thorough understanding of all the equipments in the laboratory was made sure. The hazards of chemicals were also taken into consideration while working in the laboratory. Pyrolysis was carried inside the fume hood to ensure the safety as well as the purge of gaseous wastes produced.

#### **2.4 Waste Management**

In a chemical laboratory, it is as important to take care of the chemical wastes as long as the reactions undergone. All chemical wastes were disposed according to the University Safety Standards and regulations. Heavy metal solutions were disposed in separate container along with their concentrations considering their risk impact when exposed to groundwater. Pyrolytic oil and liquids were collected separately and disposed. Solid chemical wastes, glass wastes and recyclable wastes such as syringes were disposed separately too.

## Chapter 3 – Literature Review

### 3.1 Biochar

Biochar is a solid residue, rich in carbon, formed from partial or full biomass decomposition in an oxygen-limited environment at comparatively low temperatures (Figure 3.1) [25]. Biochar is used exclusively in different research fields, including soil sedimentation, agricultural and environmental gains, CO<sub>2</sub> sequestration and as an excellent emerging adsorbent [26-29]. The element that distinguishes biochar from charcoal is that charcoal is used as a fuel for heat or in metallurgical processes as a reducing agent. Unique properties exhibited by biochar including large specific surface area, porous structure, enriched surface functional groups and mineral components, and ion exchange capacity have inspired mainstream researchers to explore their potential to remove pollutants from aqueous solutions as an alternative to activated carbons [30-32]. The ease of feedstock availability, low energy requirements for production has also made it more interesting over other expensive adsorbents.



**Figure 3.1** Biochar produced from softwood chips

### 3.1.1 Synthesis methods for biochar

Biochar is obtained through various thermochemical processes such as pyrolysis, hydrothermal carbonization, torrefaction and gasification (Figure 3.2) [33,34]. These processes result in three main products, namely liquid bio-oil, solid biochar and non-condensable gas products called syn-gas. Depending on the heating rate and solid residence time, biomass pyrolysis can be divided into three main types including slow (conventional) pyrolysis, fast pyrolysis and flash pyrolysis. The major product and its ratio will also vary with the technique used for thermal conversion of feedstock.

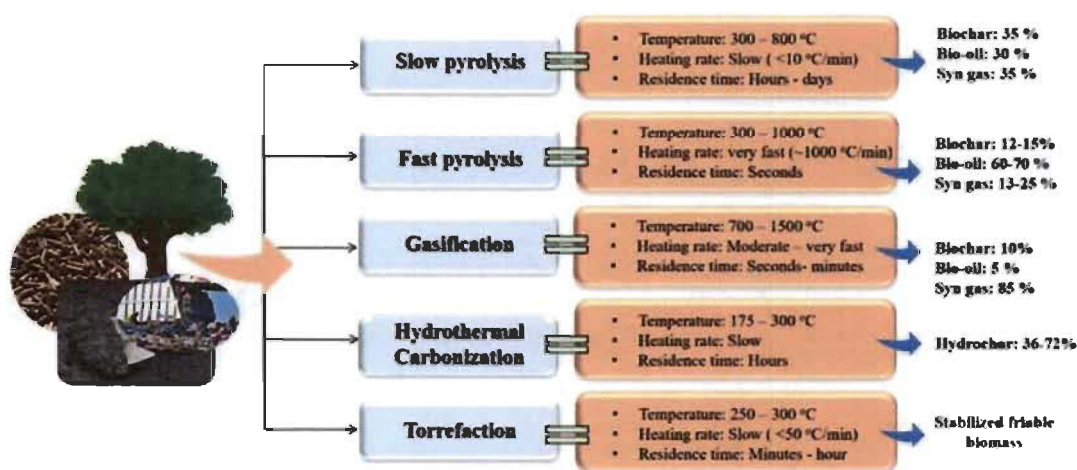


Figure 3.2 Various thermal conversion methods for biomass feedstocks

#### 3.1.1.1 Slow pyrolysis

Slow pyrolysis, also known as conventional pyrolysis, belong to a long history of applications. Initially used to produce charcoal, it has emerged as one of the main techniques to produce biochar. It is an inexpensive and robust technology which typically produce materials with yields: bio-oil 30 wt%, biochar 35 wt%, and gas 35 wt% [25,35]. Unlike normal combustion which is carried out in the presence of oxygen, pyrolysis is performed under no or limited oxygen environment. The normal temperature range for slow pyrolysis is 300 to 800 °C and the residence time is usually long (hours to days). The thermal decomposition of biomass proceeds under a very low heating rate with sufficient time allowed for repolymerisation reactions to maximise the solid yields. Pyrolysis temperatures ranging from 300 to 800 °C favours the production of biochar by reducing the yield of

bio-oil. Likewise, a rise in the peak temperature (the highest temperature reached), during slow pyrolysis, could lead to an increase in the fixed carbon content of biochar. Higher aromaticity is observed for biochars produced from slow pyrolysis [36,37].

A significant number of simultaneous and serial reactions occurred during biomass pyrolysis, includes dehydration, depolymerisation, isomerization, aromatisation, decarboxylation, and charring [38]. Biomass pyrolysis is widely believed to consist of three intermingled major stages: (i) initial free moisture evaporation, (ii) primary decomposition followed by (iii) secondary reactions (oil cracking and repolymerisation). Biomass decomposition generally occurs during the primary decomposition to form solid char at 200–400 °C, which is responsible for the largest degradation of biomass. Secondary reactions take place within the solid matrix with further rise of the temperature. Decomposition of hemicellulose, generally represented by xylan, mainly takes place between 250 and 350 °C, followed by cellulose decomposition which primarily occurs between 325 and 400 °C with levoglucosan as the main pyrolysis product. Lignin remains the most stable component; it decomposes at higher temperature between 300–550 °C.

### ***3.1.1.2 Fast and flash pyrolysis***

Fast or flash pyrolysis is preferred when the primary product of interest is bio-oil [39]. Fast pyrolysis typically uses very short residence time of 2-60 seconds and the peak temperature is set between 300 and 1000 °C in order to achieve the maximum yield of bio-oil. The biomass particle size used is less than 2 mm under heating rate of 103 to 105 °C per second. The major product being bio-oil (60-70 wt %) biochar and syn-gas are produced as by-products with yields of 12-15 wt% and 13-25 wt%, respectively. The rapid quenching of pyrolytic vapors prevents secondary reactions during the process. Rapid elimination of primary carbon is a general requirement, as it acts as a catalyst for the cracking of primary organic vapors into secondary carbon, gas and water, leading to lower bio-oil yields.

Flash pyrolysis is a similar method which transforms biomass into high-pressure gas (about 1–2 MPa). The reaction time for this process is below 30 min, and the temperature is between 300 and 600 °C. Typical feed particle sizes of not more than 200 mm are required, giving a typical bio-oil yield of 75 wt percent and gas and char yields of 12-13 wt% [40].

### ***3.1.1.3 Hydrothermal carbonization***

Hydrothermal carbonization (HTC) uses unconventional wet biomass sources to produce hydrochars without any pre-drying processes. Main feedstocks used in this process are sewage sludge, city wastes, animal and human excreta. This technique is also known as wet pyrolysis. Hydrothermal carbonization is carried out upto 16 h by submerging feedstock biomass into water in a sealed container system and under saturated pressure at a temperature range of 175–300 °C and results in 36–72 percent of solid residue as major product [41]. Hydrochar is formed by a sequence of simultaneous reactions such as hydrolysis, dehydration, aromatization, condensation and decarboxylation. Aliphatic compounds are mostly primary components of the hydrocarbon than aromatic compounds of biochars. The moderate reaction of the hydrothermal carbonization process and the presence of subcritical water produces biochar with a significant amount of oxygen containing functional groups. Hydrochar typically has higher cation exchange capacity is readily biodegradable, but has lower surface area, poor microporosity and lower carbon stability [42,43].

### ***3.1.1.4 Torrefaction***

Torrefaction usually entails slow heating in a temperature range of 250–300 °C, under minimal to no oxygen supply along with low heating rate of  $<50^{\circ}\text{C min}^{-1}$  and long residence time up to 1 h. This process releases both moisture and carbon dioxide from wood, resulting in a solid fuel with a lower oxygen/carbon ratio. Solid products derived from torrefaction have certain benefits, such as: (1) high energy density and heating value, (2) minimal shipping costs due to reduced moisture content of the end product, (3) high tolerance of torrefied biomass to fungal attacks due to its hydrophobic nature, (4) reduced energy requirements for grinding and (5) the production of a uniform fuel for gasification or co-firing of electricity [44,45].

### ***3.1.1.5 Gasification***

During gasification processes, biomass is converted into gasses in the high-temperature gasification chamber (700–1500 °C) at ambient or elevated pressure than pyrolysis technique without combustion. The yield and carbon content of the solid biochar using the gasification

process is considerably lower [46]. Gasifying agents such as air, steam, and air-steam, etc., are used for the processing of syngas. The carbon dioxide emitted during the gasification process also acts as a gasifying agent. During the biomass gasification process, 80% of the mass loss is attributed to the removal of certain permanent gasses and volatile components. The parameters governing the gasification process are the temperature, the pressure, the gasification agent and the biomass ratio gasification agent. Temperature is one of the main parameters that specifically affects the phase of gasification. The rise in temperature favours the production of hydrogen, carbon monoxide and carbon, while contents of tar, hydrocarbons, carbon dioxide and methane remain limited.

#### ***3.1.1.6 Type of pyrolysis used***

The temperature range of lab-scale pyrolysis system we have used for this project was set between 500- 550 °C. The heating rate was approximately 15 °C/min and the time of reaction between 1 to 1.5 h. The pyrolysis resulted in almost equal percent of products. These observations demonstrate that the type of pyrolysis we are using belongs to slow pyrolysis category [47-49].

#### **3.1.2 Factors affecting biochar properties**

Biochar exhibit difference in its physicochemical properties depending mainly on the feedstock type, production conditions and post and pre-processing of feedstocks [50-53]. In most of the pyrolysis process, conditions of higher heating rate, lower pressure, higher reactor temperature, and smaller biomass particle sizes have shown improvements in biochar properties and yield. These conditions have an effect on carbon content, higher surface area and greater pore volume.

A study conducted by Manyà [54] showed that an increase of peak temperature seems to lead to the generation of biochar with higher aromatic character, fixed carbon, and higher porosity. Kim and co-workers [55] have also investigated the Influence of pyrolysis temperature on physicochemical properties of biochar obtained from the fast pyrolysis of pitch pine. Authors state that obtained biochar at 400 and 500 °C was composed of a highly ordered aromatic carbon structure.

The feedstock type is also an important parameter that affects the properties of the biochar. As an example, optimal biochar properties for filtration purposes with surface area of 1400 m<sup>2</sup>/g and micro pore volume of 0.7 cm<sup>3</sup>/g were obtained from coconut shells with a particle diameter of 1.55 mm, reaction temperature of 850 °C, and a retention time of 1.5 h under steam using a fluidise bed reactor [56]. A biochar with similar properties (surface area of 1690 m<sup>2</sup>/g and micro pore volume of 0.7 cm<sup>3</sup>/g) was obtained by pyrolyzing olive seed waste in a fixed bed heated under N<sub>2</sub> at 800 °C for 1 h and activating the produced biochar with KOH [57]. In 2013, Mukome and co-workers [58,] studied the physical and chemical properties of commercially available biochars and investigated trends in biochar properties related to feedstock material to develop guidelines for biochar use. They tested twelve biochars for physical and chemical properties. This study has reported that feedstock was a better indicator of the quality of biochar ash and carbon/nitrogen ratio, but for wood-derived biochar, the surface area was also temperature dependent.

The adsorption capability of biochar was also significantly influenced by the natural compositions of feedstock. Given the same pyrolysis condition, the adsorption capacity of biochars for contaminants varied with the types of raw biomass [59,60]. Xu et al. [61] reported that dairy manure biochar was more effective than rice husk biochar in removing Pb, Cu, Zn, and Cd from both mono and multi-metal solutions. The adsorption of methyl violet by the biochars from four crop residues was demonstrated in a study [62]. Indeed, the adsorption capacity varied with their feedstock in the following order: canola straw char > peanut straw char > soybean straw char > rice husk char. This order is generally consistent with the amount of negative charges on biochars.

### **3.1.3 Biochar for heavy metal adsorption**

As a natural resource and because of its economic and environmental advantages, biochar is a valuable resource for environmental technologies that can be used in the treatment of water pollutants. Most researches have indicated that biochar has demonstrated excellent capacity to extract pollutants such as heavy metals [29,63]. Several biochars exhibit comparable or even better adsorption capacity than commercially activated carbon [64-66]. Typical biochar is less carbonized than activated carbon. Nevertheless, more hydrogen and oxygen remain

in its structure along with the ash originating from the biomass: both seemed to improve its physicochemical properties.

Efficient physicochemical properties of biochar arose from the feedstock type, pyrolysis conditions and processing techniques make them a good candidate as a low-cost adsorbent. Removal rates of various heavy metals like arsenic (As), cadmium (Cd), chromium (Cr), copper (Cu), lead (Pb), mercury (Hg), nickel (Ni), uranium (U), and zinc (Zn) were well studied with biochar as adsorbent [67-70]. Adsorption of anionic contaminants and organic pollutants (i.e. pharmaceutical residues, dyes, pesticides etc) are also investigated using biochar as an adsorbent [71-73]. According to the literatures available, the removal efficiency of biochars is based on various surface mechanisms (Figure 3.3).

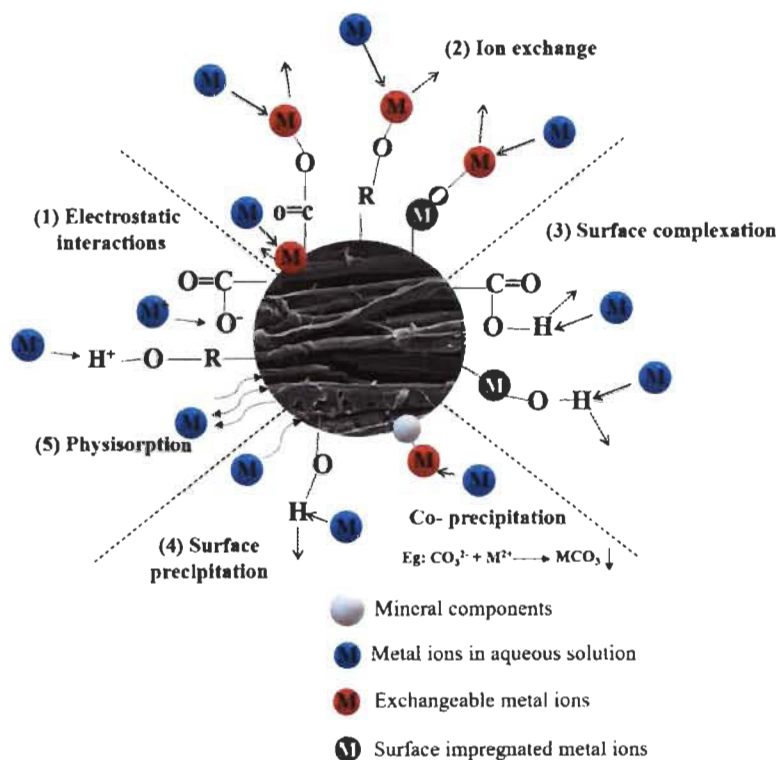


**Figure 3.3** Different surface interactions for heavy metal adsorption

They include: (1) electrostatic interactions between metals and biochar surface; (2) cation exchange between metals and protons or alkaline metals on biochar surface; (3) metal complexation with functional groups and  $\pi$  electron rich domain on the aromatic structure of

biochar; (4) metal precipitation to form insoluble compounds; and (5) physical adsorption on surface pores.

Sorption mechanisms and capacity vary considerably with biochar properties and target metal. Available surface functionalities help to improve the positively charged metal ions adsorption through the above-mentioned mechanisms. As an example, a study by Lu et al. [74] proposed that the functional groups played an important role in Pb adsorption on a sludge derived biochar, including metal exchange with  $K^+$  and  $Na^+$  due to the electrostatic outer-sphere complexation. Tong et al. [75] have used peanut, canola, and soybean straw biochars, prepared in a 400 °C muffle furnace for  $Cu^{2+}$  adsorption. All three biochars had higher adsorption capacities than commercial activated carbon at pH 3.5–5.0. Lead adsorption by slow pyrolysis (at 600 °C) biochars from raw (BC) and anaerobically digested sugarcane bagasse (DBC) was studied by Inyang et al. [76]. These biochars possessed far lower surface areas than activated carbon. However, the sorption capacity of DBC (653.9 mmol/kg) was twice that of AC (395.3 mmol/kg) and twenty times higher than BC (31.3 mmol/kg).

Additional studies proved the ability of biochars to remove heavy metals from water. However, researches are still devoted to the improvement of the efficiency of these materials in a low-cost method. This can be done by understanding the surface morphology of biochar related to its physicochemical properties. Various modification techniques, theoretical isotherm and kinetic models with thermodynamic studies are implemented on biochar adsorption mechanism. These topics will be discussed in the following sections.

#### **3.1.4 Modifications on biochar**

Several alteration methods have been used to boost the physicochemical properties of biochar. Through increasing specific surface area, porosity and introducing new functionalities as anchoring sites on the surface, these methods help to improve the adsorption properties of biochar [77,78]. Intense research is being carried out in a cost-effective, environmentally sustainable and feasible manner to develop modified biochars. The engineered biochars can be used as a potential alternative to existing adsorbent

materials like activated carbons. Few of the major modification techniques are discussed below.

#### ***3.1.4.1 Activation***

Activation is an important and key step in material synthesis in order to enhance the performance of adsorption by modifying the surface morphology with improved specific surface area and porosity. Activation processes establish a network of interconnecting micropores that eventually increases the surface area on which chemical or physical adsorption of metal cations can take place. Biochar can be activated mainly using physical and chemical activation methods [79-81]. Physical activation methods force high temperature steam through the pores of the biochar, which increases the surface area, while chemical activation methods expose the biochar to acidic or alkaline solutions which oxidise the surface and create oxygen-containing functional groups.

##### **a) Physical activation**

Physical activation is the development of porosity by gasification with an oxidizing agent at relatively high temperatures. The increased internal surface area and accessibility of pores is achieved by using activation agents like CO<sub>2</sub>, steam or their combination [82-84]. They can be injected either at the end of the pyrolysis process or as a separate activation to the synthesized biochar. Compared to CO<sub>2</sub>, the smaller size of water molecule facilitates better activation. A series of reactions happening during the activation process which involves surface oxide groups and carbon monoxide, enable non-condensable gas formation and improves the porous structure of biochar by removing the trapped products. The mechanism of activation with CO<sub>2</sub> involves the Boudouard reaction ( $C + CO_2 \leftrightarrow 2CO$ ). In this process, CO<sub>2</sub> undergoes dissociative chemisorption on the carbon surface to form a surface oxide and carbon monoxide. The surface oxide, C(O), is subsequently desorbed from the surface, further developing the pore structure [80].

Lima and Marshall [85] produced activated biochars from poultry manure feedstocks using steam activation with a range of water flow rates and durations. It was observed that higher flow rates and longer activation times increased the sorption of Cd, Cu and Zn on the surface

of the biochar. Even though steam activation increases the surface area and porosity of biochar, Shim et al. [86] found that the  $\text{Cu}^{2+}$  sorption capacity of biochar produced by slow pyrolysis of Miscanthus at 500 °C was not significantly changed by activation with steam. There was an increase in specific surface area, but the abundance of functional groups decreased with an increase in aromaticity. Similarly, Lou et al. [87] observed that steam activation of biochar prepared with pine sawdust increased the surface area but had little effect on the characteristics of surface functional groups. Azargohar and Dalai [88] studied the activation of wood-derived biochar using steam followed by chemical activation to understand the activation effect on its BET surface area and product yield. They found that the steam activation increases the specific surface area, however, decreases the pyrolytic product yield.

These methods are clean and simple but energy intensive since they normally need high temperatures. To rectify the problem caused by steam and  $\text{CO}_2$  activations, activation by microwave, ultrasound irradiation, plasma treatment, and electrochemical modification methods have recently emerged to improve BC characteristics at a reasonable cost.

#### b) Chemical activation

Oxidation reagents like hydrogen peroxide, phosphoric acid, strong alkali (i.e. KOH, NaOH, etc) are the most common chemical activation agents. Many articles showed the efficiency of these agents to significantly enhance the surface properties and adsorption ability [89-92]. Chemical activation is preferred over physical activation owing to the higher yield, simplicity, lower temperature, shorter activation time, and good development of the porous structure. Although this method should have great potential for biochar engineering, its effects on biochar's surface properties and sorption ability are still not well understood. Nevertheless, it appears that the chemical agent dehydrates the sample, inhibits the tar formation and volatile compounds evolution, and therefore enhances the yield of the carbonization process [78]. After impregnating the precursor by chemical agent and heat treatment of the mixture, the impregnating agent and its salts are removed by washing with acid/base and water, which makes the pore structure available. In comparison to acid

activations, use of alkali as activation agent is more effective in generating high BET surface area and altering surface functional groups.

Physicochemical activation of rice husk biochar using KOH was achieved according to the study by Prapagdee et al. [93] large specific surface area was obtained and the Cd (II) removal efficiency of the activated biochar was increased from 13–20% to 95–97% over non-activated biochar. In another study by Angin et al. [94], activation by KOH improved the specific surface area and porosity of the material with efficient removal of reactive dyestuff from wastewater. Biochar activation with NaOH has also proved its efficiency in removing hazardous contaminants from aqueous solution [95,96]. Wood derived biochar was activated using high temperature oven by Braghiroli et al. for the application of phenolic removal. It was found that activated biochars presented higher phenol adsorption capacity compared to biochars due to their improved textural properties, higher micropore volume, and proportion of oxygenated carbonyl groups connected to their surface [97]. In a study conducted by same authors, they have shown that physically and chemically activated biochars can be efficiently used in the treatment of Cu in synthetic and actual contaminated mine drainage [98]. The results were interesting because CO<sub>2</sub>-activated biochar showed better efficiency for Cu in synthetic effluent at up to 200 mg L<sup>-1</sup>, whereas KOH-activated biochar was the most efficient material for Cu from high concentration synthetic effluent (1000 mg L<sup>-1</sup>) and from multimetal actual effluent.

#### ***3.1.4.2 Metal impregnation***

Biochars generally have a high surface area but a negative surface charge and high pH. These properties make biochars excellent sorbents for metal cations due to specific adsorption on oxygenated functional groups, electrostatic attraction to aromatic groups and precipitation on the mineral ash components of the biochar. However, because of the same reason, they are poor adsorbents for anionic contaminants. By exploiting the high surface area of biochars as a platform to embed a metal oxide with contrasting chemical properties (and usually a positive charge), biochar-based composites are developed to remove negatively charged oxyanions from aqueous solutions [99,100]. The objective of most methodologies to create metal oxide biochar-based composites is to ensure a homogenous

spread of the metal over the biochar surface. The biochar is essentially used as a porous carbon scaffold upon which metal oxides precipitated to increase the surface area of the metal oxide. Generally, impregnation of biochar with metal oxides is performed by soaking biochars or their feedstocks in solutions of metal nitrate or chloride salt solutions [78]. The most frequently used impregnation agents in the literature are  $\text{FeCl}_3$ ,  $\text{Fe}^0$ ,  $\text{Fe}(\text{NO}_3)_3$  and  $\text{MgCl}_2$ . This process can be done directly to the feedstock prior to pyrolysis as well. These metal impregnated biochars are used as efficient catalyst for photoreduction reactions and bio-oil productions [101-103]. They also have proved its efficiency in removal heavy metal as well as anionic contaminants from aqueous solution [104-106]. Hasan et al. [107] have proved the efficiency of biochar-supported nanoscale zerovalent iron (BC-nZVI) for removing heavy metals (Cu, Cd, and Zn) from synthetic stormwater. Recently, Bao et al. [108] have studied the characteristics and mechanism of metal-modified sludge-based biochar for enhance catalytic capacity. The metal-modified (Fe, Ce, La, Al, Ti) sludge-based biochars were prepared and applied for  $\text{H}_2\text{O}_2$  activation. It was seen that the metals loaded significantly changed the surface morphology, element compositions, and structural defects of the biochar and enriched the metal oxides on it. The ability of modified biochars to activate  $\text{H}_2\text{O}_2$  to generate hydroxyl radicals found to be stronger than that of the unmodified biochar, indicating that the catalytic performance of modified biochars was mainly related to the metal oxides loaded and the defect structure on the surface of biochars.

As an extension of study on ultrasonic pre-treatment effects of biochar and adsorption properties, the effect of iron impregnation was also investigated in this project. The ultrasound pre-treated woodchips and biochar derived were subjected to Fe-impregnation and physicochemical properties were examined. These modified biochars can be a cost-efficient alternative in catalysis applications.

### ***3.1.4.3 Other Modifications***

Functionalising the biochar with organic molecules, graphene oxides, nanocomposite materials are also emerging techniques to improve adsorption of solid as well as gaseous molecules from different medium [109-111]. Here, the biochar is essentially used as a high surface area scaffold to support the materials being deposited. Composites are distinguished

from chemical activation because they involve the creation of completely new functional groups on surfaces that did not previously exist on the biochar or feedstock surface. Literatures prove the efficiency of these methods thereby promoting engineered biochars as a potential candidate to remove hazardous contaminants [112,113]. For example, a redox precipitation method was used to load manganese dioxide ( $\text{MnO}_2$ ) nanoparticles on biochar (BC) ( $\text{BC@MnO}_2$ ) pyrolyzed from the invasive water hyacinth, and the adsorption of  $\text{Cd(II)}$ ,  $\text{Cu(II)}$ ,  $\text{Zn(II)}$ , and  $\text{Pb(II)}$  was investigated by Zhang et al. [114]. The results revealed that the BC surface was covered by many intertwined thin amorphous  $\text{MnO}_2$  nanosheets, which significantly increased its specific surface area and pore volume. The adsorption of heavy metal ions by BC was negligible, whereas the  $\text{MnO}_2$ -containing adsorbents exhibited a high capacity for adsorbing heavy metal ions.

### **3.1.5 Wood biochar and its application on heavy metal removal**

Lignocellulosic materials are commonly used as precursors to activated carbon due to its two essential characteristics. First, owing to its low inorganic material content, which results in the production of activated biochars with a lower ash content. Second, they have a relatively high volatile content that helps to regulate the different production processes [115]. The availability of feedstock, the renewability and the eco-friendly nature have enabled them to gain worldwide consideration. The residues from agricultural activities and forest environment are the important source of the lignocellulosic biomass. The Food and Agricultural Organization (FAO) estimated the wood volume and aboveground woody biomass in forests in the year 2000 and reported that the global volume of forests was 386 billion cubic metres and the worldwide aboveground woody biomass was about 422 billion tonnes. Over the 1990s, the amount of wood increased by 2 percent, so the volume of wood biomass in 2020 will be about 401 billion cubic meters [116].

However, the properties of biochar derived from wood feedstock are difficult to control because of the highly hygroscopic nature of wood and heterogeneity in structure. The structural heterogeneity is mainly arising from the three basic components of wood, namely: cellulose, hemicellulose and lignin.

### *3.1.5.1 Components of wood and effect of slow pyrolysis*

The major structural chemical components of wood with high molar masses are carbohydrate polymers and oligomers (65%-75%) and lignin (18%-35%). Minor amounts of organic extractives and inorganic minerals are also present in wood (usually 4%-10%). The weight percent of these components varies in different biomass species of wood. For example, hardwoods contain 38–51% cellulose, 17–38% hemicellulose, 21–31% lignin, and 3% extractives. Whereas in softwood it is 33–42% cellulose, 22–40% hemicellulose, 27–32% lignin, and 2–3.5% extractives [117].

#### a) Cellulose

Cellulose is the most abundant organic polymer on earth. It is a high molecular weight linear polymer of  $\beta$ -(1 $\rightarrow$ 4)-D-glucopyranose units in the  ${}^4C_1$  conformation. Cellulose fibres provide wood strength and comprise almost 40-50 wt % of dry wood. The basic repeating unit of the cellulose polymer consists of two glucose anhydride units, called a cellobiose unit (Figure 3.4). Cellulose is insoluble, consisting of between 2000 and 14000 residues. The crystalline structure resists thermal decomposition better than hemicelluloses. Amorphous regions in cellulose contain waters of hydration, and free water that is present within the wood. This water, when rapidly heated, disrupts the structure by a steam explosion-like process prior to chemical dehydration of the cellulose molecules. Cellulose degradation occurs at 240-350 °C to produce anhydro cellulose and levoglucosan [118].

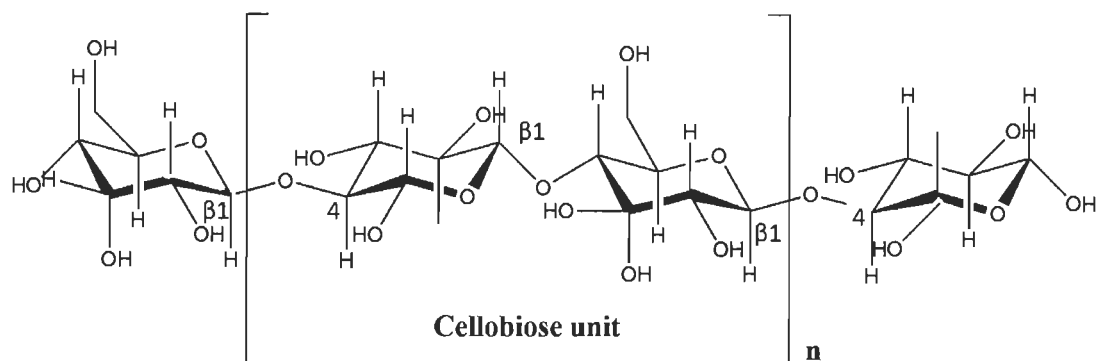


**Figure 3.4** Chemical structure of cellulose

b) Hemicellulose

A second major wood chemical constituent is hemicellulose (Figure 3.5). A variety of hemicelluloses usually account for 25%-35% of the mass of dry wood, 28% in softwoods, and 35% in hardwoods. Hemicellulose is a mixture of various polymerized monosaccharides such as glucose, mannose, galactose, xylose, arabinose, 4-*O*-methyl glucuronic acid and galacturonic acid residues.

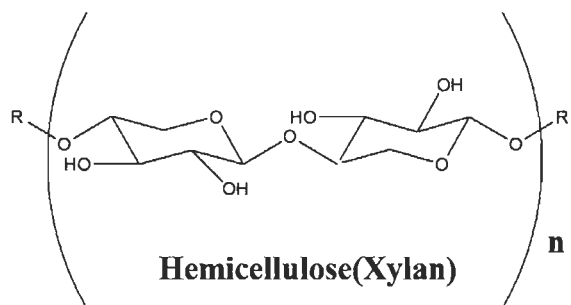


**Figure 3.5** An example for hemicellulose

Hemicelluloses exhibit lower molecular weights than cellulose. The number of repeating saccharide monomers is very less when compared to cellulose. Cellulose has only glucose in its structure, whereas hemicellulose has a heteropolysaccharide makeup and some contains short side-chain “branches” pendent along the main polymeric chain. Hemicellulose decomposes at temperatures of 200-260 °C, giving rise to more volatiles, less tars, and less chars than cellulose [118,119]. Most hemicelluloses do not yield significant amounts of

levoglucosan. The loss of hemicellulose occurs in slow pyrolysis of wood in the temperature range of 130-194 °C, with most of this loss occurring above 180 °C.

### c) Lignin

The third major component of wood is lignin which is an amorphous cross-linked resin with no exact structure. It is the main binder for the agglomeration of fibrous cellulosic components while also providing a shield against the rapid microbial or fungal destruction of the cellulosic fibres. Lignin has an amorphous structure, which leads to a large number of possible interlinkages between individual units, because the radical reactions are non-selective random condensations. Ether bonds predominate between lignin units, unlike the acetal functions found in cellulose and hemicellulose, but carbon-to-carbon linkages also exist. Lignin is the most stable component which decomposes at higher temperature range of 300 – 550 °C. Pyrolysis of biomass with higher lignin content will result in more biochar yield [25,120].

Hardwood and softwood lignin have different structures. “Guaiacyl” lignin, which is found predominantly in softwoods, results from the polymerization of a higher fraction of coniferyl phenylpropane units. “Guaiacyl-syringyl” lignin, which is typically found in many hardwoods, is a copolymer of both the coniferyl and sinapyl phenylpropane units where the fraction of sinapyl units is higher than that in softwood lignins (Figure 3.6).

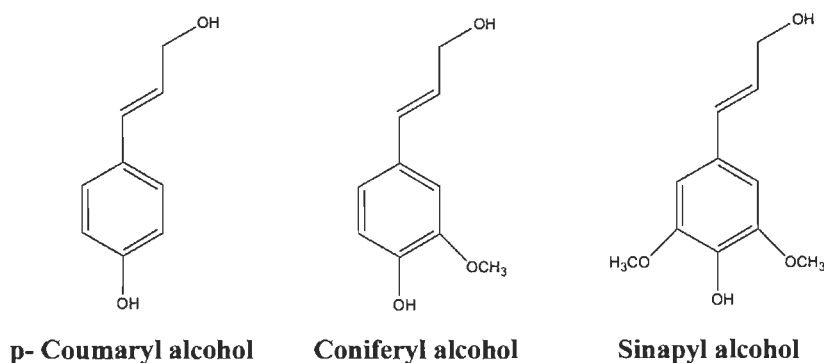


**Figure 3.6** Components of lignin

### 3.1.5.2 Heavy metal adsorption using wood biochars

The abundance of negatively charged surface sites on wood biochars due to the presence of functional groups such as carboxyl, hydroxyl, and phenolic ( $-\text{COO}^-$  and  $-\text{OH}^-$ ) could bind cationic contaminants such as As, Pb, Cu, Zn, and Cd from aqueous solution. For instance, the potential applicability of Japanese oak wood biochar for removal of As in As-contaminated drinking well water was investigated by Niazi et al. [121]. The authors demonstrated that 92–100% of dissolved As was removed from the drinking well water despite the presence of co-occurring anions. It is also shown that the presence of electron donor functional groups ( $-\text{C}-\text{OH}$ ,  $\text{C}-\text{O}$ ,  $\text{C}-\text{O}-\text{R}$ ) could promote sorption of Cr(VI) on wood biochar by sorption-coupled reduction of Cr(VI) to Cr(III) in order to enable surface sorption [122]. Huggins et al. [64] examined the efficiency of granular wood-derived biochar to remove contaminants such as heavy metals (As, Cd, Cr, Pb, Zn, Cu) and  $\text{PO}_4$ ,  $\text{NH}_4$ . They found that biochar has considerably higher adsorption ability relative to granular activated carbons for the treatment and nutritional recovery of actual wastewater in both batch and column tests. The properties of wood biochar (e.g. organic functional groups, mineral content, ionic content, and  $\pi$ -electrons) have a direct influence on sorption mechanisms of metal removal from aqueous solution. Cation exchange, pH, and surface complexation promotes the removal efficiency and literatures are available to prove the potential of wood derived biochars to remove toxic contaminants from wastewater [123-127].

## 3.2 Ultrasound

The oscillation of pressure travelling through solid, liquid, or gas medium in a wave pattern results in mechanical and longitudinal waves and are called *Acoustic waves*. These waves are defined by different parameters such as wavelength, frequency, period and amplitude (Figure 3.7). Depending on the frequency of the waveform, sound waves can be classified as infrasonic, sonic, and ultrasonic. Sonic waves have frequencies between 20 and 20,000 Hz, which correspond to the frequency range of the human hearing. Waves with frequencies below 20 Hz are classified as infrasonic, while waves with frequencies above 20,000 Hz are classified as ultrasonic [128].

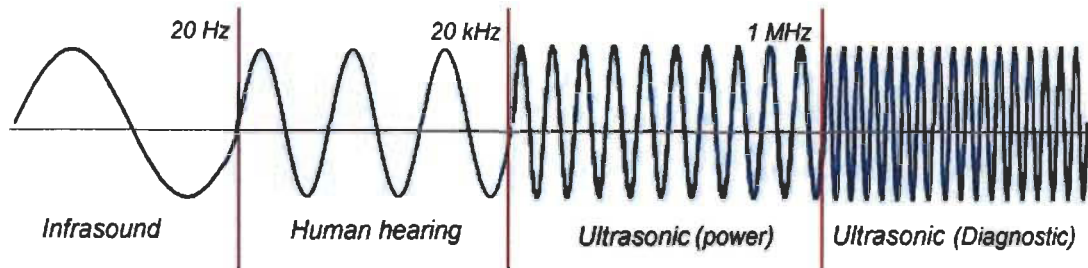


**Figure 3.7** Type of sound waves and frequency range

Within the ultrasound range, acoustic techniques can be categorized into different groups according to the frequency and power of operation. High frequency and low power techniques are classified into diagnostic and high frequency ultrasound, while low frequency and high-power techniques are classified into power ultrasound. They have wide range of applications in medical industry, engineering, manufacturing industry, etc.

### 3.2.1 Types of ultrasound

#### 3.2.1.1 Diagnostic Ultrasound

Diagnostic ultrasound is mainly used in medical sciences to study the internal tissue structure. It makes use of a series of pulse-echo technique which are non-invasive with combination of low-power ( $< 100 \text{ mW cm}^{-2}$ ) and high-frequency (1-10 MHz) wave forms. They are low intensity sound waves and therefore do not affect the physicochemical properties of the tissue.

Ultrasound with intensity around  $1 \text{ W cm}^{-2}$  is used for deep-heating therapeutic tools [129] and higher intensity waves ( $\sim 10 \text{ W cm}^{-2}$ ) are used in oncology treatments [130]. Ultrasound with higher power intensities ( $10^3 \text{ W cm}^{-2}$ ) are used in small duration to modify tissue structures [131].

#### 3.2.1.2 High Frequency Ultrasound

Frequencies between 100 kHz and 1 MHz are classified as higher frequency ultrasound. They also make use of lower intensities therefore do not cause any change in material

structure while application. They are non-invasive and can be used in concentrated and opaque materials [132-134].

### ***3.2.1.3 Power Ultrasound***

Power ultrasound or high intensity ultrasound uses significantly lower frequencies than those used in diagnostic and high frequency ultrasound. Frequencies used in power ultrasound range between 20 kHz and 1 MHz. These are highly invasive techniques that uses high intensity acoustic waves to purposely change the properties of materials [128]. Acoustic cavitation and events associated with this phenomenon are responsible for inducing several physicochemical changes in the material. Some of the main advantages of using power ultrasound in various industries include: (a) improvements in product quality, (b) reduction in food processing costs, (c) decreased processing times, (d) reduced chemical and physical hazards, (e) environmentally friendly and sustainable, and (f) scalable throughput. The application of this technique extends to the fields such as therapeutic medicine, physiotherapy, chemotherapy, ultrasonic thrombolysis, and drug delivery [135]. Power ultrasound is also used for inducing crystallization of materials (sonocrystallization) and inducing or causing chemical reactions (sonochemistry) that would not occur in the absence of ultrasound [1363].

### **3.2.2 Cavitation**

The basis of many applications of ultrasound in this frequency range is acoustic cavitation, which is the formation, growth and collapse of microbubbles within an aqueous solution resultant from pressure fluctuations that occur in the applied sound field.

In 1895, Thornycroft and Barnaby reported cavitation for the first time when they observed that the propeller of their submarine became pitted and eroded over a relatively short operation period [137]. Their observation was the consequence of collapsing bubbles due to hydrodynamic cavitation that generated intense pressure and temperature gradients in the local vicinity of the propeller blades. In 1917, Lord Rayleigh published the first mathematical model describing a cavitation event in an incompressible fluid [138]. Later in 1927, Loomis reported the first chemical and biological effects of ultrasound, that workers

recognised that cavitation could be a useful tool in chemical reaction processes [139]. Since then, cavitation has been effectively applied in various field of research including production of polymer, for the enhancement of chemical reactions, emulsification of oils and degradation of chemical or biological pollutants.

In acoustic cavitation, a sound wave imposes a sinusoidally varying pressure upon existing cavities in solution (Figure 3.8). During the negative pressure cycle, the liquid is pulled apart at sites containing such a gaseous impurity, which are known as “weak spots” in the fluid. The number of bubbles that are produced during this rarefaction cycle is proportional to the density of such weak spots present in the fluid. There are two known mechanisms for cavity or bubble formation. One mechanism involves pre-existing bubbles in the liquid which are stabilised against dissolution because the surface is coated with contaminants such as a skin of organic impurity. A second mechanism relies on the existence of solid particles (motes) in the liquid with gas trapped in these particles, where nucleation takes place.

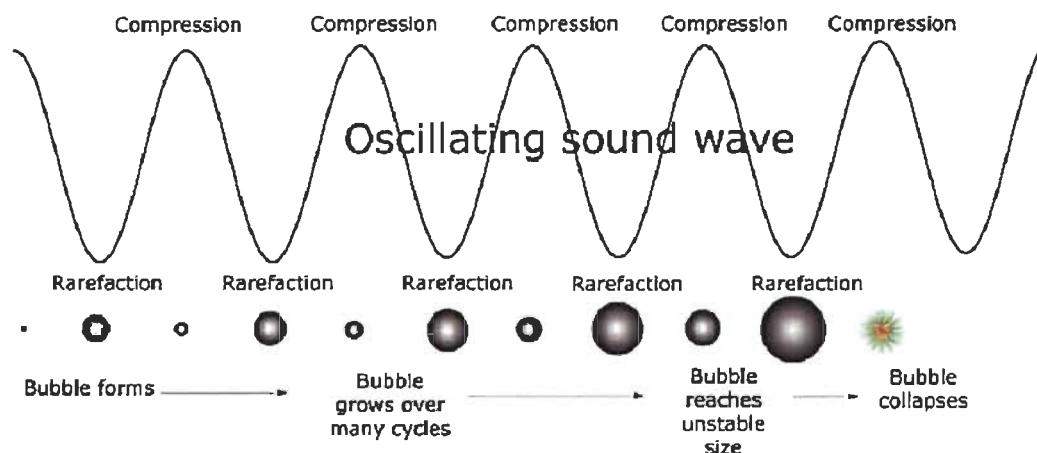


**Figure 3.8** Formation and growth of cavitation bubbles with wave cycle

As can be seen in Figure 3.9, a bubble formed in one of these ways may then grow until it reaches a critical size known as its resonance size.

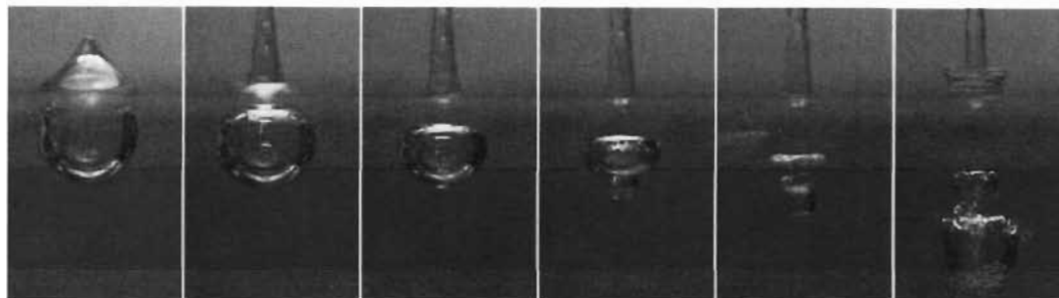
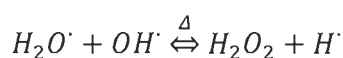
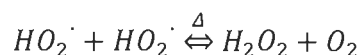
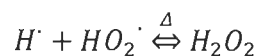
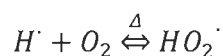
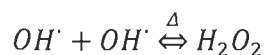
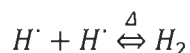
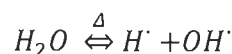


**Figure 3.9** Bubble collapse and microjet formation

The resonance size of a bubble depends on the applied frequency of the sound field. When bubbles reach their resonance size due to growth by processes called rectified diffusion or coalescence, two possible events may occur. The bubble may become unstable and collapse, often violently, within a single acoustic cycle or over a small number of cycles. This is termed transient cavitation. The other possibility is that the bubble oscillates for many cycles at, or near, the linear resonance size. This is termed stable cavitation. The terms transient and stable cavitation are also used to define whether or not the bubbles are active in light emission (sonoluminescence) or chemical reactions [140].

The event of a collapsing bubble is a microscopic implosion that generates high local turbulence and the release of heat energy. The consequence is a significant increase of temperature and pressure of up to several thousand degrees Kelvin and several hundred Bar. These causes different mechanical and sonochemical effects depending on the nature of the cavitation bubble. These physical phenomena are the same as those reported in hydrodynamic cavitation which results in damage of mechanical items such as pumps and propellers.

Low frequency ultrasound normally produces mechanical change on the material surface while high frequency results in various sonochemical reactions. The extreme temperature conditions generated by a collapsing bubble will lead to the formation of radical chemical species, depending on the liquid medium [141]. Ultrasonic waves in water have been shown to form radicals by the following series of reactions due to homolytic cleavage:



The hydroxy and hydroxyl radical formed in this reaction are highly reactive and rapidly interact with other radical or chemical species in solution.  $H\cdot$  atoms are highly reducing in nature and  $OH\cdot$  radicals are highly oxidizing. A common product of this reaction in water is hydrogen peroxide.

### ***3.2.2.1 Influence of frequency and power on cavitation***

The size of cavitation bubbles produced in an ultrasonic bath depends primarily on the ultrasonic frequency. The number of cavitation bubbles depends on both the ultrasonic frequency and the ultrasonic power [142].

Higher ultrasonic frequencies produce smaller cavitation bubbles than lower frequencies. At lower frequencies, cavitation bubbles have more time to grow due to the increased wavelength and, therefore, become larger before they implode. The energy required to produce a cavitation bubble, and, in turn, the energy released as it implodes are directly related to its size. Larger cavitation bubbles require more energy to produce and, in turn, release a larger amount of energy when they implode which cause mechanical effect. Increasing the ultrasonic frequency while maintaining the same ultrasonic power will result

in a larger number of smaller cavitation bubbles, which are normally less impact bubbles and causes sonochemical effects.

Increasing the ultrasonic power in ultrasonic bath results in a larger number of cavitation bubbles being produced. Since the size of the cavitation bubbles is dictated primarily by the ultrasonic frequency, an increase in the number of bubbles is the only way that the energy balance can be resolved. The cavitation bubbles are created as defects in the structure of the liquid act as “weak spots” for the growth of cavitation bubbles. At lower energy, only the most favourable sites grow into cavitation bubbles. As power is increased, there is sufficient to cause less favourable sites to grow into cavitation bubbles and the overall number of bubbles increases.

### **3.2.3 Power ultrasound on biomass applications**

The combined primary sonochemical reactions in the gas phase, secondary sonochemical reactions in the liquid phase, and the physical impact of bubble collapse have generated many novel technological concepts in the last three decades. The idea of cavitation has been utilized to provide a unique physicochemical environment for processing biomass. As an example, the conversion of lignocellulosic biomass for biofuels and biorefinery applications is limited due to the cost of pre-treatment used to separate or access the main usable components of biomass (i.e. cellulose, hemicellulose, and lignin). Ultrasound pre-treatment has been efficiently utilized for this purpose and revealed that ultrasound has the potential to enhance the separation and hydrolysis of lignocellulosic materials for the use in biofuel production and biorefineries whether the enhancement be from physical or chemical mechanisms [143]. Ultrasound provides physical augmentation via shear forces, mass transfer, and surface erosion as well as chemical effects of producing oxidizing radicals.

One of the most common uses of ultrasonic pre-treatment is high-efficiency extraction of biomass. As an example, He and co-workers [144] investigated the influence of ultrasonic pre-treatments on eucalyptus wood. They proved that the ultrasound could modify the physiochemical structure of the wood. Ultrasound pre-treatment increased the samples' crystallinity up to 35.5%, and could successfully remove the cellulose, hemicellulose, and lignin from the samples. Also, the pre-treatment has increased the exposure of the sample to

the treatment solutions, broke down sample pits, and generated collapses and microchannels on sample pits, and removed attachments in the samples. A report from Qui et al. [145] has demonstrated that, ultrasound pre-treatments on hardwood could increase its dimensional stability by chemical modification and it is an effective way to reduce water adsorption rate in wood. Wang et al. [146] has also proved the effect of ultrasound-assisted pre-treatments using borax and sodium hydroxide on the physicochemical properties of Chinese fir. The thermal degradation processes, changes in chemical structures, and crystallinity of the treated samples were studied, and it was noticed that the ultrasound pre-treatments positively influenced the physicochemical properties of wood and its crystallinity. Later, they have also shown that ultrasound-treated eucalyptus showed higher activation energy at the primary portion of thermal degradation during pyrolysis and the physicochemical properties were modified [147].

Ultrasound assisted TEMPO oxidation is also an interesting power ultrasound application. Literatures prove the significance of TEMPO - Sodium bromide - Sodium hypochlorite oxidation system, used in nanocellulose production, and can be further optimized with the use of low frequency ultrasound. The efficiency of cellulose oxidation mediated by the 4-acetamido-TEMPO radical under ultrasonic cavitation was investigated using two ultrasonic systems by Loranger et al. [148]. A batch lab scale ultrasonic bath equipped with a glass reactor and a semi-continuous flow-through sonoreactor were used to comparative studies. The possibility of scaling up the production of some oxidized cellulose under ultrasound from a lab scale process to a pilot plant process was explored. It was found that under acoustic cavitation, the efficiency of TEMPO-mediation oxidation of native cellulose was significantly improved, particularly in the flow-through sonoreactor [149]. The impact of transducers configuration in a pilot sonoreactor used for nanocellulose production and sonoreactors for kraft lignin fractionation were also studied in order to evaluate the efficiency of power ultrasound systems to potentially use in industrial-grade biomass processing [150].

Cherpozat et al. have demonstrated the effect of ultrasonic pre-treatments on the pyrolysis product yield [48]. This work was recognized as a great progress in ultrasonic enhanced lab-scale pyrolysis. The effect of ultrasound frequency, power, exposure time and bath temperature on wood treatment were examined to understand the effect on bio-oil yield.

Authors have reported that a combination of 0.5 h at 170 kHz and 1.5 h at 40 kHz was the most effective, enabling an increase of almost 12% of bio-oil yield compared to untreated wood. However, the limitation of this technique was associated to their scale-up using pilot unit. The powerfulness of the pilot scale unit, especially at high frequencies, seemed too strong for the goal aiming the enhancement of the pyrolytic bio-oil yield [151]. The post treatment effect power ultrasound on bio-oil yield was investigated by Pichon et al. [49]. To protect the ultrasonic bath and minimize the amount of raw material, bio-oils were placed in a sealed plastic bag before their treatment. It was interesting to note that the presence of the plastic bag has influenced the ultrasound diffusion. Moreover, ultrasonic post-treatment has modified the composition, calorimetry, and time stability of bio-oils.

### **3.2.4 Power ultrasound on biochar**

Application of ultrasound to improve the physical activation process is a recently developed area with studies that showed the influence of ultrasonication in the activation process of biochar. As discussed previously, ultrasonication made possible the use of the effect of cavitation and the bubbles that collapses near the solid surfaces, disrupts the spherical shape and induces the formation of microjets which can impact the biochar surfaces. For this reason, ultrasound was used to explore hard-to-reach surfaces. Results of this physical process include mixing, erosion, and particle collisions. Activation using ultrasonication is thus a cleaner method which improves the surface morphology of the material by improving the accessibility of adsorption sites.

There are only a few studies available in literature which discusses the effect of ultrasonication on biochar properties. Chatterjee et al. [152] conducted a study on ultrasound cavitation by intensifying the amine functionalization for enhancing the CO<sub>2</sub> capture capacity of softwood biochar. They have shown that low-frequency ultrasound irradiation exfoliated and broke apart the irregular graphitic layers of biochar and creates new/opens the blocked micropores. This further enhanced the porosity and permeability of biochar and influenced the amine functionalization. As a result, the CO<sub>2</sub> uptake capacity of the biochar was significantly increased. Later in 2019, they have confirmed the low frequency ultrasound effect of dual amination of biochar and mentioned that the sonochemical technique is an

energy efficient technique since it is done at near room temperature [153]. In another study by Sajjadi et al. [154], it was seen that the ultrasound assisted urea functionalization on softwood biochar has significantly improved the Ni (II) adsorption capacity. Biochar samples were physically modified by low-frequency ultrasound waves and were chemically treated by phosphoric acid ( $H_3PO_4$ ) and then functionalized by urea ( $CO(NH_2)_2$ ). Cavitation induced by ultrasound exfoliates and breaks apart the regular shape of graphitic oxide layers of biochar, cleans smooth surfaces, and increases the porosity and permeability of the carbonaceous structure of biochars. These modified biochars exhibited more than 99 percent efficiency in removal of heavy metal from water. Very recently Sajjadi et al. [155] have also developed a double layer magnetized/functionalized biochar composite through a hybrid post-pyrolysis magnetization for enhanced adsorption capacity of microporous carbonaceous biochar. The developed process included i) structural modification of biochar under ultrasound waves, ii) magnetization with magnetite ( $Fe_3O_4$ ) nanoparticles, and iii) functionalization with 3-aminopropyltriethoxysilane. The adsorption results demonstrated that while raw biochar could remove only 13% and 68% of Ni(II) and Pb(II), with some signs of leaching, the biochar activated under 60 s of ultrasound irradiation, magnetized with  $Fe_3O_4$  in the ratio of 2:1, and functionalized with the lowest concentration of TES exhibited 32% and 90% of Ni and Pb removal, without any leaching. The highest adsorption capacity was associated with the maximum ultrasound activation of 60 s, which suggests the impact of porosity and surface area on the subsequent functionalization and the removal of metal ions. Similarly, Wang and co-workers [156] investigated on ultrasound assisted alkali activation of biochar derived from *Cinnamomum camphora* and found that the two-step activation results in more surface groups, larger surface area and a pore volume contributing to a larger sorption capacity towards Pb (II). Recently, a study by Hazrati et al. [157] shown that ultrasound pre-treatment having low-time, low-frequency, and chemical functionalization using citric acid could enhance the physicochemical properties of sewage sludge-derived biochar. Enhanced ammonium removal was obtained by biochar from forestry waste using ultrasonic activation [158]. The results showed that the ultrasonic activation significantly enhanced the  $NH_4^+$  adsorption efficiency of biochar by approximately 5 times than non-activated. The material exhibited the best performance at 500 °C with an ultrasonic activation time of 480 min, frequency of 45 kHz, and power of

700 W. The ultrasonic activation reduced the biochar ash and induced pore formation, which increased the specific surface area through cavitation corrosion and micro-acoustic flow mechanism.

### **3.2.5 Other applications of power ultrasound**

Lim et al. [159] have evaluated the feasibility of regeneration of granular activated carbon (GAC) using ultrasound techniques. The desorption of trichloroethylene (TCE) from GAC by ultrasound was investigated at 20 kHz. They observed that the TCE can be desorbed from activated carbon in the presence of ultrasound at 20 kHz. However, desorption of TCE by ultrasound occurred only at a nearby surface layer of GAC. The effect of ultrasound on adsorption and desorption process was studied by Breitbach and co-workers [160]. They observed that the ultrasonic power input clearly indicated that adsorbent particles absorbed the ultrasonic energy very effectively if they were in resonance with the ultrasonic field. The ultrasonic energy is dissipated into heat. Hence, desorption processes are promoted because at elevated temperatures the equilibrium loading is lower and mass-transfer processes are quicker. The ultrasonic power has a major effect on the efficiency of the desorption process. Effects of frequency and power of ultrasound on the size reduction of liposome was investigated by Yamaguchi et al. [161]. Their results indicated that the small number of cavitation events with stronger physical disturbance on liposome could reduce the size of the liposome more efficiently than the large number of cavitation events with weaker disturbance.

These studies encouraged us to deepen our investigation on influence of ultrasound treatments on biochar characteristics and the adsorption properties. These findings also motivate us to optimize the parameters such as frequency, power, time and treatment temperature. Though the power ultrasound provides a wide range of applications with improved material efficiency, some drawbacks arise from this technique. A few main constraints of using power ultrasound for large-scale applications are high energy consumption, need of liquid medium to diffuse ultrasounds waves, cavitation effects, practical difficulties for scaling-up reactions (mainly in probes and bath ultrasound techniques). The total destruction of material surface under mechanical effect (at low

frequency range) can also be a disadvantage for applications of molecular level modifications [162,163].

### 3.3 Theory of Adsorption

In 1881, a German physicist named Heinrich Kayser coined the word *Adsorption*, defined as the adhesion of atoms, ions, or molecules from a gas, liquid, or dissolved solid (adsorbate) to a nearby surfaces or pores of a solid (adsorbent). Adsorption is a surface phenomenon which unlike absorption that is related to the permeability or dissolution of a fluid (i.e. adsorbate) by a liquid or solid (i.e. adsorbent). In principle adsorption can occur at any solid fluid interface, such as a gas-solid interface and a liquid-solid interface (Figure 3.10) [164].

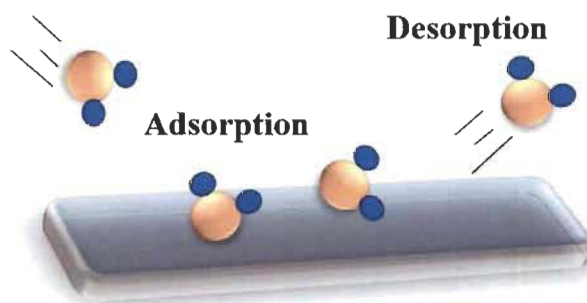


**Figure 3.10** Representation of adsorption and desorption on to a surface

#### 3.3.1 Factors affecting adsorption

There are some important factors that affects adsorption of adsorbates onto a solid surface. These parameters are described below.

- (a) Surface area and porosity: the adsorption capacity of a material increases if it has larger surface area. Likewise, if a greater number of pores are available, the intake of adsorbate into these pores will also increase.
- (b) Particle size of adsorbent: smaller the particle size is, higher will be adsorption rate. The specific surface area of the material will increase, and more sites will be available for the adsorption.

- (c) Contact time: The adsorbent-adsorbate contact time is an important factor affecting adsorption rate. As the contact time increases, the adsorption becomes more complete. This parameter also gives an idea the required time of a particular adsorbent to reach its maximum capacity or saturation.
- (d) Adsorbent-adsorbate affinity: if the adsorbent is polar, non-polar adsorbates are more easily adsorbed on the surface and vice-versa.
- (e) pH: the effect of pH is depending on the surface charge of both adsorbent and adsorbate. At different pH, with the number of protons available on the medium, the competition of charged adsorbates to access the adsorption sites will be varied. As an example, at low pH, the functional groups present on the adsorbent surface will be protonated and positively charged. This will favour the adsorption of negative ions. If the solution pH is less than the point of zero charge (PZC) (which is defined as the pH at which the surface of adsorbent is neutral), the adsorbent surface will be positively charged. Thus, the degree of ionisation of the charged particles varies with a change in pH and affects the rate of adsorption.
- (f) Initial concentration of adsorbate: to understand the effect of initial adsorbate concentration on adsorption behaviour, different theoretical models are implemented on experimental data. They are called adsorption isotherms, and they provide significant information about how the change in initial concentration influence the adsorption behaviour of the material.
- (g) Amount of adsorbent: higher the amount of adsorbent is, higher will be the amount of adsorbate. However, while the efficiency of adsorption increases with mass of adsorbent, the adsorption capacity of the sample decreases. This is related with the total number of active sites available for adsorption.
- (h) Temperature: temperature is an important parameter while defining adsorption capacity of a material. Depending on the mechanism of adsorption happening in the system, temperature improves or reduces the efficiency of adsorption. The change in adsorption capacity with temperature can explain the thermodynamic state of the

system like heat of enthalpy, degree of freedom or entropy. The Gibb's free energy equation can be used to determine if the adsorption is spontaneous or non-spontaneous.

We will be discussing more about some of these important factors in coming sections.

### 3.3.2 Modes of adsorption and mechanism

#### 3.3.2.1 Physisorption and Chemisorption

The adsorption of a molecule to a solid surface occurs mainly through two modes, called *Physisorption* and *Chemisorption* [165]. In physisorption, the target molecules are attracted to the surface of pore walls within a high surface-area sorbent by van der Waals forces (Figure 3.11). The energy of interaction between the adsorbate and adsorbent has the same order of magnitude but is usually greater than the energy of condensation of the adsorptive. Therefore, no activation energy is needed. In this case, low temperature is favourable for the adsorption with exothermic reactions. Physical adsorption is relatively non-specific due to the operation of weak forces of attraction between molecules. The adsorbed molecule is not affixed to a particular site on the solid surface; therefore, it is free to move over the surface creating a multilayer adsorption behaviour. Physical adsorption is generally reversible in nature and has low enthalpy of adsorption (i.e.  $\Delta H_{\text{ads}}$  is  $\sim 20\text{-}40$  kJ/mol).

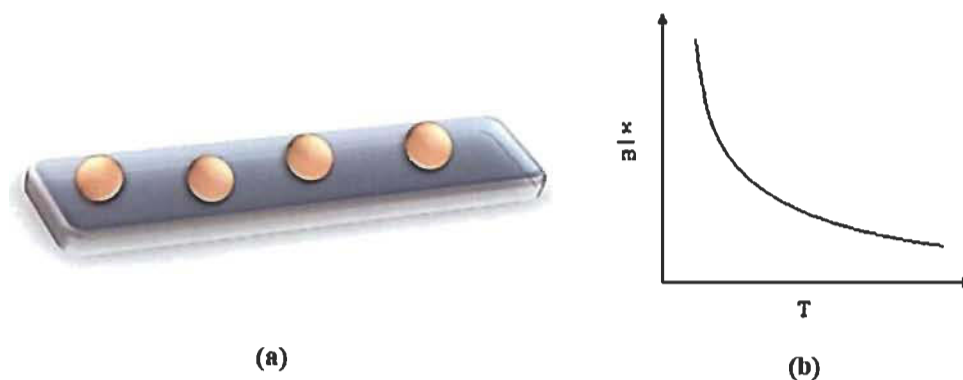


**Figure 3.11** (a) Representation of physisorption, and (b) rate of adsorption with increase in temperature ( $x$  is the amount of adsorbate,  $m$  is the amount of adsorbent and  $T$  is the temperature)

Chemisorption is a chemical adsorption in which the adsorption caused by the formation of chemical bonds between the surface of the adsorbent and adsorbate (Figure 3.12). Therefore, the energy of chemisorption is considered like chemical reactions. The strong chemical bonds involved in the mechanism makes them irreversible. It may be exothermic or endothermic processes ranging from very small to very large energy magnitudes. The elementary step in chemisorption often involves large activation energy with high magnitude of  $\Delta H_{\text{ads}}$  ( $\sim 40 - 200 \text{ kJ mol}^{-1}$ ). The temperature influences the kinetics of the chemisorption by accelerating the amount adsorbed. As the temperature increases, the rate of adsorption also increases till it reaches the activation energy level, and then decreases with further increase in temperature. Chemisorption occurs only in the adsorption sites present on the surface of the adsorbent, resulting in monolayer adsorption.

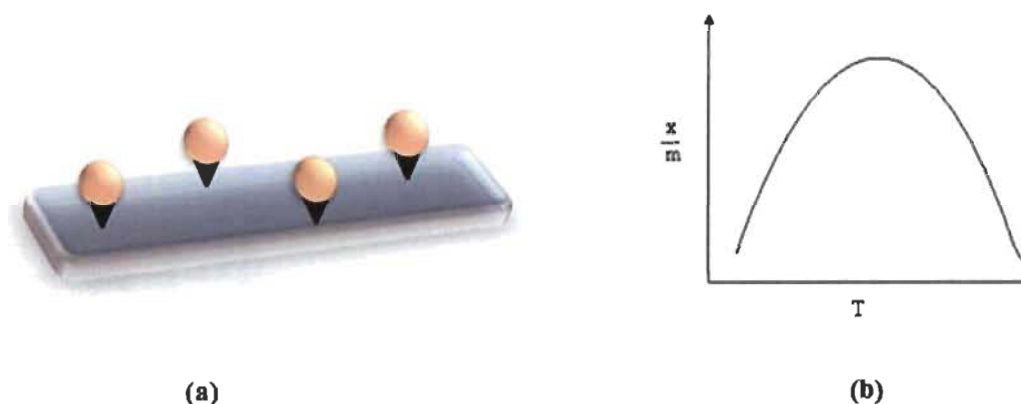


**Figure 3.12** (a) Representation of chemisorption, and (b) amount of adsorption with increase in temperature ( $x$  is the amount of adsorbate,  $m$  is the amount of adsorbent and  $T$  is the temperature)

### 3.3.2.2 Kinetic models

The evolution of the amount adsorbed with time is known as adsorption kinetics. The adsorption reactions generally proceed through the following steps: (i) transfer of adsorbate from bulk solution to adsorbent surface, also referred as diffusion, (ii) migration of adsorbate into pores, and (iii) interaction of adsorbates with available sites on the surface. The intensity of each of these steps define the rate limiting factor of the overall adsorption process [166]. Normally, the driving force for the adsorption process is the concentration

difference between the adsorbate in the solution at any time and the adsorbate in the solution at equilibrium ( $C_{\text{initial}} - C_{\text{equilibrium}}$ ).

At any given conditions the amount of adsorbate adsorbed on a material is known as the adsorption capacity ( $Q$ ) of the material and it is described by the following equation,

$$Q = \frac{(C_{\text{initial}} - C_{\text{final}}) * V}{m} \quad \text{Equation 3.1}$$

Where  $Q$  is the adsorption capacity (mg/g),  $C_{\text{initial}}$  is the initial concentration of adsorbate (mg/L),  $C_{\text{final}}$  is the final concentration of adsorbate (mg/L),  $V$  is the volume of solution (L) and  $m$  is the mass of adsorbent (g).

To determine which step controls the adsorption rate, different kinetic models are evaluated. The four most popular kinetic models are the pseudo-first-order kinetic model, the pseudo-second-order kinetic model, the intra-particle diffusion model, and the Elovich model are discussed here. These kinetic models provide valuable information about the adsorption process involving adsorbent surface, chemical reaction, and/or diffusion mechanisms.

#### a) Pseudo First Order

The pseudo first order kinetics was proposed at the end of the 19th century by Lagergren [167]. It is a simple rate equation that describes the process of adsorption as Physisorption. It is represented by the following equation,

$$Q_t = Q_e(1 - e^{-k_t t}) \quad \text{Equation 3.2}$$

Where  $Q_t$  (mg g<sup>-1</sup>) is adsorption capacity at time  $t$ ,  $Q_e$  is adsorption capacity at equilibrium and  $k$  is rate constant (min<sup>-1</sup>).

#### b) Pseudo Second Order

The pseudo second order kinetics were introduced in the middle of 80's however it was not really popular until in 1999. Ho and McKay significant contributions and findings related to pseudo second order reactions [168]. According to them, reactions involving pseudo-second-

order processes are greatly influenced by the adsorbate amount on the adsorbent's surface and adsorbate amount adsorbed at equilibrium [169]. This means that the reaction rate is directly proportional to the number of active sites on the adsorbent's surface. This indicates that the rate limiting mechanism involved in this phenomenon is Chemisorption.

The pseudo second order kinetic equation is represented as follow:

$$Q_t = \frac{k_2 Q_e^2 t}{1 + k_2 Q_e t} \quad \text{Equation 3.3}$$

Where  $Q_t$  ( $\text{mg g}^{-1}$ ) is adsorption capacity at time  $t$ ,  $Q_e$  is adsorption capacity at equilibrium and  $k$  is rate constant ( $\text{g mg}^{-1} \text{min}^{-1}$ ).

### c) Intraparticle Diffusion

The theoretical relationship common to most treatments of intraparticle diffusion during the retention process uptake varies almost proportionately with the half-power of time,  $t^{0.5}$ , rather than  $t$ . A nearly linear variation in the quantity sorbed with  $t^{0.5}$  is predicted for a large initial fraction of reactions controlled by rates of intraparticle diffusion. Good linearization of data is observed for the initial phase of the reaction in accordance with the expected behaviour if intraparticle diffusion is the rate-limiting step. According to Weber and Morris, if the rate-limiting step is the intraparticle diffusion, a plot of solute sorbed against the square root of the contact time should yield a straight line passing through the origin [170]. The equation is represented by,

$$Q_t = kt^{1/2} + C \quad \text{Equation 3.4}$$

Where:

$C$  is the constant related to diffusion resistance ( $\text{mg g}^{-1}$ ),  $k$  is Intraparticle diffusion coefficient ( $\text{mg g}^{-1} \text{min}^{-1/2}$ ). The constant  $C$  gives an idea of the thickness of the boundary layer. As the value of  $C$  increases, the effect of boundary layer will also increase.

d) Elovich

The Elovich equation is one of the most widely used equations to describe the kinetics of heterogeneous chemisorption of gases on solid surfaces [171] and therefore it is not a better model to explain adsorption of ions in liquid phase. This equation assumes a heterogeneous distribution of adsorption energies which increases linearly with surface coverage.

$$Q_t = \frac{1}{\beta} \ln(\alpha\beta) + \frac{1}{\beta} \ln t \quad \text{Equation 3.5}$$

$\alpha$  is the initial adsorption rate ( $\text{mg g}^{-1} \text{min}^{-1}$ ),  $\beta$  ( $\text{g mg}^{-1}$ ) is a constant related to surface coverage and activation energy and  $t$  (min) is the contact time.

### 3.3.3 Adsorption isotherms

The determination of equilibrium state is crucial to understand the adsorption processes. This can be achieved by an adsorption isotherm which is a curve relating the equilibrium concentration of a solute on the surface of an adsorbent  $Q_e$  to the concentration of the solute in the liquid  $C_e$  with which it is in contact. The experimental data can be fitted to one or more equilibrium isotherm models to understand the parameter dependence. Till date, there is no isotherm equation describing properly all experimental isotherm curves. In contrast, many isotherm equations have been obtained from theoretical or empirical models.

#### 3.3.3.1 Langmuir isotherm

Irving Langmuir, 1932 Nobel prize winner, proposed an isotherm as one of the simplest theoretical models [172]. Langmuir adsorption considers adsorption and desorption as totally reversible process with few more assumptions as mentioned below:

- (i) Adsorption occurs at specific binding sites that are localized on the surface of the adsorbent.
- (ii) All adsorption sites on the surface of the adsorbent are identical.
- (iii) The surface of the adsorbent is covered with a monolayer of adsorbed molecules.

(iv) There is no interaction between the adsorbed molecules on the adsorbent surface.

The Langmuir equation is explained as:

$$Q_e = \frac{(Q_{\max} * b * C_e)}{(1 + b * C_e)} \quad \text{Equation 3.6}$$

In Equation 3.6 above,  $C_e$  ( $\text{mg L}^{-1}$ ) and  $Q_e$  ( $\text{mg g}^{-1}$ ) are the concentration of the molecules at equilibrium and the amount of adsorbed molecules on the surface of the adsorbent at any time, respectively.  $Q_{\max}$  shows the maximum adsorption capacity ( $\text{mg g}^{-1}$ ) and  $b$  represents the Langmuir constant ( $\text{L mg}^{-1}$ ).

The Langmuir model represents one of the first theoretical treatments of non-linear sorption and suggests that uptake occurs on a homogenous surface by monolayer sorption without interaction between adsorbed molecules. The Langmuir isotherm assumes that all adsorption sites on the adsorbent surfaces are occupied by the adsorbate in the solution. Therefore, the Langmuir constant ( $b$ ) represents the degree of adsorption affinity of the adsorbate. The maximum adsorption capacity ( $Q_{\max}$ ) associated with complete monolayer cover is typically expressed in ( $\text{mg/g}$ ). High value of  $b$  indicates for much stronger affinity of adsorbate towards adsorbent.

The shape of the isotherm is a gradual positive curve that flattens to a constant value. The effect of isotherm shape is discussed from the direction of predicting whether and adsorption system is "favorable" or "unfavorable". In 1966, Hall et al. [173] proposed a dimensionless separation factor or equilibrium parameter,  $R_L$ , as an essential feature of the Langmuir isotherm to predict if an adsorption system is "favourable" or "unfavourable", which is defined as

$$R_L = \frac{1}{(1 + bC_i)} \quad \text{Equation 3.7}$$

Where,

$C_i$  = initial adsorbate concentration (For a single adsorption system,  $C_i$  is usually the highest initial concentration)

$b$  = Langmuir constant ( $\text{ml mg}^{-1}$ )

Value of  $R_L$  indicates the shape of the isotherm accordingly,

$0 < R_L < 1$ : Favourable

$R_L > 1$ : Unfavourable

$R_L = 1$ : Linear

$R_L = 0$ : Irreversible

The Langmuir adsorption model deviates significantly in many cases, primarily because it fails to account for the surface roughness of the adsorbent. Rough heterogeneous surfaces have multiple site-types available for adsorption, with some parameters varying from site to site, such as the heat of adsorption. The model also ignores adsorbate/adsorbate interactions.

### 3.3.3.2 *Freundlich isotherm*

The Freundlich isotherm is commonly used to describe the adsorption characteristics for the heterogeneous surface [174]. It represents an initial surface adsorption followed by a condensation effect resulting from a strong adsorbate-adsorbate interaction. The heat of adsorption, in many instances, decreases in magnitude with increasing extent of adsorption. This decline in heat is logarithmic implying that the adsorption sites are distributed exponentially with respect to adsorption energy. This isotherm does not indicate an adsorption limit when coverage is sufficient to fill a monolayer.

The Freundlich isotherm is represented by the equation:

$$Q_e = K_f C_e^{1/n} \quad \text{Equation 3.8}$$

$K_f$  = Freundlich constant related to maximum adsorption capacity ( $\text{mg g}^{-1}$ ). It is a temperature-dependent constant.

$n$  = Freundlich constant related to surface heterogeneity (dimensionless). It gives an indication of how favourable the adsorption processes are.

With  $n = 1$ , the equation reduces to the linear form:  $Q_e = k \times C_e$

A value of  $n$  higher than 1 indicates a favourable adsorption of the molecules onto the adsorbent surface.

Unlike the Langmuir model, the Freundlich equation does not approach linearity at low  $C$ , nor does it approach a limiting (fixed) adsorption capacity as  $C$  reaches saturation. These features are opposed to the general adsorption characteristics. Basically, the Freundlich equation with its adjustable parameters offers a simple mathematical tool rather than a physical model to account for the energetic heterogeneity of adsorption at different regions of the isotherm.

### 3.3.3.3 Dubinin-Radushkevich (DR) isotherm

The adsorption of molecules into the micropores of the adsorbents is described by the Dubinin-Radushkevich adsorption model [175]. According to this model, molecular adsorption occurs in micropores (pore filling) instead of adsorption on the surface of the adsorbents that leads to monolayer or multilayer formation. The Dubinin-Radushkevich adsorption model is commonly applied to the adsorption processes of the subcritical vapors in pores of the adsorbents such as zeolites and activated carbons. It is represented by the equation:

$$\ln Q_e = \ln Q_m - \beta * \varepsilon^2 \quad \text{Equation 3.9}$$

where  $Q_e$  is the amount of adsorbed molecules per gram of adsorbent ( $\text{mg g}^{-1}$ ),  $Q_m$  represents the adsorption capacity ( $\text{mg g}^{-1}$ ) and  $\varepsilon$  demonstrates the Polanyi potential as given in the following formula:

$$\varepsilon = RT * \ln\left(1 + \frac{1}{C_e}\right) \quad \text{Equation 3.10}$$

where  $R$  is the ideal gas constant ( $\text{J mol}^{-1} \text{K}^{-1}$ ),  $T$  is the temperature (K), and  $C_e$  is the concentration of the molecules at equilibrium ( $\text{mg L}^{-1}$ )

$\beta$  is the activity coefficient ( $\text{mol}^2 \text{J}^{-2}$ ), which represents the adsorption energy ( $\text{kJ mol}^{-1}$ )

$$E = \frac{1}{\sqrt{2\beta}} \quad \text{Equation 3.11}$$

### 3.3.3.4 Redlich-Peterson isotherm

The Redlich-Peterson isotherm is a combined model that exhibits the features of both Langmuir and Freundlich isotherm models [176]. It is used to describe the adsorption process to the homogenous and heterogeneous surfaces of adsorbents over a wide range of adsorbate concentrations. This isotherm model shows the features of the Freundlich isotherm model at higher adsorbate concentrations while it obeys the Henry's law at lower adsorbate concentrations.

$$Q_e = \frac{K_{RP} * C_e}{(1 + \alpha_{RP} * C_e^\beta)} \quad \text{Equation 3.12}$$

where  $K_{RP}$ ,  $\alpha_{RP}$  and  $\beta_{RP}$  are Redlich-Peterson constants. The exponent  $\beta$  lies between 0 and 1. When the  $\beta$  value is close to unity, it means that the adsorption is closer towards Langmuir model.

There are few other isotherm models available on literature namely Temkin isotherm (adsorption heat effect) [177], Harkins-Jura and Halsey isotherms (multilayer adsorption processes to the adsorbent surfaces having heterogeneous pore distribution) [178], and Brunauer-Emmett-Teller isotherm (adsorption processes in the gas-solid systems) [179]. However, these models are less used to explain adsorption of metal ions on material surfaces, mainly because of the mechanism followed [180]. Most of the literatures reported Langmuir or Freundlich isotherms as the best fit models to explain heavy metal adsorption on biochars [30,115]. Therefore, in our adsorption results only these two models were evaluated.

### 3.3.4 Thermodynamics of adsorption

In order to fully understand the nature of adsorption, the thermodynamic parameters such as change in Gibb's free energy ( $\Delta G^0$ ), enthalpy change ( $\Delta H^0$ ) and entropy change ( $\Delta S^0$ ) should be calculated. It is possible to estimate these thermodynamic parameters for an adsorption

reaction by considering the equilibrium constants under the several experimental conditions [166]. They can be calculated using the following equations.

$$K_e = \frac{Q_e}{C_e} \quad \text{Equation 3.13}$$

$$\Delta G^0 = -RT \ln K_e \quad \text{Equation 3.14}$$

$$\Delta G^0 = \Delta H^0 - T\Delta S^0 \quad \text{Equation 3.15}$$

$$\ln K_e = \frac{\Delta S^0}{R} - \frac{\Delta H^0}{RT} \quad \text{Equation 3.16}$$

Where  $Q_e$  is the amount of metal adsorbed per unit weight of biochar at equilibrium ( $\text{mg g}^{-1}$ ),  $C_e$  is the equilibrium concentration of solution ( $\text{mg L}^{-1}$ ),  $R$  is gas constant  $8.314$ ,  $T$  (K) absolute temperature and  $K_e$  ( $\text{L g}^{-1}$ ) the equilibrium adsorption constant.

The values of enthalpy  $\Delta H^0$  and entropy  $\Delta S^0$  can be determined from the slope and intercept of the plot  $\ln K_e$  vs  $1/T$ . Gibb's free energy  $\Delta G^0$  can be obtained using Equation (3.15) with the values of  $\Delta H^0$  and  $\Delta S^0$ . In general, these parameters indicate whether the adsorption process is spontaneous and whether it is exothermic or endothermic. For a positive standard enthalpy change ( $\Delta H^0$ ) the adsorption is endothermic, which means it requires additional energy to complete the process. If the  $\Delta H^0$  is negative it implies the reaction is exothermic, which liberates heat while reaction. The positive value of entropy change ( $\Delta S^0$ ) indicates an increase in the degree of freedom (or disorder) of the adsorbed species. All chemical reactions tend naturally towards minimal state of Gibb's free energy. The negative value of  $\Delta G^0$  indicates a spontaneous reaction, on the other hand if it is positive it is non-spontaneous. When  $\Delta G^0 = 0$  the reaction is said to be at equilibrium.

## Chapter 4 – Scientific Article 1: Synthesis and Characterisation of Ultrasound Pre-treated Softwood Biochar

### 4.1 Preface

This part of work was presented during a poster session in 2019 at the International Ultrasonic Symposium held at Glasgow, UK (October 2019). It was published in the conference proceedings of IUS-2109 (available online on IEEE-Xplore, (DOI: [10.1109/ULTSYM.2019.8925793](https://doi.org/10.1109/ULTSYM.2019.8925793)) The article entitled *Enhancing Surface Properties of Softwood Biochar by Ultrasound Assisted Slow Pyrolysis* mainly deals with the biochar production, the chemical and physical characterisation and effect of ultrasound pre-treatments in surface morphology with proving its application for heavy metal adsorption using copper as model metal.

#### Author Details:

Aneeshma Peter, Int. BS-MS

Ph.D. Student, Sciences de l'énergie et des matériaux

I2E3 – Institut d'Innovations en Écomatériaux, Écoproduits et Écoénergies, à base de biomasse, Université du Québec à Trois-Rivières, P.O. Box 500, Trois-Rivières, Québec, Canada, G9A 5H7

Email: [Aneeshma.Peter@uqtr.ca](mailto:Aneeshma.Peter@uqtr.ca)

Eric Loranger, Ph.D.

Research director and corresponding author

I2E3 – Institut d'Innovations en Écomatériaux, Écoproduits et Écoénergies à base de biomasse, Université du Québec à Trois-Rivières, P.O. Box 500, Trois-Rivières, Québec, Canada, G9A 5H7

Email: [Eric.loranger1@uqtr.ca](mailto:Eric.loranger1@uqtr.ca)

Bruno Chabot, PhD.

Co-director and co-author

I2E3 – Institut d’Innovations en Écomatériaux, Écoproduits et Écoénergies à base de biomasse, Université du Québec à Trois-Rivières, P.O. Box 500, Trois-Rivières, Québec, Canada, G9A 5H7

Email: [Bruno.Chabot@uqtr.ca](mailto:Bruno.Chabot@uqtr.ca)

#### **Author Credits:**

**Aneeshma Peter:** Methodology, Validation, Investigation, Data curation, Formal analysis, Writing - original draft, Visualization

**Bruno Chabot:** Conceptualization, Project administration, Writing - review & editing

**Eric Loranger:** Conceptualization, Project administration, Supervision, Writing - review & editing, Funding acquisition

## **4.2 Résumé**

Au cours des dernières décennies, le biochar a été largement utilisé dans la chimie de l'adsorption et dans des principaux secteurs industriels (ex. les biocarburants, les pâtes et papiers, les bioraffineries, etc.) en raison de ses propriétés exceptionnelles dues à sa fonctionnalisation de surface, sa disponibilité et une capacité de traitement à faible coût. Des études sur le biochar dérivé de bois résineux ont révélé des propriétés physicochimiques efficaces. Ces propriétés dépendaient de différents paramètres tels que l'origine de la biomasse, les différentes méthodes de traitement, les conditions de pyrolyse, etc. L'application des ultrasons dans les matériaux lignocellulosiques est un domaine de recherche en développement avec très peu d'études examinant l'effet des ultrasons pour des applications de traitement sur de la biomasse. La formation de microjets lors de l'implosion de bulles de cavitation perturbe la surface solide qui subit le contact et fournit un environnement physicochimique unique aux matériaux. La littérature a prouvé l'influence des ultrasons sur la stabilité dimensionnelle du bois, la structure physicochimique et le

rendement des produits de pyrolyse. Une étude récente a démontré l'effet positif des prétraitements par ultrasons sur le rendement en produits de pyrolyse. Dans la présente étude, nous introduisons l'ultrasonication comme un outil pour améliorer les propriétés physiques du biochar résineux et comme une technique de traitement efficace, élargissant ainsi son application au niveau industriel. Le biochar utilisé dans ce travail a été synthétisé à l'aide d'une pyrolyse lente à l'échelle laboratoire. Une caractérisation détaillée des effets du prétraitement par ultrasons sur la structure chimique globale du biochar a été réalisée. Les effets mécaniques et sonochimiques ont été étudiés avec différentes combinaisons de fréquence et de puissance à une température de bain de 80 °C pendant 2 heures d'exposition. Le biochar résultant a été caractérisé en utilisant différentes techniques de caractérisation, notamment, le pH, l'analyse proximale, l'analyse élémentaire (AE), la spectroscopie infrarouge à transformée de Fourier (FT-IR), la microscopie électronique à balayage (MEB), l'analyse thermogravimétrique (ATG), le potentiel Zeta, la charge de surface et les isothermes BET. Les caractéristiques chimiques du biochar sont restées les mêmes après les prétraitements par ultrasons. Ceci a confirmé que l'ultrasonication est un phénomène physique qui n'affectait pas la structure chimique du bois, mais modifie physiquement la surface des matériaux. La surface négativement chargée et les caractéristiques globales ont révélé que le biochar prétraité par ultrasons avait de meilleures propriétés physicochimiques par rapport au biochar non traité. Les ultrasons basse fréquence généraient des effondrements, décomposaient les fosses et ouvraient les microcanaux du biocharbon, ce qui améliorait les propriétés de surface. Le biochar avec des propriétés physiques améliorées a été utilisé pour différentes expériences d'adsorption, et ce, avec une meilleure efficacité.

### **4.3 Abstract**

In recent decades, biochar, by virtue of its exceptional properties of surface functionalisation, easy availability and low-cost processability, has been extensively applied in adsorption chemistry and major industrial sectors such as biofuels, pulp and paper, biorefineries, etc. Studies on biochar derived from softwood have revealed its efficient physicochemical properties. These properties depend on different parameters such as biomass feedstock, different processing methods and pyrolysis conditions. Application of ultrasound in lignocellulosic materials is a developing area of research, which implement the effect of

cavitation bubbles. Herein, we introduce ultrasonication as a tool to enhance the physical properties of the softwood-derived biochar and a feasible processing technique for potential application of biomass feedstock, thus expanding its application in industrial level. Biochar used in this work was synthesized using a laboratory scale slow pyrolysis. A detailed investigation on the ultrasonic pre-treatment effects on the overall structure of biochar has been done. The mechanical and sono-chemical effects were studied with different combination of frequency and power at bath temperature of 80 °C for 2 h exposure time.

**Keywords:** Softwood chips, Biochar, Ultrasound pre-treatments, Pyrolysis, Physio-chemical properties

#### 4.4 Introduction

The history of carbon materials began at *terra preta* times, from which evolved diverse forms of charcoal. The potential application of these eco-friendly materials in different sectors of day-to-day life increased rapidly because of the environmental issues arose especially after the green revolution. The physicochemical properties of carbon-based materials like biochar has motivated many researchers to investigate the benefit in terms of mitigating global warming, soil amendment, enhancing crop yield, adsorption of contaminants and carbon capture. The unique properties of biochar, such as large specific surface area, porosity, mineral components along with enriched surface functional groups and ion exchange capacity makes it interesting over activated carbon [1]. There are studies to prove that these properties can be facilitated by controlling the choice of biomass feedstock, pyrolysis conditions and different processing techniques [2-3].

Studies with wood biochar is getting considerable attention in Canada, especially in Quebec where most of the forest trees are softwood. They are mostly processed into lumbers for the construction industry, leaving large volumes of biomass in the form of wooden chips. These wood chips come under the tertiary level of biomass processing which is post-consumer residues of feedstock. These biomass residues are challenging to handle because of the hygroscopic nature and heterogeneity in physical and chemical properties that arises from cellulose, hemicellulose and lignin components. An efficient method of processing techniques is required in order to overcome the challenges related to material quality and

convert them into a usable form of energy. Various pre-treatment methods can be adopted and employed at the level of moisture management, density management and physical property management.

Application of power ultrasound in biomass is a recently developed area of research. It has been shown that ultrasound pre-treatment is an effective technique to modify the physicochemical structure of the biomass [4], increasing the stability [5] and mostly, contributing to the pyrolysis product yields [6]. Ultrasonication makes use of the effect of cavitation and the bubbles collapsing near the solid surfaces disrupts the spherical shape and induces the formation of microjets, which can impact the surfaces. For this reason, ultrasound has been used to explore hard-to-reach surfaces [7]. In the same perspective, cavitation effects can be utilized to modify the surface morphology of biochar to have improved physicochemical properties. Ultrasound enhanced activation and organic functionalisation are one of the very recent developments in biochar research [8-9].

Understanding the ability of ultrasound to promote chemical and thermal decomposition reactions during pyrolysis with better efficiency in terms of product yield and physicochemical properties will be a key step to introduce ultrasound in industrial level of feedstock processing. Introducing ultrasound transducers into a pyrolysis reactor is not a feasible idea in this scenario. However, it is possible to incorporate ultrasound prior to the use of the pyrolysis reactor, as a pre-treatment. The balance between the mechanical and sonochemical effect in different combinations of frequencies, power, exposure time and bath temperature may have a different attack mechanism on biomass, hence could lead to different biochar properties. The current study is economic and practically feasible since the biochar being a byproduct during bio-oil production by lab-scale slow pyrolysis in a temperature range of 500-550 °C. To the best of our knowledge, this work is unique in terms of ultrasound pre-treatment effect on biochar surface morphology.

## 4.5 Materials and Methods

### 4.5.1 Biomass feedstock

The biochar used in this project were obtained from softwood chips (mix of spruce, fir, pine and larch) provided by an eastern Canadian pulp and paper mill. Wood chips were washed to remove impurities, dried in air and then grinded to 5 mm by 5 mm sized needles prior to the experiments. The wood chips were then dried in an oven at 105 °C for at least 24 h before being used in the pyrolysis reactor (48 h for ultrasound treated samples).

**Table 4.1** List of pre-treatments performed on wood chips

Sample	Frequency (kHz)	Power (W)	Temp (° C)	Time (h)
UST-1	40	1000	80	2
UST-2	40	250	80	2
UST-3	170	1000	80	2
UST-4	170	250	80	2

### 4.5.2 Ultrasonic pre-treatments

Ultrasonic treatments were performed in a 34 L ultrasonic bath, model BT90 from Ultrasonic Power Corporation (USA), made of 316 L stainless steel, equipped with 12 transducers located below the bottom plate of the bath. Commercially available frequency generators of 40 and 170 kHz were used to produce between 250 and 1000 W of nominal ultrasonic energy to study the mechanical and sonochemical effects, respectively. The exposure time was fixed for 2 h at a bath temperature of 80 °C (Table 4.1). For each treatment, 200 g of wood chips were dipped into 4 L of deionized water in a weighed mesh bag, to ensure that the wood chips are completely submerged in water and homogenously treated by ultrasound.

### 4.5.3 Lab-scale pyrolysis

The pyrolysis was performed using method previously reported by Loranger et al. [10] and as explained in Cherpozat et al. [6] At least three trails were performed to confirm the average yield of biochar and other pyrolysis products. The biochar was cleaned from tar and

was stored in plastic bags. Prior to each analysis, prepared biochar was dried at 105 °C for at least 12 h and stored in desiccator.

#### **4.5.4 Chemical and physical characterisations**

The elemental composition of C, H and N were analyzed using elemental analyzer, EA 1108 Fisons, CHNS instrument. The oxygen content was determined by mass difference. Proximate analysis (Ash, moisture and volatile content) were performed using the method described by American Society for Testing and Materials D1752-84, which is recommended by the International Biochar Initiative. pH of the material was measured using Accumet XL20, Thermo Fisher Scientific pH-meter in deionized water at 1:2 weight by volume ratio after stirred at room temperature for two hours. Conventional back titrations were performed using 0.05M NaOH and 0.05M HCl to understand the nature of functional groups, keeping the Boehm assumption in mind, which proves that the NaOH will neutralize the acidic carboxylic, lactonic and phenolic functional groups present on the biochar surface [11]. Zeta Potential of untreated and ultrasound pre-treated wood biochar was measured for a suspension of biochar powder in deionized water with pH 6.14 using Zetasizer-nano series from Malvern Instruments. Infrared spectra of each prepared biochar and untreated wood were obtained in Nicolet iS10 Smart iTR Infrared Spectroscopy instrument at room temperature using biochar mixed with spectroscopic grade pre-dried KBr pellet. The spectra were obtained in reflection mode in the range of 400-4000  $\text{cm}^{-1}$  for a minimum of 16 scans with 1  $\text{cm}^{-1}$  resolution. To understand the thermal stability of the material, Thermogravimetric Analysis (TGA) was performed on Mettler Toledo TGA 2. Samples were heated under nitrogen to provide inert atmosphere and prevent combustion of the samples. The sample was heated from room temperature to 100 °C by ramping at 20 °C/min, and then heated to 700 °C. Scanning Electron Microscopy (SEM) images were captured using Hitachi SU1510 instrument to understand the changes in biochar surface. Energy Dispersive X-ray Spectroscopy (EDX) was obtained with X-Max, Oxford instrument to verify the surface carbon and oxygen content. Surface area was measured via the Brunauer, Emmett and Teller (BET) method that measures  $\text{N}_2$  gas sorption ( $0.162 \text{ nm}^2$ ) at 77 K. Approximately 100 mg of biochar was outgassed at 200 °C (16 h) and then analyzed on an Autosorb-1 Surface Area Analyzer (Quantachrome Instruments).

#### **4.5.5 Adsorption of Cu using biochar**

Adsorption of metal is an efficient method to understand the surface property of the material. Cu (II) has been selected for the batch adsorption tests, as it is easily available and less toxic heavy metal. 100 ppm solution of Cu (II) was prepared from stock CuSO<sub>4</sub> solution (1000 ppm). A ratio of 5 g/L adsorbent was added to metal solution and then the mixture was agitated on a reciprocating shaker at room temperature. The kinetics of the material were studied from 0.5 to 24 h. Samples were taken at desired intervals and subsequently filtered with Whatman No. 1 filter paper. The filtrates were analyzed for residual heavy metal concentration in the solution [12]. Pseudo first order and Pseudo second order kinetic models were examined by linearizing the experimental data.

### **4.6 Results & Discussion**

The pyrolysis product yield exhibited the common trend, which is dependent on pyrolysis temperature and reaction time. However, a small decrease in yield was observed for ultrasound pre-treated samples which could be happened to adjust with the mass balance between bio-oil and syngas. Chemical and physical characterisations are performed to understand the pre-treatment effect of ultrasound on material properties.

#### **4.6.1 Chemical characterisation of biochar**

Proximate and ultimate analysis of biochar were performed and summarized in Table 4.2. Proximate analysis results indicated the stability of biochar produced during pyrolysis at a given temperature range. Dry biomass feedstock contains around 46 percent of carbon. The pyrolysis temperature range for all the experiments performed is responsible for different dehydration and decarboxylation reactions and increases the degree of carbonization with a subsequent decrease in hydrogen and oxygen content. It is clear from the result that the biochar is rich in carbon which is an indication of increase in aromaticity hence the properties could be similar to activated carbon. The biomass contains rapidly reacting oxygen fractions which are lost after the initial heating and reluctant oxygen which will retain in the matrix of the final product. This can be responsible for the ten percent oxygen in the synthesized samples.

**Table 4.2** Proximate and ultimate analysis of biochar

Parameters	Biochar Weight (%)	Feedstock Weight (%)
Moisture	4	-
Volatile	23	-
Ash	< 1	-
C	86.5 ±1.09	46.7
H	2.7 ±0.1	6.4
N	0.05 ±0.02	0.04
O*	10.7	46.9

\*Oxygen content was determined by mass balance

To confirm the presence of oxygen contained functional groups on the biochar surface, the acidic sites are determined by conventional back titration method. The Boehm back titration determines the total concentration of phenolic, lactonic and carboxylic functional groups on the surface. The results (Table 4.3) indicated that the approximate ten percent oxygen content in the biochar is from the functional groups present on the carbon surface which are impervious to different reaction mechanisms during the pyrolysis. Zeta potential of biochar (Table 4.3) in water also confirmed that the surface of biochar is negatively charged. The surface functionality makes biochar different and preferred over activated carbons since the oxygen sites could be utilized for different ionic interactions.

**Table 4.3** Surface charge nature of biochar

pH*	6.14
Zeta Potential (mV)	-2.63
Acidic sites (mmol/g)	1.27

\* pH of deionized water: 5.92

The infrared spectra of the base wood and ultrasound pre-treated wood biochar samples were analysed and compared with base activated biochar to confirm the different functional groups present. The adsorption bands were less intense for the biochar samples (Figure 4.1a). It was interesting to note that the spectral pattern for all ultrasound treated or untreated biochar were similar except slight intensity changes due to the pyrolysis temperature difference. O-H peak at 3340 cm<sup>-1</sup> was almost disappeared which clearly represents the oxygen content loss during

carbonization. Observed aromatic C-H stretching at  $3130\text{ cm}^{-1}$ , aromatic C=C stretching and  $\text{CH}_2$  bending vibrations at  $1500\text{--}1300\text{ cm}^{-1}$ , and aromatic C-H out of plane vibrations at the range of  $800\text{ to }700\text{ cm}^{-1}$  are characteristic bands for conjugated aromatic rings. At the same time, carbonyl C-O band around  $1600\text{ cm}^{-1}$  was very less intense which explains the low oxygen content in biochar samples.

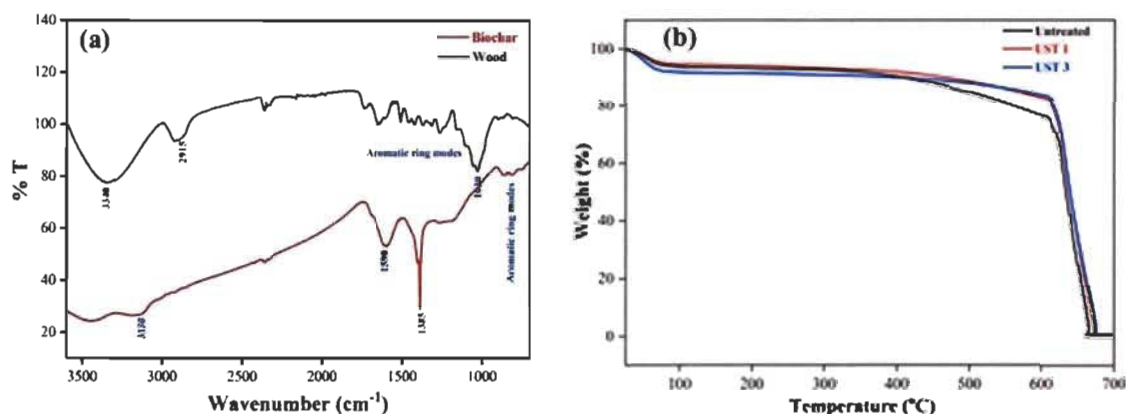


**Figure 4.1** a) Infrared spectra of feedstock and ultrasound pre-treated biochar. b) Thermogravimetric analysis of ultrasound untreated and pre-treated wood biochar

TGA analysis shown that the samples are thermally stable up to  $600\text{--}650\text{ }^{\circ}\text{C}$  (Figure 4.1b). It was well observed that the ultrasound pre-treated samples are structurally more stable than the untreated.

Chemical characteristics of synthesized biochar verified the efficiency of laboratory scale pyrolysis to produce biochar with good material quality. The chemical characteristics remained consistent and identical for all ultrasound pre-treated wood biochar. Thus, the pre-treatment with ultrasonication is confirmed to be physical phenomenon which does not affect the chemical structure and composition of feedstock. Since pyrolysis does not affect the physiology of the wood, the effect of ultrasound pre-treatments is expected to be evident in physical characteristics and surface morphology.

#### 4.6.2 Ultrasonic pre-treatment effects on surface morphology

To understand the physical effect of ultrasound pre-treatment, surface morphology studies has been performed using SEM images and metal adsorption studies. Figure 4.2 shows the comparison image for ultrasound pre-treated and untreated wood biochar. It was observed that unlike the untreated wood biochar, in all the ultrasonic conditions, the slit like channels on the wood surface were cleaned from different attachments. As expected, the mechanical effect on surface of biochar were more evident in 40 kHz samples. The surface ruptures were less apparent in 170 kHz treated samples though the channels were clean from the microfibers.

The specific surface area of UST-1 is slightly increased compared to the untreated one but there is a significant decrease in the case of UST-3 (Table 4.4).

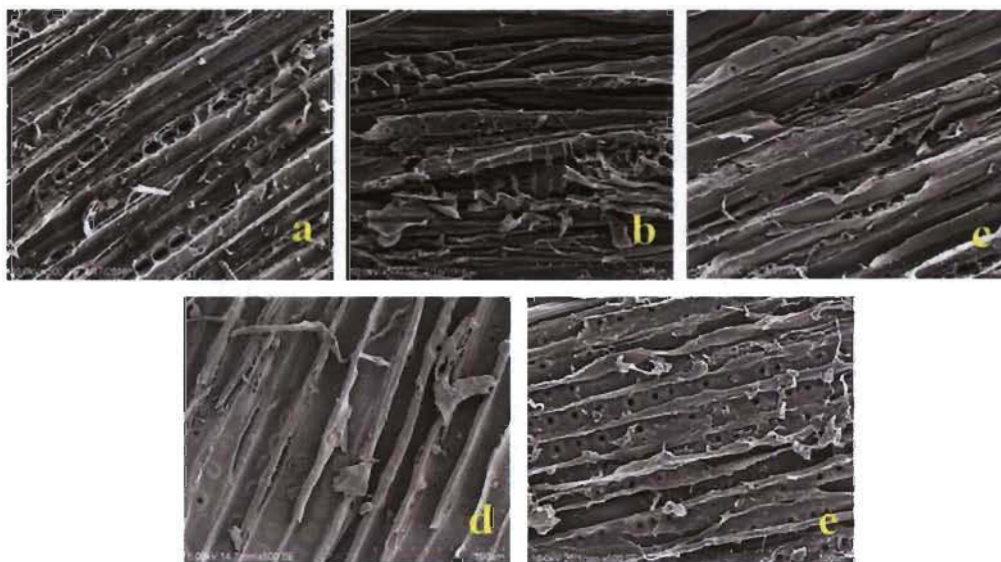


**Figure 4.2** SEM images of biochar derived from ultrasound pre-treated wood chips. a) Untreated, b) UST 1, c) UST 2, d) UST 3, e) UST 4

In higher frequency ultrasound, even though the microchannels were smoothed, it could happen that the surface sites were blocked because of the breaking down of microparticles or structural rearrangement.

**Table 4.4** Adsorption kinetics of biochar

Adsorbent	BET-N <sub>2</sub> Specific Surface Area (m <sup>2</sup> /g)	Pseudo Second order		
		Q <sub>e</sub>	k	R <sup>2</sup>
Untreated	10.48	1.09	0.051	0.993
UST 1	12.40	1.542	0.022	0.987
UST 2	nd*	1.539	0.040	0.988
UST 3	3.31	0.739	0.042	0.911
UST 4	nd*	0.729	0.22	0.992

\*nd: not determined

Adsorption experiments provided a better understanding about the surface change on biochar. Figure 4.3 is an example for the effect of contact time of Cu (II) on biochar.

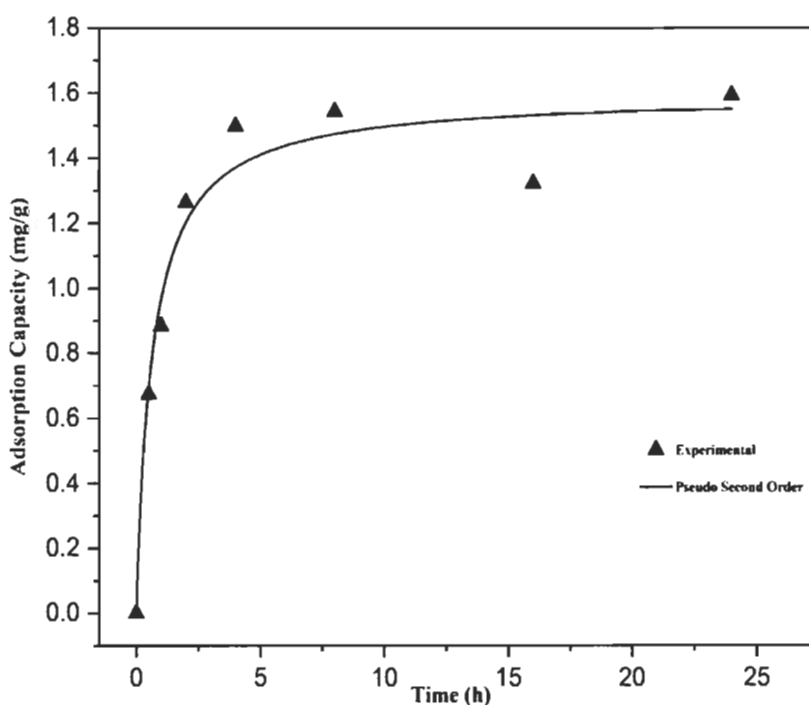


**Figure 4.3** Pseudo second order kinetic model for ultrasound pre-treated wood biochar UST-1

Almost 80 percent adsorption occurred in the first 4 hours and then a slow approach to the equilibrium over 24 hours. This trend was visible for ultrasound untreated and pre-treated samples. The adsorption kinetics was fitted to pseudo second order model only, indicating

that the adsorbate-adsorbent interaction follows physisorption. The adsorption capacity at equilibrium and rate constant were calculated by linearizing the experimental data (Table 4.2). The regression coefficient  $R^2$  indicates the fit of experimental points to the pseudo second order model.

The 40 kHz pre-treated samples showed better adsorption of Cu (II) on biochar surface. The 170 kHz samples were shown almost half less adsorption than 40 kHz samples. This was also evident in the BET surface area. The low frequency ultrasound alters the surface by exposure of the material to the treatment solution and enhances its accessibility by generating collapses. On the other hand, it could happen that the high frequency smoothed the microchannels but also decreased the accessibility of the pits which resulted in significant decrease of the adsorption capacity.

#### **4.7 Conclusions**

Ultrasound pre-treatments affects the surface morphology of biochar without changing the chemical characteristics. Low frequency ultrasound generates collapses, break down the pits and open up the microchannels which positively affects the adsorption behaviour of the material. It can be an effective method to process biomass feedstock at the property management level, thus leads to potential application of derived products by tuning the physical morphology. However, detailed comparison studies must be done in order to explore the effect of each ultrasound pre-treatment conditions.

#### **4.8 Acknowledgment**

The authors gratefully acknowledge all the members of I2E3 for their great support and help during the period of this work. Financing was provided by the Natural Sciences and Engineering Research Council of Canada (NSERC) and by Queen Elizabeth II Diamond Jubilee Scholarship.

#### 4.9 References

- [1] F. R. Oliveira, A. K. Patel, D. P. Jaisi, S. Adhikari, H. Lu and S. K. Khanal, Environmental application of biochar: Current status and perspectives, *Bioresource Technol.*, 2017
- [2] Y. Sun, B. Gao, Y. Yao, J. Fang, M. Zhang, Y. Zhou, H. Chen and L. Yang, Effects of feedstock type, production method, and pyrolysis temperature on biochar and hydrochar properties, *Chem. Eng. J.*, 2014, 240, 574-578
- [3] S. Jiang, T. A. Nguyen, V. Rudolph, H. Yang, D. Zhang, Y. S. Ok and L. Huang, Characterization of hard-and softwood biochars pyrolyzed at high temperature, *Environ. Geochem. Health*, 2017, 39, 403-415
- [4] Z. He, Z. Wang, Z. Zhao, S. Yi, J. Mu and X. Wang, Influence of ultrasound pretreatment on wood physiochemical structure, *Ultrason. Sonochem.*, 2017, 34, 136-141
- [5] S. Qiu, Z. Wang, Z. He and S. Yi, The Effect of Ultrasound Pretreatment on Poplar Wood Dimensional Stability, *BioResources*, 2016, 11, 7811-7821.
- [6] L. Cherpozat, E. Loranger and C. Daneault, Ultrasonic pretreatment effects on the bio-oil yield of a laboratory-scale slow wood pyrolysis, *J. Anal. Appl. Pyrolysis*, 2017, 126, 31-38
- [7] T. Leong, M. Ashokkumar and S. Kentish, The fundamentals of power ultrasound-A review, 2011
- [8] R. Chatterjee, B. Sajjadi, D. L. Mattern, W.Y. Chen, T. Zubatiuk, D. Leszczynska, J. Leszczynski, N. O. Egiebor and N. Hammer, Ultrasound cavitation intensified amine functionalization: A feasible strategy for enhancing CO<sub>2</sub> capture capacity of biochar, *Fuel*, 2018, 225, 287-298.

- [9] B. Sajjadi, J. W. Broome, W. Y. Chen, D. L. Mattern, N. O. Egiebor, N. Hammer and C. L. Smith, Urea functionalization of ultrasound-treated biochar: A feasible strategy for enhancing heavy metal adsorption capacity, *Ultrason. Sonochem.*, 2019, 51, 20-30.
- [10] É. Loranger, A.-O. Piché and C. Daneault, Ultrasonic pre-treatments of wood chips used in a conventional pyrolysis and their effect on bio-oil composition and calorimetry, *SAMPE Conference Proceedings*, 2016.
- [11] H. P. Boehm, Chemical identification of surface groups: Advances in catalysis, Elsevier, 1966, 16, 179-274.
- [12] X. Chen, G. Chen, L. Chen, Y. Chen, J. Lehmann, M. B. McBride and A. G. Hay, Adsorption of copper and zinc by biochars produced from pyrolysis of hardwood and corn straw in aqueous solution, *Bioresource Technol.*, 2011, 102 ,8877–8884.

#### 4.10 Highlights

- Softwood derived biochars were synthesized using ultrasound assisted lab-scale pyrolysis
- The chemical characteristics remained unchanged even after ultrasonic pre-treatments
- Surface morphology and adsorption behaviour was positively affected by ultrasonic pre-treatments
- Synthesized biochars can be potentially used for adsorption of heavy metals from aqueous solution

## Chapter 5 – Scientific Article 2: Heavy Metal Adsorption using Synthesized Biochars

### 5.1 Preface

Article 1 demonstrated the effect of ultrasound on physicochemical properties and surface morphology of biochar. However, the adsorption characteristics were not completely investigated. Hence, based on the results obtained from first article, this study discuss about the detailed examination of how each ultrasonic pre-treatment affects the heavy metal adsorption behaviour of synthesized biochar. Different combinations of ultrasound frequency, power, bath temperature and time were investigated. The adsorption behaviour of each pre-treated biochar was examined with copper as a model metal contaminant using kinetics, isotherm and thermodynamic parameters. This work was published in Bioresource Technology Reports on May 2020 entitled *The influence of ultrasonic pre-treatments on metal adsorption properties of softwood-derived biochar* (DOI: <https://doi.org/10.1016/j.biteb.2020.100445>) The results were also presented in poster session conducted in I2E3-Innofibre colloque 2020, Trois-Rivieres (January 2020).

#### Author Details:

Aneeshma Peter, Int. BS-MS

Ph.D. Student, Sciences de l'énergie et des matériaux

I2E3 – Institut d'Innovations en Écomatériaux, Écoproduits et Écoénergies, à base de biomasse, Université du Québec à Trois-Rivières, P.O. Box 500, Trois-Rivières, Québec, Canada, G9A 5H7

Email: [Aneeshma.Peter@uqtr.ca](mailto:Aneeshma.Peter@uqtr.ca)

Eric Loranger, Ph.D.

Research director and corresponding author

I2E3 – Institut d’Innovations en Écomatériaux, Écoproduits et Écoénergies à base de biomasse, Université du Québec à Trois-Rivières, P.O. Box 500, Trois-Rivières, Québec, Canada, G9A 5H7

Email: [Eric.loranger1@uqtr.ca](mailto:Eric.loranger1@uqtr.ca)

Bruno Chabot, PhD.

Co-director and co-author

I2E3 – Institut d’Innovations en Écomatériaux, Écoproduits et Écoénergies à base de biomasse, Université du Québec à Trois-Rivières, P.O. Box 500, Trois-Rivières, Québec, Canada, G9A 5H7

Email: [Bruno.Chabot@uqtr.ca](mailto:Bruno.Chabot@uqtr.ca)

#### **Author Credits:**

**Aneeshma Peter:** Methodology, Validation, Investigation, Data curation, Formal analysis, Writing - original draft, Visualization

**Bruno Chabot:** Conceptualization, Project administration, Writing - review & editing

**Eric Loranger:** Conceptualization, Project administration, Supervision, Writing - review & editing, Funding acquisition

## **5.2 Résumé**

Les biochars dérivés de biomasse sont étudiés de manière approfondie en raison de leurs propriétés de surface uniques et de leur efficacité à éliminer les métaux lourds d'une solution aqueuse. Différents prétraitements effectués sur la biomasse peuvent affecter les propriétés de surface du biochar obtenu, ce qui peut affecter par la suite les propriétés d'adsorption. Une bonne compréhension et un contrôle de la relation structure-propriétés du biochar peuvent ainsi améliorer ou faciliter son application dans le domaine de l'élimination des métaux lourds. Cette approche peut également corriger les problèmes de qualité des

matériaux des matières premières de post-consommation et les convertir en sous-produits réutilisables. Les prétraitements par ultrasons de puissance sont intéressants dans ce contexte, car ils peuvent apporter des changements significatifs dans les caractéristiques physicochimiques de la biomasse. Les effets mécaniques et sonochimiques des ultrasons peuvent potentiellement améliorer les propriétés du biochar pour les applications d'élimination des métaux lourds. Ici, nous avons étudié leurs effets sur les caractéristiques d'adsorption d'un biochar de résineux produit dans différentes conditions de fréquence, de puissance, de température et de temps d'exposition aux ultrasons. Les études détaillées sur la cinétique d'adsorption, les isothermes et effets thermodynamiques ont été réalisés en utilisant le cuivre comme contaminant métallique modèle. Les résultats ont été analysés à l'aide de l'outil statistique JMP pour comprendre comment chaque condition du prétraitement affecte la capacité d'adsorption ( $Q_e$ ) du biochar. Les échantillons prétraités à 40 kHz présentaient une augmentation d'environ 0,3 à 0,65 mg/g de la capacité d'adsorption à l'équilibre en montrant une forte dépendance de la combinaison de la puissance des ultrasons en fonction du temps d'exposition et de la température. Les études des isothermes et thermodynamiques ont également montré que l'effet mécanique des ultrasons joue un rôle essentiel dans l'amélioration de la surface. L'adsorption par unité de surface de UST-biochars a été comparée au charbon actif disponible dans le commerce. Le biochar prétraité à haute fréquence a montré une meilleure efficacité en termes d'adsorption par unité de surface, contrairement aux résultats d'adsorption initiaux. Les résultats de cette étude ont donc démontré que les conditions de prétraitement par ultrasons influencent fortement et positivement le comportement du biochar vis-à-vis de l'adsorption des métaux et que les prétraitements par ultrasons peuvent être utilisés comme méthode de traitement efficace pour les résidus de biomasse et ses produits dérivés.

### 5.3 Abstract

Biomass-derived biochars are studied extensively because of their unique surface properties and efficiency in removing heavy metals from aqueous solution. Power ultrasound pre-treatments is interesting in this context, as they can make significant changes in the physicochemical characteristics of biomass. Herein, we studied their effect on adsorption characteristics of softwood biochar under different conditions of frequency, power,

temperature and exposure time of ultrasound. The 40 kHz pre-treated samples exhibited around 0.3 to 0.65 mg/g increase in equilibrium adsorption capacity ( $Q_e$ ) which highly depends on the combination of power versus time and temperature of ultrasound. The isotherm and thermodynamic studies also showed that the mechanical effect of ultrasound plays a vital role in enhancing the surface. Results from this study demonstrated that ultrasound pre-treatment conditions influence the behaviour of biochar towards metal adsorption and ultrasonic pre-treatments can be used as an efficient processing method for biomass residues and the derived products.

**Keywords:** Biochar, ultrasonic pre-treatments, metal adsorption, adsorption capacity, surface modification

#### 5.4 Introduction

Biochar is a solid residue obtained from thermochemical conversion of biomass in an oxygen-limited environment (Manyà, 2012). Due to the similar physical appearance, biochars are often misinterpreted with charcoal and other carbonised materials, which mainly are thermal residues after complete combustion of feedstocks. The basic difference being the source material, which is mostly fresh residual matter in case of biochar rather than fossilized or good quality biomass in other carbonised materials. This carbon-rich, semi-crystalline, porous material has emerged as an alternate to activated carbons and proved its efficiency in removing organic and inorganic contaminants from industrial effluents (Mohan et al., 2014, Tan et al., 2015, Inyang et al., 2016). Modified biopolymers, membranes, hydrogels are few of the existing adsorbents available, though their application in industrial scale is limited because of the expensive activation methods, operational costs, low selectivity and production of hazardous waste after adsorption (Barakat, 2011, Oliveira et al., 2017). The unique properties of biochar such as good specific surface area, surface functionality, easy availability, and low-cost processability popularised the material and preferred over other existing adsorption materials.

The properties of wood derived biochar have been extensively studied during recent decades, especially in Quebec (Canada), because of the abundance of forest trees, which are mostly softwoods. Different research policies have been adopted to facilitate and enhance the

properties of softwood derived biochar. This is mostly attributed to their physical as well as the chemical properties that are highly dependent on feedstock type, production methods, pre and post processing of feedstocks and reaction conditions involving temperature, pressure, residence time (Nartey and Zhao, 2014, Jindo et al., 2014; Chowdhury et al., 2016; Behazin et al., 2016). For example, the effect of temperature, production method and feedstock type on the physicochemical and biological properties of different biochars were explored by Sun et al. (2014) and they have shown that production method and feedstock type have high influence on the properties. Mukome et al., (2013) also studied the trend of feedstock type on biochar properties. They have analysed biochar from twelve different feedstocks and stated that physical and chemical properties vary depending on the feedstock type. Similarly, in a study by Jiang et al. (2017) the physicochemical properties of different varieties of hardwood and softwood were examined and showed that the properties are dependent on the pyrolysis temperature. They have also stated that the properties vary depending on the cellulose, hemicellulose and lignin content of the wood. Therefore, developing and optimising an efficient treatment method can be interesting for tuning the physicochemical properties of the material for the same feedstock and pyrolysis conditions.

Application of power ultrasound in biomass processing is a recently developed area. The invasive technique uses high intensity acoustic waves to change or modify the properties as well as promote chemical and thermal decomposition reactions within the material. The formation of cavitation bubbles followed by the microjet collision experienced during the bubble implosions were employed to expose inaccessible regions on the surface (Leong et al., 2011). Limited reports are available in literature that examine the effect of ultrasound for different biomass applications. He et al. (2017) investigated the influence of ultrasonic pre-treatments on eucalyptus wood. They proved that the ultrasound can modify the physicochemical structure of the wood and can significantly increase the crystallinity of the material. Qui and co-workers (2016) demonstrated that ultrasound pre-treatments on hardwood can increase its dimensional stability by chemical modification and it is an effective way to reduce water adsorption rate in wood. A recent study by Chatterjee et al. (2018) examined the effect of ultrasound cavitation induced physical activation to enhance the chemical modification of biochar for CO<sub>2</sub> sequestration. Sajjadi et al. (2019) also have demonstrated the physical modification of biochar by low frequency ultrasound to enhance

the urea functionalisation, which enhances the adsorption capacity of the material. Recently, Cherpozat et al. (2017) have investigated the effect of ultrasonic pre-treatments on the pyrolysis biooils yield giving a significant progress in ultrasonic enhanced lab-scale pyrolysis and hence motivating the further investigation on the effect of ultrasonic pre-treatment in pyrolysis product characteristics.

In this study, we aim at investigating the ultrasonic pre-treatment effects on the overall structure of biochar and its adsorption behaviour. Proper understanding and controlling the structure-property relationship of biochar can improve its application in the field of heavy metal removal. It can also rectify the issues regarding material quality of post-consumer feedstocks and convert them into useable by-products. To the best of our knowledge, this is the first study to evaluate ultrasound pre-treatment effects on biomass and change in properties of biochar via systematic analysis methods. The adsorption behaviour of mixed softwood is very rarely investigated because of their heterogeneity in properties. Shen et al. (2018) used mixed softwood chips to compare effect of feedstocks on Ni and Cu adsorption properties. However, the maximum copper adsorption capacity obtained were very less in comparison with our present study. Hence to understand the pre-treatment effects on metal adsorption, ultrasound untreated biochar is used as control sample for a proper comparison.

## **5.5 Materials and Methods**

### **5.5.1 Biochar production and characterisation**

The biochar samples were prepared using mix of processed softwood chips (spruce, fir, pine and larch) from an eastern Canadian pulp and paper mill (Peter et al., 2019). A lab-scale pyrolysis set up was used as previously reported by Loranger et al. (2016). 34 L ultrasonic bath (model BT90, Ultrasonic Power Corporation USA) made of 316 L stainless steel and equipped with 12 transducers below the bottom plate was used to carry out the ultrasonic pre-treatments. 40 and 170 kHz frequency generators were used to study the mechanical and sonochemical effects, respectively with energies of 250 and 1000 W. The bath temperature was fixed at 20 °C and 80 °C for the exposure time of 1 and 2 h. The list of ultrasound pre-treatments is given in Table 5.1.

To obtain the pH of the material, biochar was mixed in deionized water at 1:2 weight by volume ratio (g:mL), stirred at room temperature for 2 h and measured using Accumet XL20, Thermo Fisher Scientific pH-meter. Zeta Potential was measured in Zetasizer-nano series from Malvern Instruments using the suspension of biochar powder in deionized water (pH 6.14). The point zero charge was determined from the plot of pH against Zeta potential. Surface morphology was examined using Scanning Electron Microscopy (SEM) images, captured using Hitachi SU1510 instrument.

**Table 5.1** List of ultrasonic pre-treatments on wood chips

Sample Code	Frequency (kHz)	Power (W)	Temperature (°C)	Time (h)
UST 1	40	1000	80	1
UST 2	40	1000	20	1
UST 3	40	1000	80	2
UST 4	40	1000	20	2
UST 5	40	250	80	1
UST 6	40	250	20	1
UST 7	40	250	80	2
UST 8	40	250	20	2
UST 9	170	1000	80	1
UST 10	170	1000	20	1
UST 11	170	1000	80	2
UST 12	170	1000	20	2
UST 13	170	250	80	1
UST 14	170	250	20	1
UST 15	170	250	80	2
UST 16	170	250	20	2

Brunauer, Emmett and Teller (BET) method with N<sub>2</sub> gas sorption (0.162 nm<sup>2</sup>) at 77 K was used to calculate specific surface area of the biochar. Approximately 100 mg of biochar was outgassed at 200°C for 16 h and analysed on an Autosorb-1 Surface Area Analyzer (Quantachrome Instruments).

### 5.5.2 Cu (II) adsorption experiments

To understand the metal adsorption behaviour of the biochar samples, batch adsorption studies were carried out using copper as model metal. A 1000 ppm stock solution of Cu (II)

was prepared by dissolving analytical grade anhydrous CuSO<sub>4</sub> in deionized water. The pH of the copper solution ranged from 4.8 to 5. The kinetic experiments for all the biochar samples were conducted in 125 mL Erlenmeyer flask with 5 g/L biochar mixed in 100 ppm Cu (II) solution by agitated on a reciprocating shaker at room temperature (22 ± 2 °C) at 150 rpm. Samples were taken at desired intervals and immediately filtered using Whatman No. 1 filter paper. The residual heavy metal concentration in the filtrate was measured using EDTA titration described by Prasad and Raheem, (1992). The amount of adsorbed metal ions, Q (mg/g), was calculated using Equation 3.1.

$$Q = \frac{(C_{initial} - C_{final}) * V}{m} \quad \text{Equation 3.1}$$

Experimental data were fitted to linear forms of pseudo first order (Equation 5.1) and pseudo second order (Equation 5.2) kinetic models, since in most of the cases, heavy metal adsorption on biochar follows pseudo first or second order kinetics (Tan et al., 2015).

$$\text{Log}(Q_e - Q_t) = \log Q_e - \frac{k_1 * t}{2.303} \quad \text{Equation 5.1}$$

$$\frac{1}{Q_t} = \frac{1}{k_2 * Q_e^2} + \frac{1}{Q_e} \quad \text{Equation 5.2}$$

Where Q<sub>t</sub> and Q<sub>e</sub> (mg/g) are adsorbed metal amount at time t (minute) and equilibrium, k<sub>1</sub> and k<sub>2</sub> (g/mg. min) are the rate constants for pseudo first order and second order kinetic model, respectively. The regression factor R<sup>2</sup> determines the best fit model which helps to understand the mechanism of adsorbent-adsorbate interaction. Slope and intercept values were used to calculate Q<sub>e</sub> and rate constant, k.

Adsorption isotherms for selected samples were obtained with initial Cu (II) concentrations varied from 10 to 200 ppm. The linearized Langmuir and Freundlich models were used to fit the experimental data as they are the most commonly used and well fitted adsorption models for heavy metal adsorption on biochar. (Zhang et al., 2013; Jia et al., 2013; Chen et al., 2011).

The linear equations of the Freundlich and Langmuir adsorption models are expressed respectively, by Equations 5.3 and 5.4:

$$\text{Log}Q_e = \log K_f + \frac{1}{n} \log C_e \quad \text{Equation 5.3}$$

$$\frac{C_e}{Q_e} = \frac{1}{b \cdot Q_{\max}} + \frac{1}{Q_{\max}} C_e \quad \text{Equation 5.4}$$

Where  $Q_e$  is the amount of the metal adsorbed per unit weight of biochar at equilibrium (mg/g),  $C_e$  is the equilibrium concentration of solution (mg/L).  $K_f$  and  $n$  are indicators of relative adsorption capacity and surface heterogeneity, respectively. The maximum monolayer adsorption capacity is represented by  $Q_{\max}$  (mg/g) and Langmuir constant related to the degree of adsorption affinity is denoted by  $b$ .

Model fitness for a particular system is denoted by a dimensionless constant  $R_L$ , which was calculated (Equation 3.7) using Langmuir constant and initial concentration (Ozcan et al., 2006; Brandes et al., 2019). If value of  $R_L$  falls between 0 and 1, the system is considered appropriate for adsorption purpose.

$$R_L = \frac{1}{(1 + bC_i)} \quad \text{Equation 3.7}$$

Where  $b$  is the Langmuir constant and  $C_i$  is the initial concentration. The favourability of the adsorption is identified by the value of  $R_L$  as given below:

$R_L > 1$ , unfavourable

$R_L = 1$ , linear

$0 < R_L < 1$ , favourable

$R_L < 0$ , irreversible

The temperature effect was assessed by equilibrating 0.1 g biochar with 20 mL Cu (II) solution on shaker at 25, 40, and 60 °C. The thermodynamics of the adsorption processes were estimated using the following equations:

$$K_e = \frac{Q_e}{C_e} \quad \text{Equation 3.13}$$

$$\Delta G^0 = -RT \ln K_e \quad \text{Equation 3.14}$$

$$\Delta G^0 = \Delta H^0 - T\Delta S^0 \quad \text{Equation 3.15}$$

$$\ln K_e = \frac{\Delta S^0}{R} - \frac{\Delta H^0}{RT} \quad \text{Equation 3.16}$$

Where  $Q_e$  is the amount of the metal adsorbed per unit weight of biochar at equilibrium (mg/g),  $C_e$  is the equilibrium concentration of solution (mg/L),  $R$  is gas constant 8.314,  $T$  (K) absolute temperature and  $K_e$  (L/g) the equilibrium adsorption constant.

The values of enthalpy  $\Delta H^0$  and entropy  $\Delta S^0$  can be determined from the slope and intercept of the plot  $\ln K_e$  vs  $1/T$ . Gibb's free energy  $\Delta G^0$  can be obtained using Equation 3.15 with the values of  $\Delta H^0$  and  $\Delta S^0$ .

The effect of each ultrasonic pre-treatment on the kinetics parameters is useful to determine the change in surface property of biochar with pre-treatments. Therefore, for better understanding, statistical analysis of the kinetics data was performed using JMP Pro 14 (SAS) for the detailed investigation of ultrasound pre-treatment effects on equilibrium adsorption capacity and rate constant  $k$ .

Kinetic results of biochar samples were compared with commercially available carbon (Fluval Carbon for purifiers) to compare the adsorption per unit surface area. Equilibrium adsorption capacity was measured for activated carbon, untreated, UST-3 and UST-11 and the results were compared in terms of adsorption per unit surface area ( $\text{mg}/\text{m}^2$ ).

## 5.6 Results and Discussions

The synthesis conditions and chemical characterisations of all biochar were done and reported before (Peter et al., 2019). The pyrolysis temperature was ranged between 510 to 580 °C. In brief, the chemical characteristics of ultrasound pre-treated, and untreated biochar remained same, confirming that the ultrasound had affected only on the physical morphology of biochar. The chemical composition of feedstock and biochar synthesised is summarised in Table 5.2. Almost 87 percent is carbonised with a 10-weight percent of oxygen present, which can be from carboxylic, phenolic lactonic surface functional groups. These functionalities can act as anchoring sites for the positively charged adsorbates.

At least three replicates were performed, and the average value is reported for all the adsorption experiments. This is required considering the variations in experimental data because of the mixed feedstock softwoods, heterogeneity in structure and variations in effect of temperature inside pyrolysis reactor. The standard error has been included in the experimental graphs and has shown an average of about 15 percent variation from the mean value, which shows the consistency in values reported.

**Table 5.2** Proximate and Ultimate analyses of biochar and feedstock

Parameters	Biochar Weight (%)	Feedstock Weight (%)
Moisture	4	-
Volatile	23	-
Ash	< 1	-
C	86.5 ±1.09	46.7
H	2.7 ±0.1	6.4
N	0.05 ±0.02	0.04
O*	10.7	46.9

\*Oxygen content was determined by mass balance

### 5.6.1 Ultrasound pre-treatment effects on biochar

The microscopic images of biochar prepared from wood chips after different ultrasonic conditions were studied to understand if there are any obvious surface morphology changes. The comparison of surface images has been done for all samples (Figure A1 S1).

Unlike untreated wood biochar, in most of the ultrasonic conditions, the slit like channels on the wood surface were cleaned from the microfibrils. 40 kHz samples were expected to be more structurally disturbed because of the mechanical effect of low frequency ultrasound. As expected, this effect was more evident in 40 kHz experiments. The surface had undergone more ruptures and the channels were disturbed at 1000 W and 2 h exposure of ultrasound at a bath temperature of 80 °C (UST-3). This effect was tending to decrease slightly with decrease in power and bath temperature. The surface ruptures were less visible in 170 kHz treated samples though the channels were clean and smooth for all the power, temperature combinations. A majority of adsorption happens in micropores and functional groups attached to the surface of biochar (Mohan et al., 2011; Han et al., 2013). The pits cleared from the fibre attachments are more likely to be accessible for surface interactions. The breakdown of the pits and the collapses observed on the microchannels after ultrasound pre-treatments could lead to a change in surface morphology of biochar. This observation was not clearly visible in 170 kHz samples, which could be a result of lower impact bubbles by higher frequency ultrasound. Therefore, the breakdown and ruptures did not strongly occur. The surface of 40 kHz samples seems to be much more heterogeneous, which could affect the adsorption process. In higher frequency ultrasound, even though the microchannels were smoothed, it could happen that the surface sites were blocked because of the breaking down of microparticles or structural rearrangement.

### **5.6.2 Effect of pH and surface zeta potential**

The effect of pH on adsorption properties is an important parameter to optimize because it depends on the nature of the adsorbent surface and target contaminant. The characteristics of surface functional groups on biochar changes with the pH of the solution. Low pH makes most of the functional groups present on biochars protonated and positively charged. For  $\text{pH} < \text{pH}_{\text{pzc}}$  (point of zero charge), the biochar surface is positive and favours adsorption of the anions. The cationic adsorption sites on biochar were hindered with the presence of a large number of  $\text{H}^+$  and  $\text{H}_3\text{O}^+$  in the aqueous solution. Thus, electrostatic repulsion will occur between cation contaminants and positively charged biochars surface thus a lower adsorption was observed at low pH in most of the studies. With the increase of pH value, the competition of metal ions and protons for binding sites decreased and more binding sites are released due

to the deprotonation of functional groups. The surface of biochar is negatively charged when  $\text{pH} > \text{pH}_{\text{pzc}}$ . Therefore, in the higher pH range, the cations can be easily captured by biochar surface (Oh et al., 2012; Li et al., 2013).

Plot of pH against Zeta potential (Figure 5.1) was examined to determine the zero-point charge and the most favourable pH condition for the solution.

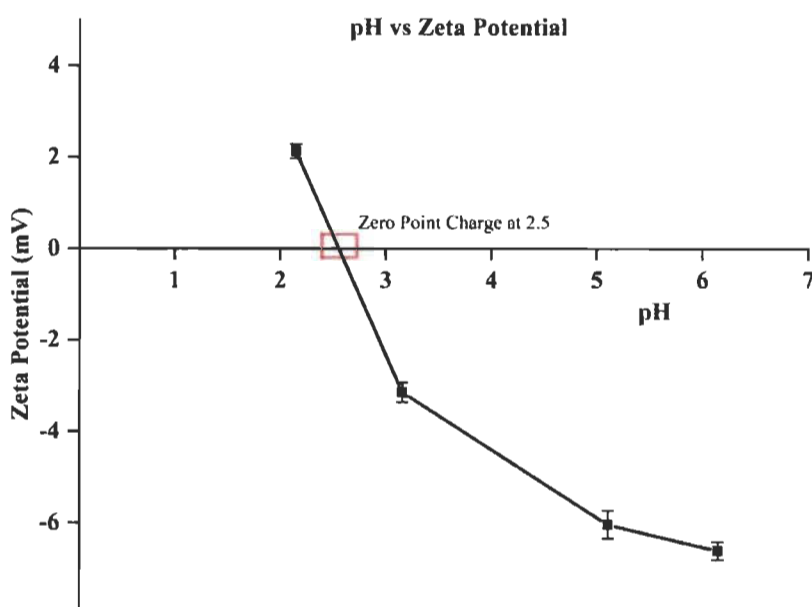


**Figure 5.1** Change in zeta potential with increase in pH of the metal solution

Biochar suspensions in copper solution with different pH were used to measure zeta potential. Since the metal ions are positively charged ( $\text{Cu}^{2+}$ ) more negative surface is favoured for adsorption. From the previous chemical characteristic studies, it was seen that the biochar we synthesized has negatively charged surface because of the acidic sites available. As seen from the plot, PZC is around 2.5 pH that means at this pH, surface is globally neutral. Any pH more than that surface will be negative. The maximum negative zeta potential occurred at pH 6.2. Since the copper from the solution precipitates at this pH or above (Liu et al., 2010), the optimal pH was determined as 5.5. Kołodynska et al. (2012) also had the same observation for pH in adsorption of Cu (II) from water. Therefore, for all the adsorption experiments, the pH of the solution was set in the range of 5.1 to 5.5.

The results were assumed to be same for all biochar samples since the chemical properties were similar for both ultrasound untreated and pre-treated biochar samples (Peter et al. 2019).

### 5.6.3 Adsorption kinetics and statistical analysis

To understand the effect of contact time with adsorption capacity, different kinetic models were examined by fitting the experimental data to corresponding linearized kinetic models. Adsorption kinetics help to describe the physical and chemical characteristics of the biochar, which can be used to explain the surface characteristics of biochar (Lu et al., 2012; Ho and McKay, 1999).

Figure 5.2 shows the evolution of Cu (II) adsorption on biochar (Untreated, UST-3, UST-6, UST-11 and UST-14 as example) with contact time. As seen in the figure, the adsorption capacity gradually increases with time until reaching a maximum value. The variation in experimental data shows that the increasing tendency of the adsorption capacity ( $Q_e$ ) is unique for each biochar samples. However, almost 70 percent of the adsorption occurred within 4 hours and then slowly approached the equilibrium time after 16-24 h. The experimental data fitted only with pseudo second order model (Table 5.3) which was similar to the report by Mohan et al. (2007) for oak and pine wood biochars. Thus, the pseudo first order calculations were omitted.

Pseudo second order kinetics signified that the rate limiting mechanism is mainly by chemisorption which controls the entire adsorption process. Chemisorption involves the valence forces through the sharing or exchange of electrons between adsorbent and adsorbate and therefore the rate of desorption is considered to be negligible. 40 kHz samples tend to show better equilibrium adsorption capacity ( $Q_e$ ) than the untreated sample. UST-8 showed 1.66 mg/g, which is the highest  $Q_e$  among 40 kHz samples. This is almost 52 percent increase when compared to Untreated sample. The lowest of 1.38 mg/g adsorption capacity (UST-4) has an increase of around 26 percent than untreated. Interestingly, the adsorption on 170 kHz was less compared to 40 kHz and showed less or almost similar adsorption with the untreated sample. However, slightly better adsorption rates ( $k$ ) were observed in general for the 170 kHz samples compared to untreated or 40 kHz samples.

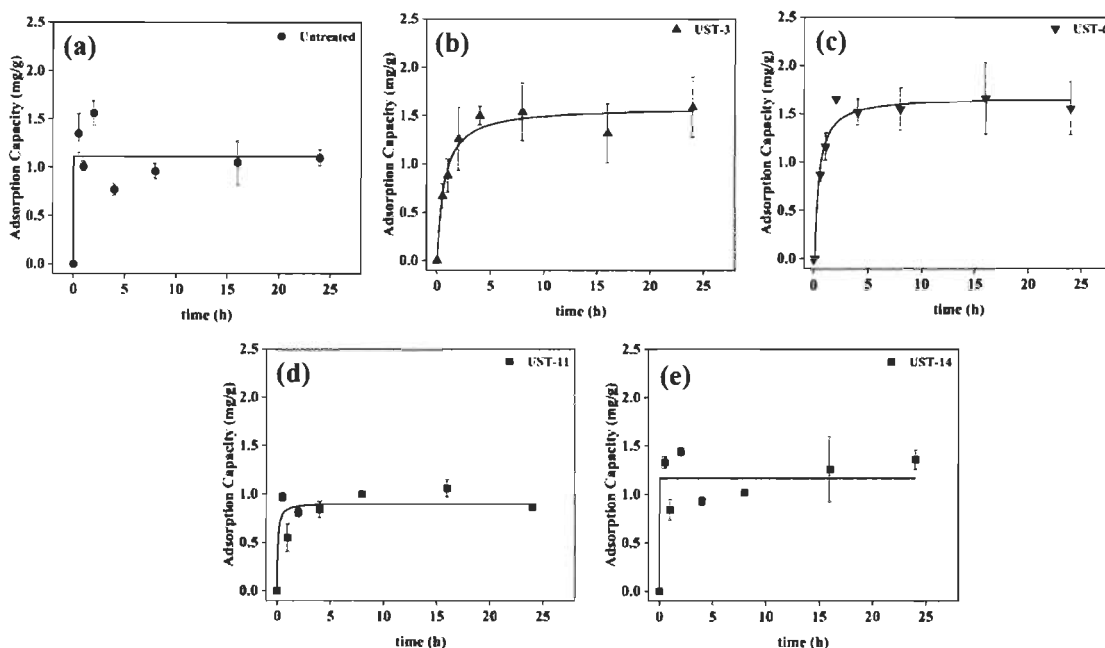


**Figure 5.2** Adsorption capacity of biochar samples with increase in contact time. (a) Untreated biochar, (b) UST-3 (40 kHz, 1000 W, 80 °C for 2 h), (c) UST-6 (40 kHz, 250 W, 20 °C for 1 h), (d) UST-11 (170 kHz, 1000 W, 80 °C for 2 h), and (e) UST-14 (170 kHz, 250 W, 20 °C for 1 h)

As evident from the kinetic data, the main driving force for the heavy metal adsorption on the surface is ionic interactions with the metal ions and surface groups. Therefore, in 170 kHz samples the only available interaction can be these ionic interactions and their specific surface area is too low for adsorptions. Nevertheless, in 40 kHz samples, in addition to the surface functional group interactions, there could be more accessibility of pores, resulting from the surface breakdowns and ruptures in the micro pits. The slight increasing tendency in equilibrium adsorption capacity can be due to this surface modification. These results are in agreement with the surface morphology observed from SEM images.

As explained by He et al. (2017), ultrasonic pre-treatments increase the exposure of the sample to the treatment solutions as well as the general accessibility of the sample, which could possibly lead to better adsorption capacity than higher frequency pre-treated samples. However, the 170 kHz experiments were better with consistency, which could be because of the less heterogeneity in surface structure.

**Table 5.3** Pseudo second order parameters for biochar samples

Sample	Pseudo Second order		
	Q <sub>e</sub> (mg/g)	k (g/mg. min)	R <sup>2</sup>
Untreated	1.09	0.051	0.9928
UST-1	1.62	0.031	0.9905
UST-2	1.59	0.017	0.9928
UST-3	1.54	0.022	0.9869
UST-4	1.38	0.015	0.9619
UST-5	1.45	0.025	0.9904
UST-6	1.6	0.068	0.9931
UST-7	1.54	0.055	0.9923
UST-8	1.66	0.020	0.9942
UST-9	0.92	0.085	0.9946
UST-10	0.98	0.080	0.9906
UST-11	0.92	0.865	0.9862
UST-12	0.79	0.321	0.9626
UST-13	0.94	0.291	0.9857
UST-14	1.42	0.015	0.9761
UST-15	0.75	0.063	0.9848
UST-16	0.78	0.179	0.9992

To understand the effect of each ultrasonic conditions on the equilibrium adsorption capacity, statistical analysis was performed on the experimental data shown in Table 5.3. It was interesting to note that the ultrasonic power, bath temperature and time together affect positively towards the adsorption capacities of 40 kHz samples. The adsorption capacity is highly dependent on the combination of power with time and power with temperature (Figure 5.3a). In case of 170 kHz samples, there was no significant trend observed (Figure 5.3c). All the ultrasound conditions equally contributed to the change in adsorption capacity. The rate constant values (k) for both 40 and 170 kHz samples did not show any significant trend with pre-treatment conditions (Figure 5.3b and 5.3d). These results also demonstrate that the low frequency ultrasound has a higher impact on equilibrium adsorption capacity of the material, yet, no appreciable effect on the speed of adsorption.

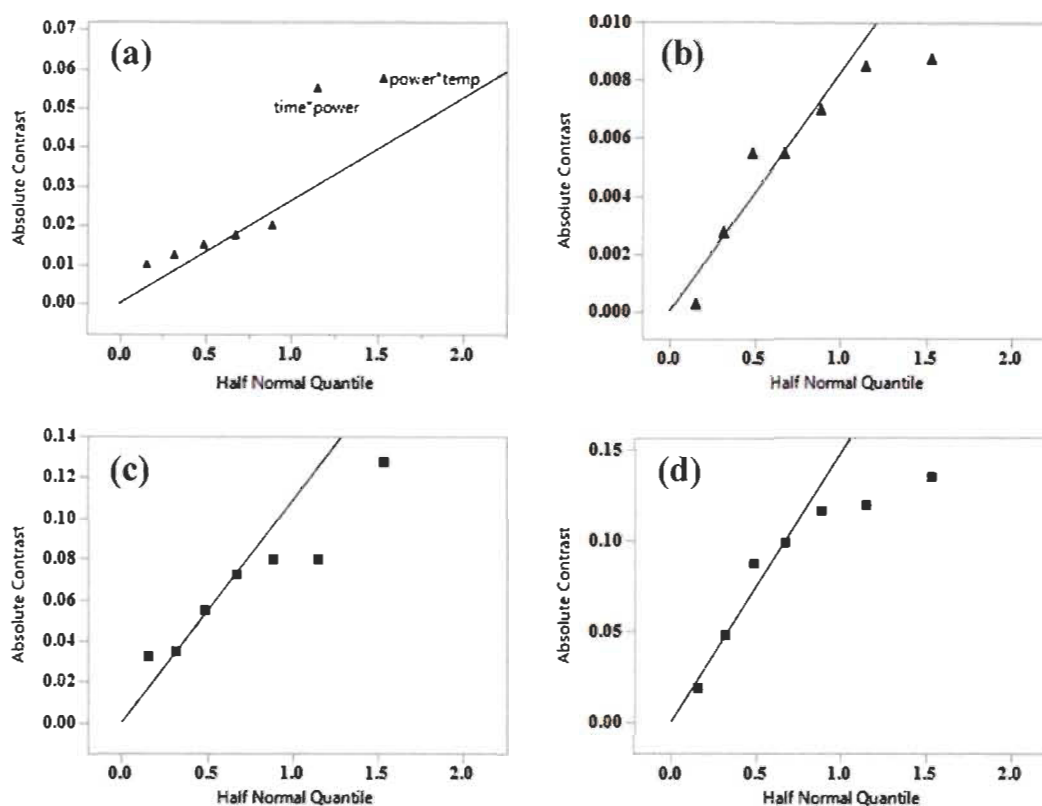


**Figure 5.3** Statistical correlation of ultrasonic pre-treatment conditions on equilibrium adsorption capacity,  $Q_e$  and rate constant  $k$ : a) effect on  $Q_e$  of 40 kHz samples, b) effect on  $k$  of 40 kHz samples, c) effect on  $Q_e$  of 170 kHz samples, and d) effect on  $k$  of 170 kHz samples

High frequency ultrasound, 170 kHz as in here, is not really improving to the adsorption mechanism. These samples are less preferred over untreated samples and 40 kHz as their adsorption capacity at equilibrium is not only improved but also, has been significantly decreased in some cases after ultrasound pre-treatments. The statistical analysis supports the observed fact that the ultrasound pre-treatments affect the surface properties and the low frequency ultrasound enhances the adsorption capacities of metal ions from water. Liu et al. (2010) and Jiang et al. (2016) reported pine wood biochar with 2.75 and 1.47 mg/g adsorption of copper ions respectively. Comparable results were able to achieve by using mixed softwood as feedstock, which is interesting since the adsorption properties are highly depending on feedstock type.

### 5.6.4 Isotherm models and thermodynamics studies

Different adsorption isotherm models were used to describe the adsorbate-adsorbents interaction. Isotherm models were studied for the untreated biochar at maximum and minimum ultrasound pre-treatment conditions (UST-3, UST-6, UST-11 and UST-14) samples for a quick comparison of ultrasound effect in adsorption behaviour. Figure 5.4 represents the trend of change in equilibrium adsorption capacity with increase in equilibrium concentration for synthesized biochar samples (Untreated, UST-3, UST-6, UST-11 and UST-14).

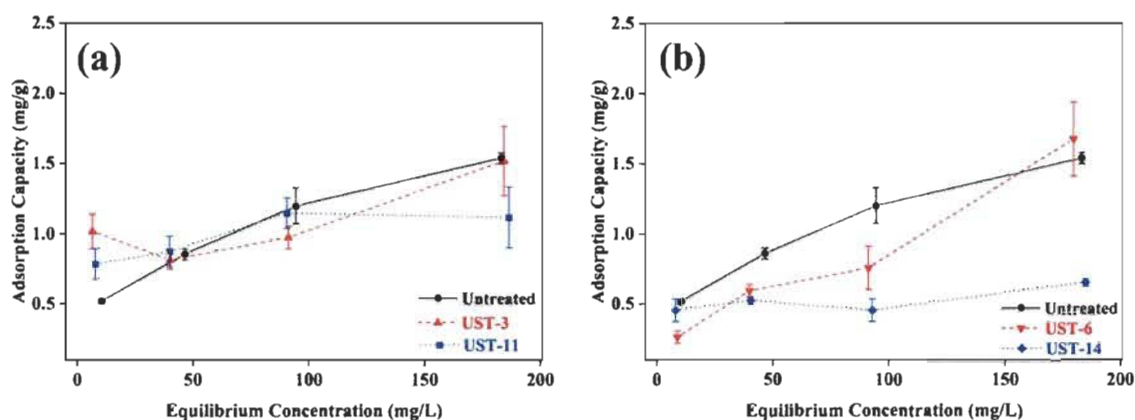


**Figure 5.4** Change in equilibrium adsorption capacity with concentration of metal at equilibrium: (a) Untreated biochar compared with UST-3 (40 kHz, 1000 W, 80 °C for 2 h) and UST- 11 (170 kHz, 1000 W, 80 °C for 2 h), (b) Untreated biochar compared with UST-6 (40 kHz, 250 W, 20 °C for 1 h) and UST-14 (170 kHz, 250 W, 20 °C for 1 h)

The detailed isotherm parameters for the samples are given in Table 5.4. From the regression coefficient  $R^2$ , it was clearly seen that the experimental data for untreated biochar was best fit to the Freundlich isotherm, which explains the heterogeneous adsorption that is not restricted to the formation of a monolayer. The adsorption capacity increased substantially with increasing concentration with a heterogeneity factor ( $n$ ) of 0.38. It could be possible that ultrasound pre-treated samples show comparatively more variation in data points, especially at lower concentrations where less Cu ions are available for adsorption sites, because of the slight irregularity in ultrasound exposure which affects the structural rearrangement.

Interestingly, for ultrasound pre-treated wood biochar, the experimental data followed Langmuir isotherm, irrespective of the ultrasound treatment condition. Langmuir model assumes monolayer adsorption of adsorbate on a homogeneous surface of adsorbent with definite number of adsorption sites having equivalent energy. A significant increase in  $Q_{\max}$  was observed for UST-3 and UST-6 compared with UST-11 and UST-14, also suggesting that the low frequency ultrasound has positive effect on adsorption capacity.

The range of value for  $R_L$  for ultrasound pre-treated samples where between 0 and 1, indicating the adsorption is favourable. As the aggressiveness of ultrasonication decreases (power, temperature and time), the value of  $R_L$  increases and approaching towards unfavourable system. This clearly indicates that the ultrasound pre-treatment favours the adsorption mechanism. Isotherm studies provided a better understanding of the fact that ultrasound pre-treatment could possibly modify the structure of biochar and make it more homogeneous surface.

**Table 5.4** Parameters of linearized Freundlich and Langmuir isotherm models for Cu adsorption on biochar

Sample	Langmuir Model				Freundlich Model		
	$Q_{\max}$	b	$R^2$	$R_L$	$K_f$	n	$R^2$
Untreated	1.82	0.082	0.9735	0.48	5.97	0.38	0.9955
UST-3	1.62	0.091	0.9015	0.47	4.99	0.37	0.2496
UST-6	1.01	0.038	0.9988	0.71	9.71	0.41	0.9621
UST-11	1.17	0.21	0.9957	0.28	5.86	0.15	0.8541
UST-14	0.67	0.030	0.945	0.75	23.4	0.19	0.4384

Most of the previous studies on biochar have reported that the adsorption of contaminants by biochars appeared to be an endothermic process and the adsorption capacity increased with increasing temperature (Liu and Zhang, 2009; Zhang et al., 2013; Meng et al., 2014). The enhanced temperature provides enough energy for metal ions to be captured onto the interior structure of biochar. The values of  $\Delta H^0$ ,  $\Delta S^0$  and  $\Delta G^0$  are used to determine thermodynamically favourable conditions for the adsorption (Al-Anber, 2011). Thermodynamic parameters were examined on the same set of samples used for isotherm studies (UST-3, UST-6, UST-11 and UST-14).

For the 40 kHz samples, higher temperature was favoured with significant increase in adsorption of Cu (II). The 170 kHz samples were not following the expected trend with increase in temperature (Figure 5.5) and hence the thermodynamic parameters were not calculated. The higherequilibrium adsorption capacity at room temperature and loweradsorption capacity at higher temperatures are contradicting the kinetic results of 170 kHz samples. Therefore, the exact adsorption mechanism followed need to be explored further.

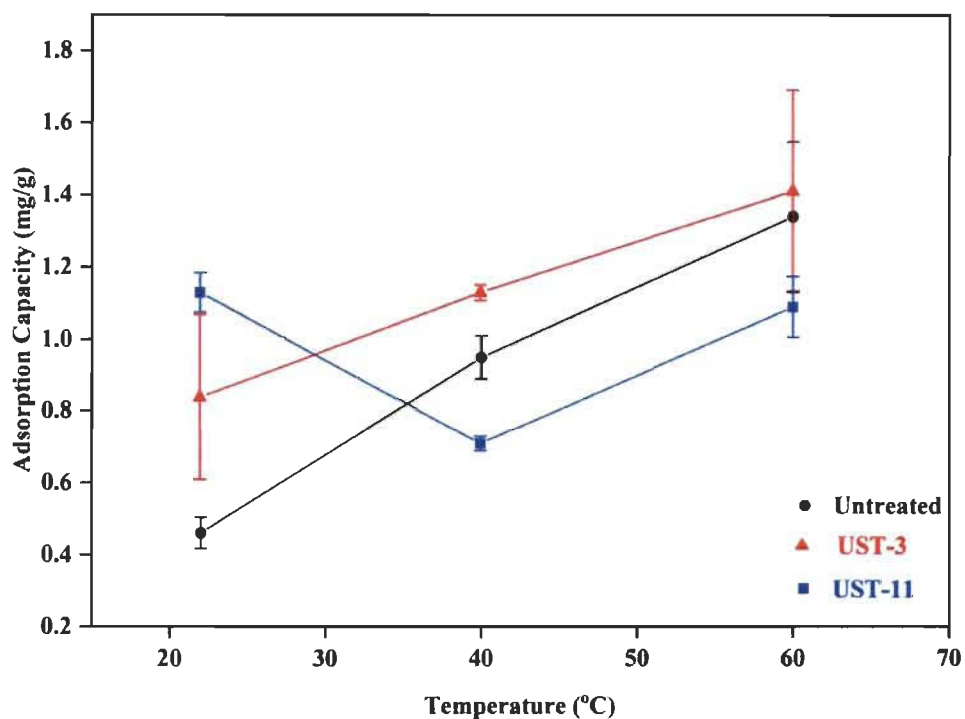


**Figure 5.5** Effect of temperature on equilibrium adsorption capacity of samples untreated, UST-3 (40 kHz, 1000 W, 80 °C for 2 h) and UST-11(170 kHz, 1000 W, 80 °C for 2 h).

The data shown in Table 5.5 describe the thermodynamic parameters of selected biochar samples pre-treated at 40 kHz. As seen in results, the value for  $\Delta H^0$  is positive in all the conditions indicating that the adsorption is endothermic. The positive value of  $\Delta S^0$  indicates the increase in degree of freedom or affinity at the adsorbate/adsorbent interface. This value is very low in case of UST-3 which means that there is not much structural change in adsorbent compared to others.

**Table 5.5** Thermodynamic parameters of copper adsorption on biochar

Sample	Temperature (K)	Thermodynamic parameters		
		$\Delta G^0$ (kJ/mol)	$\Delta H^0$ (kJ/mol)	$\Delta S^0$ (J/mol K)
Untreated	295	12.56	24.11	39.15
	313	11.85		
	333	11.07		
UST 3	295	11.51	11.63	0.43
	313	11.50		
	33	11.49		
UST 6	295	14.68	33.76	64.69
	313	13.51		
	333	12.22		

The Gibb's free energy gave positive value for all the treatments, indicating that the adsorption is non-spontaneous, hence the adsorption and desorption is not in thermal equilibrium. Since the mechanism is found to be chemisorption, the adsorption is irreversible, which can be the possible explanation for positive value of  $\Delta G^0$ . Similar trend was reported before for Cu (II) adsorption on hardwood biochar (Chen et al., 2011). However, the value of  $\Delta G^0$  decreased with increase in temperature, indicating that the system approaches spontaneous when external energy is provided. UST-3 showed almost constant  $\Delta G^0$  at all temperatures, yet the room temperature value was lesser compared with other biochar samples signifying that the adsorption on UST-3 is less non-spontaneous at room temperature and thus slightly more favourable than others. The thermodynamic results also show that the low frequency ultrasound samples are more favoured for Cu (II) adsorption compared to the untreated ones. The thermodynamic experimental values showed comparatively less consistency, especially for UST-3, which could be resulted from the variation in ambient temperature, calibration of the heating stations or higher heterogeneity in surface morphology.

Isotherm and thermodynamic data had shown that the ultrasound pre-treatments have prominent effect on tuning the adsorption behaviour of the biochar. These results also support the kinetic studies, hence motivate to assume that ultrasonic pre-treated samples can be preferred over as-synthesised untreated biochars. Mechanical effect of ultrasound plays a

vital role in enhancing the surface, yet the sonochemistry behind the adsorption mechanism needs further investigation.

### 5.6.5 Comparison with Activated carbon

It was well observed that the ultrasound pre-treated biochars are exhibiting different adsorption capacity than the untreated one. Even though, the increase in adsorption capacity was not much when compared to the materials like activated carbons. Therefore, evaluating the efficiency of biochar we prepared is an important step when it is used in real life applications. Adsorption capacity per unit surface area ( $\text{mg}/\text{m}^2$ ) is an interesting parameter to look in this perception (Choi et al., 2018). Table 5.6 represents the comparison with activated carbon and biochar we synthesised, with the BET specific surface area and corresponding equilibrium adsorption capacity  $Q_e$ . Activated carbon has an equilibrium adsorption capacity of  $4.62 \text{ mg}/\text{g}$ , for a large specific surface of  $718.42 \text{ m}^2/\text{g}$ . The value for adsorption per surface area is very less for activated carbon when compared to ultrasonic pre-treated biochar.

**Table 5.6** Comparison on adsorption capacity with specific surface area

Sample	$Q_e$ ( $\text{mg}/\text{g}$ )	Specific Surface ( $\text{m}^2/\text{g}$ )	Adsorption per unit surface ( $\text{mg}/\text{m}^2$ )
Activated carbon	4.62	718.42	0.0064
Untreated	1.09	10.48	0.104
UST-3	1.54	12.4	0.124
UST-11	0.92	3.31	0.278

Activated carbons are almost 95-99% carbonised materials with ideally no surface functionalities attached. The only interaction with the contaminants in this case is the physisorption on surface sites by Van der Waal types of interactions. Biochar has higher adsorption per specific surface which could be the result of chemisorption at the anchoring surface sites and modification by ultrasound. However, high frequency pre-treated biochar exhibited better efficiency in terms of adsorption per unit surface in contrary to the initial adsorption results. Therefore, activation or chemical modifications on these biochars is of further interest to investigate the ultrasonic pre-treatment effects on chemical modifications

on biochar. This could lead to a cost-effective replacement for activated carbons for heavy metal removal from water.

### 5.7 Conclusions

In this study, we aimed to investigate the physicochemical changes in biochar derived from softwood which are processed under different ultrasonic pre-treatment conditions. Kinetics, isotherm and thermodynamic studies proved that the adsorption properties of ultrasound pre-treated samples differ from untreated and enhanced properties are observed for low frequency pre-treated biochars. These results open the door to a new processing method on wood feedstock to enhance the physical properties of biochar derived from it, without changing the chemical properties. However, chemical modifications on these biochars could be interesting to provide an insight about the effect of ultrasonic pre-treatment on surface functionalisation towards adsorption capacity.

### 5.8 Acknowledgements

The authors gratefully acknowledge all the members of I2E3 for their great support and help during the period of this work. Financing was provided by the Natural Sciences and Engineering Research Council of Canada (NSERC) and by Queen Elizabeth II Diamond Jubilee Scholarship.

### 5.9 References

- [1] Al-Anber, M.A., 2011. Thermodynamics approach in the adsorption of heavy metals. In: Thermodynamics-Interaction Studies-Solids, Liquids and Gases. IntechOpen. <https://doi.org/10.5772/21326>
- [2] Barakat, M., 2011. New trends in removing heavy metals from industrial wastewater. Arab. J. Chem. 4 (4), 361–377. <https://doi.org/10.1016/j.arabjc.2010.07.019>

- [3] Behazin, E., Ogunsona, E., Rodriguez-Uribe, A., Mohanty, A.K., Misra, M., Anyia, A.O., 2016. Mechanical, chemical, and physical properties of wood and perennial grass biochars for possible composite application. *BioResources* 11 (1), 1334–1348. <https://doi.org/10.15376/biores.11.1.1334-1348>
- [4] Brandes, R., Belosinschi, D., Brouillette, F., Chabot, B., 2019. A new electrospun chitosan/ phosphorylated nanocellulose biosorbent for the removal of cadmium ions from aqueous solutions. *J. Environ. Chem. Eng.* 7 (6), 103477. <https://doi.org/10.1016/j.jece.2019.103477>
- [5] Chatterjee, R., Sajjadi, B., Mattern, D.L., Chen, W.-Y., Zubatiuk, T., Leszczynska, D., Leszczynski, J., Egiebor, N.O., Hammer, N., 2018. Ultrasound cavitation intensified amine functionalization: a feasible strategy for enhancing CO<sub>2</sub> capture capacity of biochar. *Fuel* 225, 287–298. <https://doi.org/10.1016/j.fuel.2018.03.145>
- [6] Chen, X., Chen, G., Chen, L., Chen, Y., Lehmann, J., McBride, M.B., Hay, A.G., 2011. Adsorption of copper and zinc by biochars produced from pyrolysis of hardwood and corn straw in aqueous solution. *Bioresour. Technol.* 102 (19), 8877–8884. <https://doi.org/10.1016/j.biortech.2011.06.078>
- [7] Cherpozat, L., Loranger, E., Daneault, C., 2017. Ultrasonic pretreatment effects on the biooil yield of a laboratory-scale slow wood pyrolysis. *J. Anal. Appl. Pyrolysis* 126, 31–38. <https://doi.org/10.1016/j.jaap.2017.06.027>
- [8] Choi, Y.-K., Jang, H.M., Kan, E., Wallace, A.R., Sun, W., 2018. Adsorption of phosphate in water on a novel calcium hydroxide-coated dairy manure-derived biochar. *Environ. Eng. Res.* 24 (3), 434–442. <https://doi.org/10.4491/eer.2018.296>
- [9] Chowdhury, Z.Z., Karim, M.Z., Ashraf, M.A., Khalid, K., 2016. Influence of carbonization temperature on physicochemical properties of biochar derived from slow pyrolysis of durian wood (*Durio zibethinus*) sawdust. *BioResources* 11 (2), 3356–3372. <https://doi.org/10.15376/biores.11.2.3356-3372>

- [10] Han, Y., Boateng, A.A., Qi, P.X., Lima, I.M., Chang, J., 2013. Heavy metal and phenol adsorptive properties of biochars from pyrolyzed switchgrass and woody biomass in correlation with surface properties. *J. Environ. Manag.* 118, 196–204. <https://doi.org/10.1016/j.jenvman.2013.01.001>
- [11] He, Z., Wang, Z., Zhao, Z., Yi, S., Mu, J., Wang, X., 2017. Influence of ultrasound pretreatment on wood physiochemical structure. *Ultrason. Sonochem.* 34, 136–141. <https://doi.org/10.1016/j.ultsonch.2016.05.035>
- [12] Ho, Y.-S., McKay, G., 1999. Pseudo-second order model for sorption processes. *Process Biochem.* 34 (5), 451–465. [https://doi.org/10.1016/S0032-9592\(98\)00112-5](https://doi.org/10.1016/S0032-9592(98)00112-5)
- [13] Inyang, M.I., Gao, B., Yao, Y., Xue, Y., Zimmerman, A., Mosa, A., Pullammanappallil, P., Ok, Y.S., Cao, X., 2016. A review of biochar as a low-cost adsorbent for aqueous heavy metal removal. *Crit. Rev. Environ. Sci. Technol.* 46 (4), 406–433. <https://doi.org/10.1080/10643389.2015.1096880>
- [14] Jia, M., Wang, F., Bian, Y., Jin, X., Song, Y., Kengara, F.O., Xu, R., Jiang, X., 2013. Effects of pH and metal ions on oxytetracycline sorption to maize-straw-derived biochar. *Bioresour. Technol.* 136, 87–93. <https://doi.org/10.1016/j.biortech.2013.02.098>
- [15] Jiang, S., Huang, L., Nguyen, T.A., Ok, Y.S., Rudolph, V., Yang, H., Zhang, D., 2016. Copper and zinc adsorption by softwood and hardwood biochars under elevated sulphate-induced salinity and acidic pH conditions. *Chemosphere* 142, 64–71. <https://doi.org/10.1016/j.chemosphere.2015.06.079>
- [16] Jiang, S., Nguyen, T.A., Rudolph, V., Yang, H., Zhang, D., Ok, Y.S., Huang, L., 2017. Characterization of hard-and softwood biochars pyrolyzed at high temperature. *Environ. Geochem. Health* 39 (2), 403–415. <https://doi.org/10.1007/s10653-016-9873-6>

- [17] Jindo, K., Mizumoto, H., Sawada, Y., Sanchez-Monedero, M.A., Sonoki, T., 2014. Physical and chemical characterization of biochars derived from different agricultural residues. *Biogeosciences* 11 (23), 6613–6621. <https://doi.org/10.5194/bg-11-6613-2014>
- [18] Kołodyńska, D., Wnętrzak, R., Leahy, J., Hayes, M., Kwapiński, W., Hubicki, Z., 2012. Kinetic and adsorptive characterization of biochar in metal ions removal. *Chem. Eng. J.* 197, 295–305. <https://doi.org/10.1016/j.cej.2012.05.025>
- [19] Leong, T., Ashokkumar, M., Kentish, S., 2011. The Fundamentals of Power Ultrasound – A Review. <http://hdl.handle.net/11343/123494>
- [20] Li, M., Liu, Q., Guo, L., Zhang, Y., Lou, Z., Wang, Y., Qian, G., 2013. Cu (II) removal from aqueous solution by *Spartina alterniflora* derived biochar. *Bioresour. Technol.* 141, 83–88. <https://doi.org/10.1016/j.biortech.2012.12.096>
- [21] Liu, Z., Zhang, F.-S., 2009. Removal of lead from water using biochars prepared from hydrothermal liquefaction of biomass. *J. Hazard. Mater.* 167 (1–3), 933–939. <https://doi.org/10.1016/j.jhazmat.2009.01.085>
- [22] Liu, Z., Zhang, F.-S., Wu, J., 2010. Characterization and application of chars produced from pinewood pyrolysis and hydrothermal treatment. *Fuel* 89 (2), 510–514. <https://doi.org/10.1016/j.fuel.2009.08.042>
- [23] Loranger, É., Pombert, O., Drouadaine, V., 2016. Ultrasonic Pre-treatments of Wood Chips Used in a Conventional Pyrolysis and their Effect on Bio-oil Composition and Calorimetry. (SAMPE Conference Proceedings).
- [24] Lu, H., Zhang, W., Yang, Y., Huang, X., Wang, S., Qiu, R., 2012. Relative distribution of Pb<sup>2+</sup> sorption mechanisms by sludge-derived biochar. *Water Res.* 46 (3), 854–862. <https://doi.org/10.1016/j.watres.2011.11.058>
- [25] Manyà, J.J., 2012. Pyrolysis for biochar purposes: a review to establish current knowledge gaps and research needs. *Environ. Sci. Technol.* 46 (15), 7939–7954. <https://doi.org/10.1021/es301029g>

- [26] Meng, J., Feng, X., Dai, Z., Liu, X., Wu, J., Xu, J., 2014. Adsorption characteristics of Cu (II) from aqueous solution onto biochar derived from swine manure. *Environ. Sci. Pollut. Res.* 21 (11), 7035–7046. <https://doi.org/10.1007/s11356-014-2627-z>
- [27] Mohan, D., Pittman Jr., C.U., Bricka, M., Smith, F., Yancey, B., Mohammad, J., Steele, P.H., Alexandre-Franco, M.F., Gómez-Serrano, V., Gong, H., 2007. Sorption of arsenic, cadmium, and lead by chars produced from fast pyrolysis of wood and bark during bio-oil production. *J. Colloid Interface Sci.* 310 (1), 57–73. <https://doi.org/10.1016/j.jcis.2007.01.020>
- [28] Mohan, D., Rajput, S., Singh, V.K., Steele, P.H., Pittman Jr., C.U., 2011. Modeling and evaluation of chromium remediation from water using low cost bio-char, a green adsorbent. *J. Hazard. Mater.* 188 (1–3), 319–333. <https://doi.org/10.1016/j.jhazmat.2011.01.127>
- [29] Mohan, D., Sarswat, A., Ok, Y.S., Pittman Jr., C.U., 2014. Organic and inorganic contaminants removal from water with biochar, a renewable, low cost and sustainable adsorbent—a critical review. *Bioresour. Technol.* 160, 191–202. <https://doi.org/10.1016/j.biortech.2014.01.120>
- [30] Mukome, F.N., Zhang, X., Silva, L.C., Six, J., Parikh, S.J., 2013. Use of chemical and physical characteristics to investigate trends in biochar feedstocks. *J. Agric. Food Chem.* 61 (9), 2196–2204. <https://doi.org/10.1021/jf3049142>
- [31] Nartey, O.D., Zhao, B., 2014. Biochar preparation, characterization, and adsorptive capacity and its effect on bioavailability of contaminants: an overview. *Adv. Mater. Sci. Eng.* 2014. <https://doi.org/10.1155/2014/715398>
- [32] Oh, T.-K., Choi, B., Shinogi, Y., Chikushi, J., 2012. Effect of pH conditions on actual and apparent fluoride adsorption by biochar in aqueous phase. *Water Air Soil Pollut.* 223 (7), 3729–3738. <https://doi.org/10.1007/s11270-012-1144-2>

- [33] Oliveira, F.R., Patel, A.K., Jaisi, D.P., Adhikari, S., Lu, H., Khanal, S.K., 2017. Environmental application of biochar: current status and perspectives. *Bioresour. Technol.* 246, 110–122. <https://doi.org/10.1016/j.biortech.2017.08.122>
- [34] Özcan, A., Öncü, E.M., Özcan, A.S., 2006. Kinetics, isotherm and thermodynamic studies of adsorption of Acid Blue 193 from aqueous solutions onto natural sepiolite. *Colloids Surf. A* 277 (1–3), 90–97. <https://doi.org/10.1016/j.colsurfa.2005.11.017>
- [35] Peter, A., Chabot, B., Loranger, E., 2019. Enhancing surface properties of softwood biochar by ultrasound assisted slow pyrolysis. In: 2019 IEEE International Ultrasonics Symposium (IUS). IEEE, pp. 2477–2480. <https://doi.org/10.1109/ULTSYM.2019.8925793>
- [36] Prasad, K.K., Raheem, S., 1992. Evaluation of colour changes of indicators in the titration of cadmium with EDTA. *Anal. Chim. Acta* 264 (1), 137–140. [https://doi.org/10.1016/0003-2670\(92\)85308-S](https://doi.org/10.1016/0003-2670(92)85308-S)
- [37] Qiu, S., Wang, Z., He, Z., Yi, S., 2016. The Effect of Ultrasound Pretreatment on Poplar Wood Dimensional Stability. *BioResources* 11 (3), 7811–7821. <https://doi.org/10.15376/biores.11.3.7811-7821>
- [38] Sajjadi, B., Broome, J.W., Chen, W.Y., Mattern, D.L., Egiebor, N.O., Hammer, N., Smith, C.L., 2019. Urea functionalization of ultrasound-treated biochar: a feasible strategy for enhancing heavy metal adsorption capacity. *Ultrason. Sonochem.* 51, 20–30. <https://doi.org/10.1016/j.ultsonch.2018.09.015>
- [39] Shen, Z., Zhang, Y., Jin, F., Alessi, D.S., Zhang, Y., Wang, F., McMillan, O., Al-Tabbaa, A., 2018. Comparison of nickel adsorption on biochars produced from mixed softwood and Miscanthus straw. *Environ. Sci. Pollut. Res.* 25 (15), 14626–14635. <https://doi.org/10.1007/s11356-018-1674-2>

- [40] Sun, Y., Gao, B., Yao, Y., Fang, J., Zhang, M., Zhou, Y., Chen, H., Yang, L., 2014. Effects of feedstock type, production method, and pyrolysis temperature on biochar and hydrochar properties. *Chem. Eng. J.* 240, 574–578. <https://doi.org/10.1016/j.cej.2013.10.081>
- [41] Tan, X., Liu, Y., Zeng, G., Wang, X., Hu, X., Gu, Y., Yang, Z., 2015. Application of biochar for the removal of pollutants from aqueous solutions. *Chemosphere* 125, 70–85. <https://doi.org/10.1016/j.chemosphere.2014.12.058>.
- [42] Zhang, W., Mao, S., Chen, H., Huang, L., Qiu, R., 2013a. Pb (II) and Cr (VI) sorption by biochars pyrolyzed from the municipal wastewater sludge under different heating conditions. *Bioresour. Technol.* 147, 545–552. <https://doi.org/10.1016/j.biortech.2013.08.082>
- [43] Zhang, Z., Cao, X., Liang, P., Liu, Y., 2013b. Adsorption of uranium from aqueous solution using biochar produced by hydrothermal carbonization. *J. Radioanal. Nucl. Chem.* 295 (2), 1201–1208. <https://doi.org/10.1007/s10967-012-2017-2>

### 5.10 Highlights

- Ultrasound pre-treatment effects on heavy metal adsorption properties of biochar
- Enhanced adsorption properties of biochar by mechanical effect of ultrasound
- $Q_e$ (mg/g) depends on the combination of ultrasound power versus time and temperature
- Adsorption per unit surface area depends on the frequency of ultrasound

## Chapter 6 – Scientific Article 3: Alkali Activation and Influence of Ultrasonic Pre-treatments

### 6.1 Preface

As a continuation of previous article, this study discusses about the two-step activation of biochar we already synthesized and its effect towards heavy metal adsorption from water. Biochar derived from ultrasound pre-treated woodchips were subjected to alkali activation for further enhancement of the adsorption properties. The adsorption kinetics, isotherm and thermodynamic parameters were examined to understand influence of ultrasound pre-treatments on chemical activation. This work was published in Journal of Environmental Management (DOI: <https://doi.org/10.1016/j.jenvman.2021.112569>) entitled *Enhanced activation of ultrasonic pre-treated softwood biochar for efficient heavy metal removal from water*.

#### Author Details:

Aneeshma Peter, Int. BS-MS

Ph.D. Student, Sciences de l'énergie et des matériaux

I2E3 – Institut d'Innovations en Écomatériaux, Écoproduits et Écoénergies, à base de biomasse, Université du Québec à Trois-Rivières, P.O. Box 500, Trois-Rivières, Québec, Canada, G9A 5H7

Email: [Aneeshma.Peter@uqtr.ca](mailto:Aneeshma.Peter@uqtr.ca)

Eric Loranger, Ph.D.

Research director and corresponding author

I2E3 – Institut d'Innovations en Écomatériaux, Écoproduits et Écoénergies à base de biomasse, Université du Québec à Trois-Rivières, P.O. Box 500, Trois-Rivières, Québec, Canada, G9A 5H7

Email: [Eric.loranger1@uqtr.ca](mailto:Eric.loranger1@uqtr.ca)

Bruno Chabot, Ph.D.

Co-director and co-author

I2E3 – Institut d’Innovations en Écomatériaux, Écoproduits et Écoénergies à base de biomasse, Université du Québec à Trois-Rivières, P.O. Box 500, Trois-Rivières, Québec, Canada, G9A 5H7

Email: [Bruno.Chabot@uqtr.ca](mailto: Bruno.Chabot@uqtr.ca)

#### **Author Credits:**

**Aneeshma Peter:** Methodology, Validation, Investigation, Data curation, Formal analysis, Writing - original draft, Visualization

**Bruno Chabot:** Conceptualization, Project administration, Writing - review & editing

**Eric Loranger:** Conceptualization, Project administration, Supervision, Writing - review & editing, Funding acquisition

## **6.2 Résumé**

L'élimination des métaux lourds en utilisant le biochar comme adsorbant efficace est un centre d'intérêt pour de nombreux chercheurs, car ils sont peu dispendieux, respectueux de l'environnement et ont de bonnes propriétés physicochimiques. La modification physique et chimique du biochar est une approche intéressante pour améliorer davantage les propriétés d'adsorption. En effet, des études ont montré que les traitements par ultrasons ainsi que l'activation alcaline sur le biochar ont un impact positif sur le comportement d'adsorption du matériau. L'activation chimique à l'aide de NaOH et KOH a démontré la capacité d'améliorer les caractéristiques de surface du biochar en augmentant la surface spécifique, la porosité et la présence de groupements fonctionnels contenant de l'oxygène sur la surface. L'activation de base sur le biochar dérivé de copeaux de bois prétraités par ultrasons a été étudiée pour comprendre l'influence du prétraitement par ultrasons sur la modification chimique du biochar et les propriétés d'adsorption qui en ont émergé. Des copeaux de bois résineux prétraités aux ultrasons de 40 et 170 kHz ont été soumis à une pyrolyse à l'échelle du

laboratoire et les biochars résultants ont été traités avec du NaOH. Les biochars synthétisés ont été caractérisés en utilisant la spectroscopie infrarouge, la microscopie électronique à balayage, la spectroscopie aux rayons X à dispersion d'énergie et la surface de Brunauer, Emmett et Teller (BET). La cinétique d'adsorption, l'isotherme et le comportement thermodynamique ont été examinés en utilisant le cuivre comme métal modèle. L'adsorption sélective des métaux lourds de l'eau a également été étudiée en utilisant des solutions métalliques mixtes de  $Pb^{2+}$ ,  $Cu^{2+}$  et  $Ni^{2+}$ . Les propriétés physicochimiques ont été examinées et les expériences d'adsorption ont révélé que les biochars fabriqués par prétraitements ultrasoniques ont une meilleure capacité d'adsorption par rapport aux échantillons de biochar non traités après activation. L'échantillon prétraité de 170 kHz a présenté une capacité d'adsorption à l'équilibre de 19,65 mg/g, ce qui est presque 20 fois plus élevé que celui de l'échantillon non activé correspondant. Les échantillons prétraités par ultrasons ont aussi montré un comportement d'adsorption compétitif amélioré vis-à-vis les ions cuivre par rapport au nickel ou au plomb. L'étude globale suggère que les biochars prétraités par ultrasons, combinés à une activation alcaline, améliorent grandement l'efficacité d'élimination des métaux lourds. Elle démontre aussi que les biochars peuvent être utilisés comme adsorbants efficaces dans le domaine du traitement des eaux usées.

### 6.3 Abstract

Physical and chemical modification on biochar is an interesting approach to enhance the properties and make them potential candidates in adsorption of heavy metals from water. Studies have shown that ultrasound treatments as well as alkali activations on biochar has positive impact on adsorption behaviour of the material. Base activation on biochar derived from ultrasound pre-treated woodchips were studied to understand the influence of ultrasound pre-treatment on chemical modification of biochar and the adsorption properties emerged from it. 40 and 170 kHz ultrasound pre-treated softwood woodchips were subjected to laboratory scale pyrolysis and the resulted biochars were treated with NaOH. The physicochemical properties were examined, and the adsorption experiments revealed that ultrasound pre-treatment assisted biochars have better adsorption capacity as compared to untreated biochar samples after activation. 170 kHz pre-treated sample exhibited an equilibrium adsorption capacity of 19.99 mg/g which is almost 22 times higher than that of

corresponding non-activated sample. The ultrasound pre-treated samples showed improved competitive adsorption behaviour towards copper ions in comparison with nickel or lead. The overall study suggests that ultrasound pre-treated biochars combined with alkali activation enhances the heavy metal removal efficiency and these engineered biochars can be used as an effective adsorbent in the field of wastewater treatment.

**Keywords:** Biochar, softwood chips, ultrasound pre-treatments, base activation, adsorption properties, heavy metal removal

#### 6.4 Introduction

Fresh water contamination prevailing due to non-biodegradable pollutants have been an alarming issue during the past few decades. Rapid industrialization, urbanization, energy generation, improper waste management and other anthropogenic sources have been significantly contributed towards the environmental and health risks arising from these contaminants (Masindi and Muedi, 2018; Inyang et al., 2016). Heavy metals subsidizing a major share have grown high concern due to their reluctance and persistence in the environment and their ability to enter food chain through bioaccumulation. Severe health hazards associated with these toxic metals require the development of effective methodologies to remove them from industrial effluents, thereby ensure sustainability of water resources and control the toxic impacts on living organisms (Barakat, 2011). Electrocoagulation, membrane filtration, and precipitation are few among them. However, higher operational cost, lower selectivity, complex processability and production of hazardous by-products made them less effective in large-scale applications (Ince and Ince, 2017).

Design flexibility and regenerability of adsorbent materials have promoted adsorption as an economic and effective method for heavy metal removal. Among them, activated carbons (AC) are most predominant due to their ability in wastewater treatment and eco-friendly nature. Nevertheless, depletion in natural reserves of coal, one of the primary sources for AC, has steeply increased the price of this material. They also lack exchange capacity depending on the synthesis routes used, which is an important physicochemical property for the removal of heavy metals (Mohan and Pittman Jr, 2007).

In recent years, biochar has motivated many researchers due to its multi-functionality and effective properties compared to charcoal or other activated carbon materials. Proper specific surface area, porosity and availability of surface functional groups etc makes them a better alternative to other carbon materials for adsorption. Adsorption of various heavy metals like aluminium, arsenic, cadmium, chromium, copper, lead, mercury, nickel, uranium, and zinc are well studied using biochar as adsorbent (Tan et al., 2015; Mohan et al., 2014). A proper understanding of the physicochemical characteristics of biochar and its structure-property relationship towards the heavy metal removal can aid to develop new methodology with enhanced adsorption properties.

Activation is the important technique to improve adsorption efficiency through modification of the surface morphology by increasing the specific surface area and porosity. Physical and chemical activations are mostly used to enhance the adsorption behaviour of materials like biochar (Sajjadi et al., 2019; Angin et al., 2013). Physical activation makes use of high temperature techniques involving steam, CO<sub>2</sub> or other gaseous forms or mechanical forces like ultrasonication to modify the structure of material. The latter technique involves the impregnation of acid or base onto the carbon materials thereby modifying the surface morphology. Chemical activation is normally preferred over physical activation because of high yield, lower temperatures and short activation time compared to other techniques. The mechanism of chemical activation is not well understood, though it assumes that the chemical activation agent forms a cluster of micro- and meso- pores that significantly enhance the surface area and activates oxygen-rich surface functional groups (Prapagdee et al., 2016). Studies suggest that physical mixing of wood biochar with NaOH increases the specific surface area and adsorption capacity of pharmaceutical compounds from aqueous solution (Taheran et al., 2016). Li et al. (2017) observed that Cd sorption capacity of NaOH activated rape straw biochar was 92% greater as compared to untreated biochar. Economically feasible and effective activation methods are recommended in this perspective, thereby improving the material efficiency.

Very few reports were encountered on investigating ultrasound assisted chemical modification of biochar. Chattergee et al. (2018) has shown that ultrasound-intensified amination enhances the CO<sub>2</sub> capture capacity of biochar derived from pinewood. Similarly,

a study by Sajjadi et al. (2019) demonstrated that functionalisation of low frequency modified biochar using urea has positively affected metal adsorption capacities of pine wood biochar. Recently, we have seen that ultrasonic pre-treatment influences the adsorption behaviour of softwood-derived biochar with an enhancement of equilibrium adsorption under low frequency exposure (Peter et al., 2020). The 40 kHz pre-treated samples exhibited maximum of 52 percent increase in equilibrium adsorption capacity ( $Q_e$ ) when compared with untreated biochars. Adsorption characteristics were dependent on the frequency in combination with power versus time and temperature of ultrasound. Detailed investigation on kinetic, isotherm and thermodynamic models showed that the mechanical effect of ultrasound plays a vital role in enhancing the surface. However, mechanism behind high and low frequency pre-treated samples were different from each other, which motivated us to explore the pre-treatment assisted activation on these biochar samples.

Herein, we are evaluating the effect of ultrasound pre-treatments towards the base activation process in biochar and thereby influencing the metal adsorption behaviour of the materials. Due to the heterogeneity and feedstock dependency for physicochemical properties, mix-wood chips are rarely used for adsorption studies, therefore comparable studies available for activation and adsorption using biochar derived from mixed softwood is limited (Chen et al., 2011; Shen et al., 2018; Tomczyk et al., 2020). To the best of our knowledge, this is the first ever study focusing on the effect of combination of alkali activation towards power ultrasound pre-treated mix-wood biochar and study its heavy metal removal efficiency from water. This study focuses on potential application of biochar from sustainable resources like biomass and validating methodologies to improve its efficiency. Efficient large-scale use of these biochars will be a significant footstep in the field of emerging materials for environmental protection.

## **6.5 Materials & Methods**

### **6.5.1 Biochar production**

The biochar used in this study were produced from mix of softwood, which are post-consumer feedstocks from a local Canadian pulp and paper mill. The wood chips (5 mm by

5 mm sized needles) were processed under different ultrasonic pre-treatment conditions as discussed in our previous publications. (Peter et al., 2020; Peter et al., 2019). It was seen that the combination of power, time and bath temperature equally contributed towards adsorption capacities of the material. Hence, the maximum and minimum pre-treatment conditions were used in this work (Table 6.1) to investigate the pre-treatment effect on activation of biochar. The pre-treated woodchips were dried in an oven at 105 °C for at least 48 h before being used in the pyrolysis reactor. Slow pyrolysis was performed in a laboratory-scale set up as reported previously by Loranger et al. (2016). Each pyrolysis was performed three times to confirm consistency and the products were collected separately. The resulting biochar was subjected to alkali activation. The physicochemical characteristics of biochar were studied before and after base-activation.

**Table 6.1** List of ultrasound pre-treatments on woodchips

Sample Code	Frequency (kHz)	Power (W)	Temperature (°C)	Time (h)
Act-Untreated	-	-	-	-
Act-UST1	40	1000	80	2
Act-UST2	40	250	20	1
Act-UST3	170	1000	80	2
Act-UST4	170	250	20	1

### 6.5.2 Base activation of as-synthesized biochar

The alkali modification was done as previously reported by Taheran et al. (2016). About 10 g of NaOH were dissolved in 50 mL of water and 5 g of biochar were added to it. The mixture was stirred at room temperature for 3 h, filtered and dried at 105 °C for 24 h. This sample was placed in a quartz-tube furnace under argon flow. The temperature was increased to 800 °C at 10 °C/min and held at this temperature for 2 h before cooling down to room temperature. Then, the product was washed with water and the NaOH was neutralized with 0.1 M HCl. Inorganic-by-product was removed by water wash and the resulting product was dried at 60 °C for 24 h. Base activated samples, pre-treated with ultrasounds, are identified as Act-UST throughout the study.

### 6.5.3 Characterisation of biochar

About 1:10 weight by volume biochar and deionized water ratio were stirred at room temperature for 2 h. The pH of the sample was measured using Accumet XL20, Thermo Fisher Scientific pH-meter and the surface zeta potential (mV) was measured with Zetasizer-nano series from Malvern Instruments. The reflection mode infrared spectra were recorded in Nicolet iS10 Smart iTR Infrared Spectroscopy instrument using KBr pellet in the range of 400-4000  $\text{cm}^{-1}$  for a minimum of 16 scans with 1  $\text{cm}^{-1}$  resolution. The surface morphology of the biochar was studied using Scanning Electron Microscopy (SEM) images captured using Hitachi SU1510 instrument. Energy Dispersive X-ray Spectroscopy (EDX) was obtained with X-Max, Oxford instrument to verify the surface carbon and oxygen content. Surface area was measured using the Brunauer, Emmett and Teller (BET) method that measures  $\text{N}_2$  gas sorption ( $0.162 \text{ nm}^2$ ) at 77 K. Approximately 100 mg of biochar was outgassed at 200  $^\circ\text{C}$  for 16 h and then analysed on an Autosorb-1 Surface Area Analyzer by Quantachrome Instruments.

### 6.5.4 Adsorption experiments

The metal adsorption behaviour of biochar was studied using batch adsorption technique with copper as model metal contaminant. 1000 ppm stock solution of Cu (II) was prepared by dissolving analytical grade anhydrous  $\text{CuSO}_4$  in deionized water. The pH of salt solution was maintained at 5 to avoid salt precipitation at higher pH. In a 125 mL Erlenmeyer flask, 5 g/L biochar was added to 100 ppm Cu (II) solution and agitated on a reciprocating shaker at room temperature ( $22 \pm 2 \text{ }^\circ\text{C}$ ) at 150 rpm. For the kinetic experiments, samples were taken at specific time intervals and immediately filtered using Whatman No. 1 filter paper. The residual heavy metal concentration in the filtrate was measured using EDTA titration described by Prasad and Raheem, (1993). The amount of adsorbed metal ions,  $Q$  (mg/g), was calculated using Equation 3.1.

$$Q = \frac{(C_{initial} - C_{final}) * V}{m} \quad \text{Equation 3.1}$$

The experimental data was fitted to nonlinear forms of Pseudo First and Pseudo Second order kinetic models using Equation 3.2 and 3.3, respectively.

$$Q_t = Q_e(1 - e^{-k_1 t}) \quad \text{Equation 3.2}$$

$$Q_t = \frac{k_2 Q_e^2 t}{1 + k_2 Q_e t} \quad \text{Equation 3.3}$$

Where  $Q_t$  and  $Q_e$  (mg/g) are adsorbed metal amount at time  $t$  (min) and equilibrium,  $k_1$  and  $k_2$  are the rate constants for pseudo first order and second order kinetic model, respectively.

Most common isotherm models for biochar adsorption, Langmuir and Freundlich were examined with initial Cu (II) concentrations ranging from 10 to 100 ppm using nonlinear regression with Eq. (3.6) and (3.8), respectively.

$$Q_e = \frac{(Q_{\max} * b * C_e)}{(1 + b * C_e)} \quad \text{Equation 3.6}$$

$$Q_e = K_f C_e^{1/n} \quad \text{Equation 3.8}$$

Where  $Q_e$  is the amount of the metal adsorbed at equilibrium (mg/g),  $C_e$  is the equilibrium concentration of solution (mg/L).  $K_f$  and  $n$  are indicators of adsorption capacity and intensity, respectively.  $Q_{\max}$  is the maximum adsorption capacity (mg/g) and  $b$  is related to degree of adsorption affinity of the adsorbate.

The temperature effect was assessed at temperatures 25, 40, and 60 °C and the thermodynamic parameters were calculated as explained in literatures (Al-Anber, 2011; Batool et al., 2018).

### 6.5.5 Multicomponent adsorption

Isotherm experiments were carried out at room temperature by adding 5 g/L biochar to 125 mL Erlenmeyer flask containing tertiary metal solutions ( $Pb^{2+}$ ,  $Cu^{2+}$  and  $Ni^{2+}$ ) were prepared respectively with  $Pb(NO_3)_2$ , anhydrous  $CuSO_4$  and  $Ni(NO_3)_2 \cdot 6H_2O$ .

The concentration of Cu (II) and Ni (II) ions were ranged from 10 ppm to around 80 ppm in the initial mixed metal solution. However, at higher concentration Pb (II) started to precipitate resulting in lower concentration in the mixed solution. Therefore, the initial concentration of Pb (II) was ranged from 10 ppm to around 40 ppm in the tertiary metal system. Initial pH of the metal solutions was adjusted to about 5.0 using 0.1 M HCl and 0.1 M NaOH to avoid precipitation. The mixture was shaken for 3 h in a rotary shaker to ensure the equilibrium was reached and filtered using Whatman 1 filter paper. Concentrations of  $\text{Pb}^{2+}$ ,  $\text{Cu}^{2+}$  and  $\text{Ni}^{2+}$  in the filtrate were determined using MP–AES (4210 Agilent CrossLab, USA). The adsorption capacities were calculated using Equation 3.1.

#### **6.5.6 Statistical regression for experimental data**

All the adsorption experiments were performed three times to ensure consistency and the mean values reported with standard error in experimental plots. Experimental data were fitted with non-linear forms of equation using OriginPro software (version 9.6).

### **6.6 Results and Discussion**

#### **6.6.1 Effect of alkali activation after ultrasound pre-treatment on surface morphology and chemical properties of biochar**

Scanning Electron Microscope images were captured and examined to understand the pre-treatment induced activation effects on surface morphology (Figure 6.1).

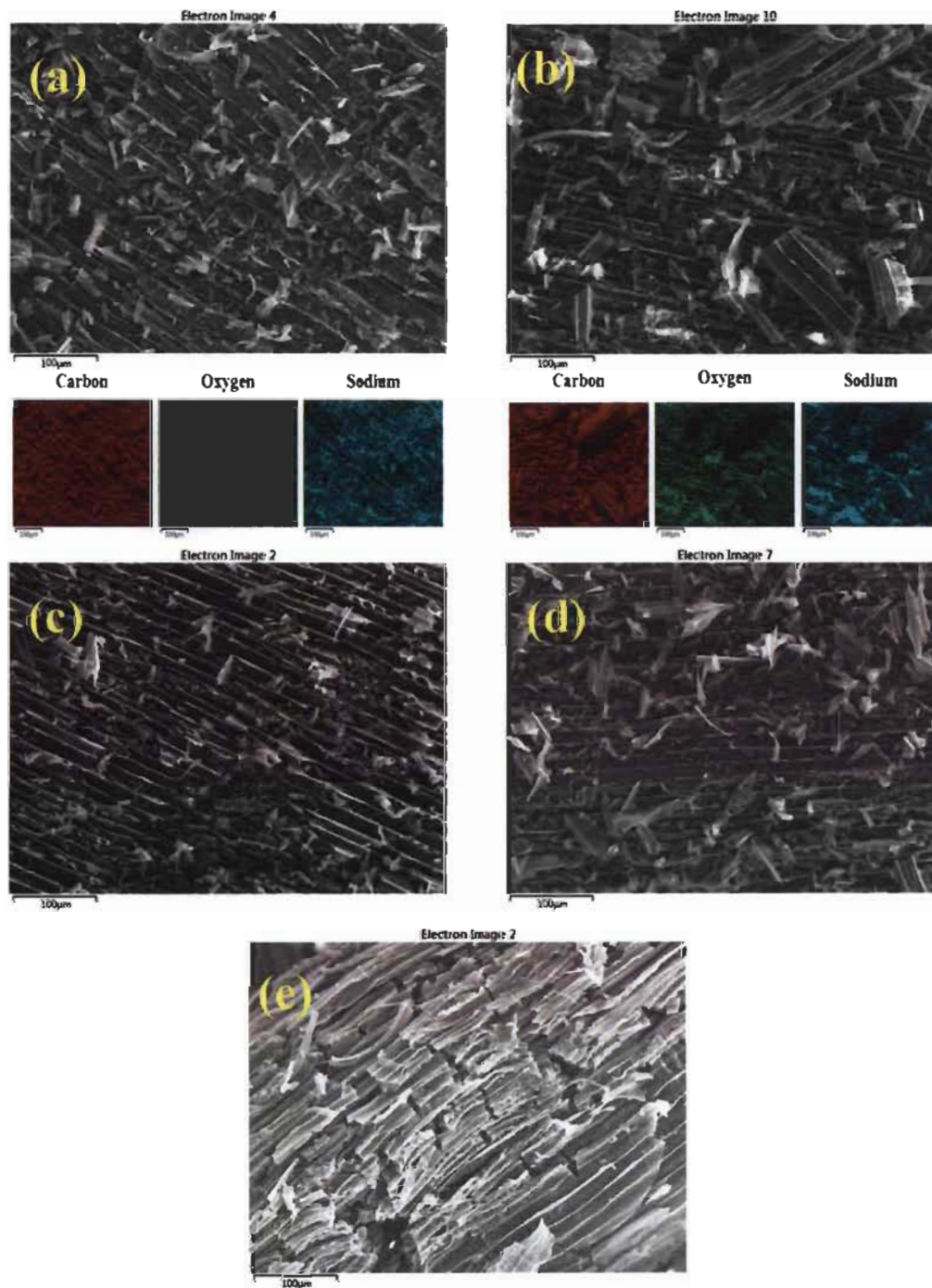


**Figure 6.1** Scanning electron Microscope images with EDX mapping of: (a) Act-UST1 (40 kHz, 1000 W at 80 °C for 2 h), (b) Act-UST3 (170 kHz, 1000 W at 80 °C for 2 h) and Scanning electron microscope images of (c) Act-UST2 (40 kHz, 250 W at 20 °C for 1 h), (d) Act-UST4 (170 kHz, 250 W at 20 °C for 1 h) and (e) Act-Untreated at magnification at 250x magnification

From common knowledge, the surface was significantly ruptured and microchannels and pits were more open after activation. These topology changes were more obvious in ultrasound pre-treated samples with a fully developed porous structure and increased heterogeneity on surface. The change in surface morphology is a positive implication since this could influence the adsorption characteristics of the material, especially after activation.

To identify the elements present on the surface, the activated biochar samples were scanned using EDX analyser and compared with corresponding as-synthesized samples. EDX give an understanding about relative atomic percent distribution on the surface for a better comparison (Figure A2 S1-S5). Results expressed in Table 6.2 excludes the count of hydrogen on the biochar surface. The major atomic percentage on surface is carbon which ranges from 81 to 87 atomic percentage compared to other elements. Almost 10 percent oxygen content in all samples could be the result of oxygen containing surface functional groups on the surface.

**Table 6.2** Surface characteristics of biochar after base activation

Sample	pH	Zeta potential (mV)	C At%	O At%	Na At%
Act-Untreated	5.4	-13.87	85.2	11.6	3.2
Act-UST1	6.3	-9.45	81.3	13.3	5.4
Act-UST2	6.4	-6.57	85.6	10.7	3.7
Act-UST3	5.3	-2.99	78.6	16.8	4.4
Act-UST4	5.3	-9.37	87.1	10.3	2.6

It was interesting to note that a significant atomic percent of sodium on the activated biochar surface were present even after thorough washing with water to remove salt. Act-UST1 and Act-UST3 has a relatively larger atomic percent of oxygen, and hence larger amount of Na compared to others. The EDX mapping results show that these sodium ions are present almost at the same position as oxygen (Figure 6.1). Na<sup>+</sup> ions could be electrostatically bonded with the remaining oxygen present on the carbon surface which was reluctant even after activation. From the image, it is clear that these sodium ions are homogeneously distributed over the surface. This is a good indication that the synthesized biochar could provide cation exchange ability, hence they can effectively replace exchangeable metal ions on the surface.

Surface charge plays important role in adsorption behaviour of biochar, especially in case of charged metal ions as contaminants. In Table 6.2, the pH and Zeta potential of biochar samples in Cu (II) solution are indicated. The pH of metal solution has increased marginally after adding biochars into it, which shows that the nature of biochars are slightly alkaline. 40 kHz pre-treated samples Act-UST1 and Act-UST2 were found to be more alkaline compared to others. The negative zeta potential of these materials confirms that the surface is negatively charged which could potentially supply adsorption sites for positively charged contaminants on to the surface. The functional groups available for different ionic interactions keeps the biochar surface charged, and they could be mainly oxygen containing functionalities, which are reluctant towards high temperature degradation during pyrolysis. However, the activation process might further remove some of these functionalities during heating, yet the surface remained negatively charged. The ultrasound pre-treated samples were slightly less negative compared to control sample (Act-Untreated), nevertheless Act-UST3 was less negatively charged amongst all.

Maximum carbonization of NaOH treated biochar was confirmed by examining FT-IR spectra (Figure 6.2, FT-IR spectra of all activated samples were identical). No significant bands were observed in higher wavelength region, indicating that most of the aliphatic chains are removed from surface and most condensed aromatic structure. However, aromatic region shows low intensity bands at  $1300\text{ cm}^{-1}$  corresponding to C-O,  $\text{COO}^-$  asymmetric stretches, which is a clear indication that a substantial amount of oxygen containing functionalities are still available for ionic interactions.

### **6.6.2 Influence of ultrasound pre-treatment assisted activation on adsorption properties**

The effect of contact time on adsorption capacity of the material is an interesting parameter to investigate in order to understand the nature of kinetic behaviour of the material. As seen in Figure 6.2, the Cu (II) uptake on biochar samples were very fast with a saturation time of approximately 30 min. The equilibrium was achieved within 1 min for Act-Untreated and 40 kHz pre-treated samples (Act-UST1 and Act-UST2). In the case of 170 kHz samples,

almost 90 percent of adsorption happened slowly during the first 15 min and then achieved equilibrium over 1 h.

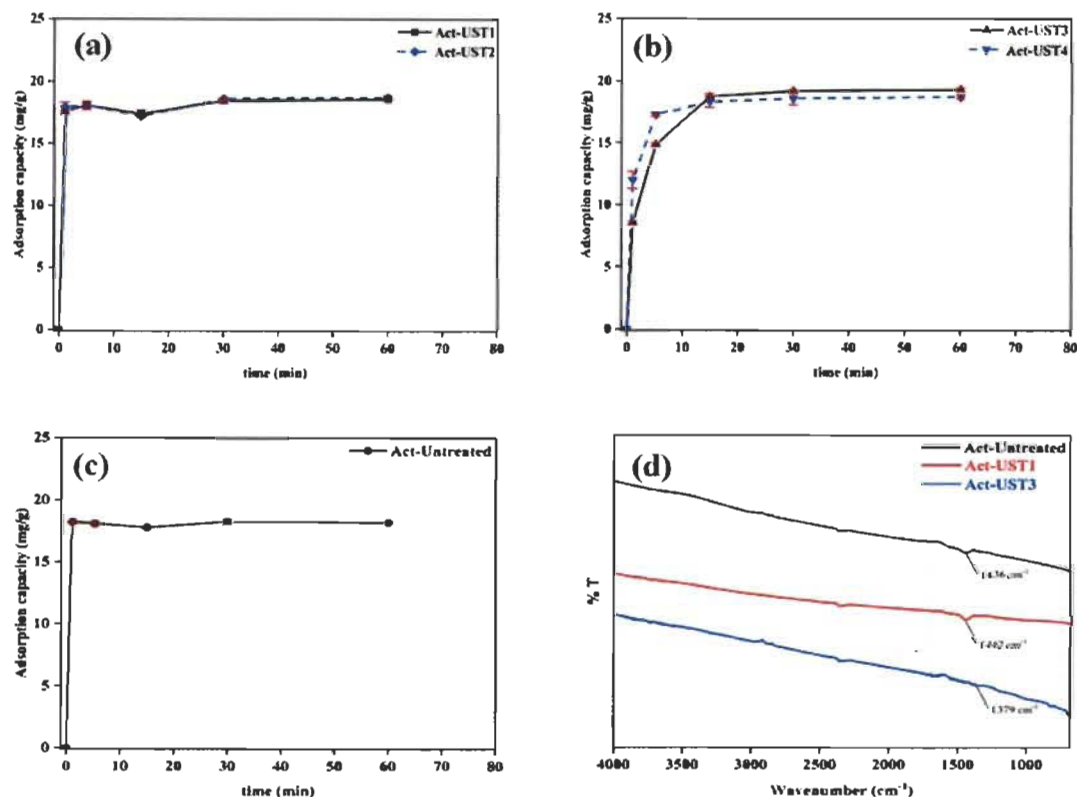


**Figure 6.2** Effect of contact time on adsorption capacity of biochar samples: (a) Activated biochar with 40 kHz ultrasound pre-treatment, (b) Activated biochar with 170 kHz ultrasound pre-treatment, (c) Activated biochar without ultrasound pre-treatment, and (d) FTIR comparison of Act-Untreated, Act-UST1 and Act-UST3 to confirm maximum carbonization

In most of the case, the mechanism of heavy metal adsorption on biochars are explained using pseudo first order and pseudo second order kinetic equations. Pseudo first order kinetics did not apply to the complete range of the contact time; therefore, the calculations were omitted. This could be possible because pseudo first order reactions depend on the concentration of both adsorbate and adsorbent and one of the components is present in large excess. They are generally classified as physisorption where adsorption rate depends on the number of available adsorption sites. Therefore, its concentration changes very slowly as the contact time increases, whereas in our case there is a rapid change in concentration of adsorbate and quick saturation on heterogenous adsorption sites (Li et al., 1999; Rudzinski

and Plazinski, 2006; Lee et al., 2011). Nevertheless, pseudo second order kinetics fitted well with the experimental data, with  $R^2 > 0.9934$ . This elucidates chemisorption as the rate limiting mechanism, mostly ion exchange interactions which are generally rapid reactions (Shen et al., 2018). The results represented in Table 6.3 shows that ultrasound pre-treated biochars have higher equilibrium adsorption capacity ( $Q_e$ ) after activation, when compared with ultrasound untreated sample. 170 kHz pre-treated samples had a better adsorption capacity in comparison to 40 kHz samples. Among them, Act-UST3 exhibited highest  $Q_e$  with  $19.99 \pm 0.13$  mg/g. However, the kinetic rate was decreased with ultrasound pre-treatments, interestingly lowest  $k$  was observed in Act-UST3 while Act-Untreated showed fastest kinetics with  $k$  value of  $7.88 \pm 0.01$  g/mg.min. This suggests that ultrasound pre-treatment enhances the activation process and thereby improves the adsorption capacity of material with higher frequency has better impacts on equilibrium adsorption capacity. Nevertheless, the rate of adsorption decreases upon ultrasonic pre-treatments. At higher frequency, a greater number of impulsive cavitation bubbles intensify the opening of existing pores of biochar, thereby increases the permeability of guest molecules into these pores. As shown by  $Q_e$  values of different pre-treated biochars (Table 6.3), the combination of higher frequency, power, bath temperature and time exhibited better adsorption when compared to other pre-treatments. This effect was marginal at lower frequency and power combinations yet showed better adsorption capacity than the untreated one. The standard deviation for  $Q_e$  value was almost  $\pm 0.21$  and  $\pm 1.9$  for  $k$ . These results demonstrate that the ultrasonic pre-treatments affect both physical and chemical characteristics of the synthesized biochars.

**Table 6.3** Parameters of Pseudo second order kinetic models for Cu (II) adsorption on biochar samples

Sample	Pseudo Second order kinetic parameters		
	$Q_e$ (mg/g)	$k$ (g/mg. min)	$R^2$
Act-Untreated	18.12	7.88	0.9993
Act-UST1	18.19	1.67	0.9961
Act-UST2	18.20	3.23	0.9934
Act-UST3	19.99	0.03	0.9962
Act-UST4	19.03	0.09	0.9997

It was clearly demonstrated that ultrasound pre-treatments have positive impact on base activation, hence the equilibrium adsorption capacities of the samples were improved. To evaluate how prominent these enhancements are, the  $Q_e$  (mg/g) and BET- $N_2$  specific surface area of synthesized samples were compared with a commercially available activated carbon samples (Fluval) along with a few of the reported wood biochars from literature (Table 6.4).

**Table 6.4** Comparison of BET surface area and copper adsorption capacities of wood-derived biochars from literature

Feedstock	Activation Method	BET Surface Area ( $m^2/g$ )	Adsorption Capacity (mg/g)	Reference
Pine wood	Hydrothermal	21	4.21	Liu et al., 2010
Pinewood	-	29	2.73	Liu et al., 2010
Hard wood	-	0.43	6.49	Chen et al., 2011
Softwood	Steam	383.66	0.476	Han et al., 2013
			(mmol/g)	
Hardwood	Steam	343.91	0.307	Han et al., 2013
			(mmol/g)	
Hickory wood	KMnO <sub>4</sub>	205	14.45	Wang et al., 2015
Hickory wood	-	101	7.6	Wang et al., 2015
Jarrah	-	309.29	4.39	Jiang et al., 2016
Pinewood	-	219.35	1.47	Jiang et al., 2016
Mix wood	-	26.40	0.019	Shen et al., 2018
			(mmol/g)	
Wood waste	-	83.6	2.9	Tomczyk et al., 2020
Willow wood	-	-	4.09	Wang et al., 2020
AC (Fluval)	-	718.42	4.62	Peter et al., 2020
UST1	40 kHz UST	12.4	1.54	Peter et al., 2020
UST3	170 kHz UST	3.31	0.92	Peter et al., 2020
Act-UST1	40 kHz UST + NaOH	<b>368.63</b>	<b>18.19</b>	This study
Act-UST3	170 kHz UST + NaOH	<b>503.60</b>	<b>19.99</b>	This study

The equilibrium adsorption capacities of Act-UST1 and Act-UST3 are considerably good among the wood biochars reported previously and almost 12 and 22 times higher than non-activated UST samples, respectively. The specific surface area was also significantly increased after activation. Ultrasound pre-treatments help the activation to develop

improved porous structure and thereby increasing the specific surface area of the material. The sono-chemical effect was dominant in this case resulting in better BET surface area of Act-UST3 (170 kHz) than Act-UST1 (40 kHz). Regardless of the higher specific surface area of activated carbon, our samples exhibited better adsorption capacity after base activation as shown in Table 6.3. The enhanced surface area along with surface functionalities facilitated the anchoring of guest contaminants towards the surface thus, resulted in better adsorption capacity of the biochars. The ultrasonic pre-treatments enhance the mass and heat transfer during various interactions, and it helps to increase the NaOH interaction with surface functionalities during alkali modification. At higher frequency and power, this effect could be considerably enhanced because of the larger number of cavitation bubbles and microjet impulses associated with it.

The initial metal concentration was linearly related to adsorption capacity of the material (Figure A2 S6) which shows that the adsorption capacity of the material increases with the number active sites available for different interactions. To better understand adsorbent-adsorbate interactions, most frequently used adsorption isotherm models Langmuir and Freundlich were applied on to the experimental data. With respect to the linear regression coefficient  $R^2$ , the adsorption of metal ions onto biochar was better described by Freundlich isotherm model, suggesting multilayer adsorption on a heterogeneous surface (Table 6.5). The surface heterogeneity constant  $n$  values were slightly higher for Act-UST samples, indicating that the isotherms changed from linear to strong nonlinear with ultrasonic pre-treatments. The highest  $n$  value for Act-UST3 indicates more heterogeneous surface. The value for  $K_f$  which is related to maximum adsorption capacity was highest for Act-UST3. Better  $K_f$  values of UST biochars further indicates that the adsorption followed by ultrasound pre-treated samples are better than the untreated biochar. The intensive support of ultrasound pre-treatments for better opening of channeled pores and larger specific surface along with the grafting of active sites using NaOH, substantially improved the adsorbent-adsorbate interactions which leads to better adsorption behaviour of the materials.

Thermodynamic parameters such as change in enthalpy  $\Delta H^0$  and entropy  $\Delta S^0$  as well as Gibb's free energy  $\Delta G^0$  were calculated in order to determine the thermodynamically favourable conditions for adsorption (Table 6.5). The positive value of  $\Delta H^0$  for all biochar

samples revealed that the adsorption is endothermic, which is similar to most of the previous studies on biochar adsorption (Chen et al., 2011; Kołodziejńska et al., 2012; Van Vinh et al., 2015). The increase in temperature provides enough energy for metal ions to be captured onto the interior structure of biochar. The change in enthalpy, and therefore, the degree of randomness  $\Delta S^0$  is less for high frequency pre-treated samples. This indicates that the structural changes occurred in these samples are lower compared to others during adsorption.

The negative value of Gibb's free energy  $\Delta G^0$  indicates that the adsorption is spontaneous, hence the adsorption and desorption is in thermal equilibrium. The system is more spontaneous when external energy is provided. These values were almost similar with all samples, however, high frequency pre-treated samples showed comparatively lower  $\Delta G^0$  value, which was also the case of  $\Delta S^0$ . Overall, it is obvious that the high frequency samples are exhibiting a different thermodynamic behaviour compared to control or low frequency samples, which could be because of the change in surface behaviour due to the two-step activation of synthesized biochars.

**Table 6.5** Freundlich isotherm and thermodynamic parameters of biochar samples

Sample	Freundlich Model			Temperature (K)	Thermodynamic parameters		
	$K_f$	$1/n$	$R^2$		$\Delta G^0$ (kJ/mol)	$\Delta H^0$ (kJ/mol)	$\Delta S^0$ (J/mol K)
Act-Untreated	1.86	0.27	0.9545	295	-1.75	14.77	56.00
				313	-2.76		
				333	-3.88		
Act-UST1	1.73	0.29	0.9828	295	-1.71	14.30	54.28
				313	-2.68		
				33	-3.77		
Act-UST2	1.80	0.30	0.8656	295	-1.52	20.48	74.58
				313	-2.86		
				333	-4.35		
Act-UST3	1.56	0.42	0.9873	295	-1.62	11.48	44.40
				313	-2.41		
				333	-3.30		
Act-UST4	2.07	0.17	0.9686	295	-1.90	6.81	29.54
				313	-2.43		
				333	-3.03		

The alkali activated biochars exhibited difference in adsorption properties with respect to the changes in ultrasound pre-treatment conditions. The surface properties and adsorption

capacities were remarkable. These engineered biochars can be an efficient cost-effective replacement for activated carbons for heavy metal removal from contaminated water.

### 6.6.3 Selectivity of heavy metals on modified biochars

For a more precise understanding on heavy metal selectivity and competitive adsorption of the material, multi metal solutions were analysed. This could give a better assessment on efficiency of the biochars in industrial wastewater recycling processes. The competitive adsorption of metals was different for ultrasound pre-treated and untreated samples. However, among the Act-UST samples, 170 kHz samples displayed effect towards heavy metal uptake. The detailed result is given in Table A2 S1 and shown in Figure 6.3.

As represented in Figure 6.3, the competitive adsorption capacity of biochar towards copper increased linearly with increase in initial concentration. However, in the case of Ni (II) and Pb (II) it did not follow the linear relation. At higher concentrations, all samples exhibited selective adsorption of Cu (II) over other two metals, with ultrasound pre-treated samples displayed a small improvement in adsorption capacity than untreated sample. On the other hand, the copper adsorption capacity of Act-UST3 at 100 ppm was reduced by approximately 20 percent as compared to single component system. A similar trend was observed by Mahdi et al. (2019) in their study with competitive adsorption of Pb (II), Cu (II) and Ni (II) ions on date seed biochars. Because of the similar ionic size of Cu (II) and Ni (II) when compared to Pb (II), their competitiveness was expected to be same onto biochars. However, despite of the higher selectivity towards copper ions, Act-UST1, Act-UST-3 and Act-UST4 exhibited better adsorption for lead over nickel. Besides, it was interesting to note that Act-Untreated and Act-UST2 behaved similar towards competitive uptake of all three ions, particularly nickel preferred over lead. This justifies that low power and frequency ultrasound does not influences the surface openings of the biochar much, which further resulted in less adsorption capacity of bigger ions in the mixed solution.

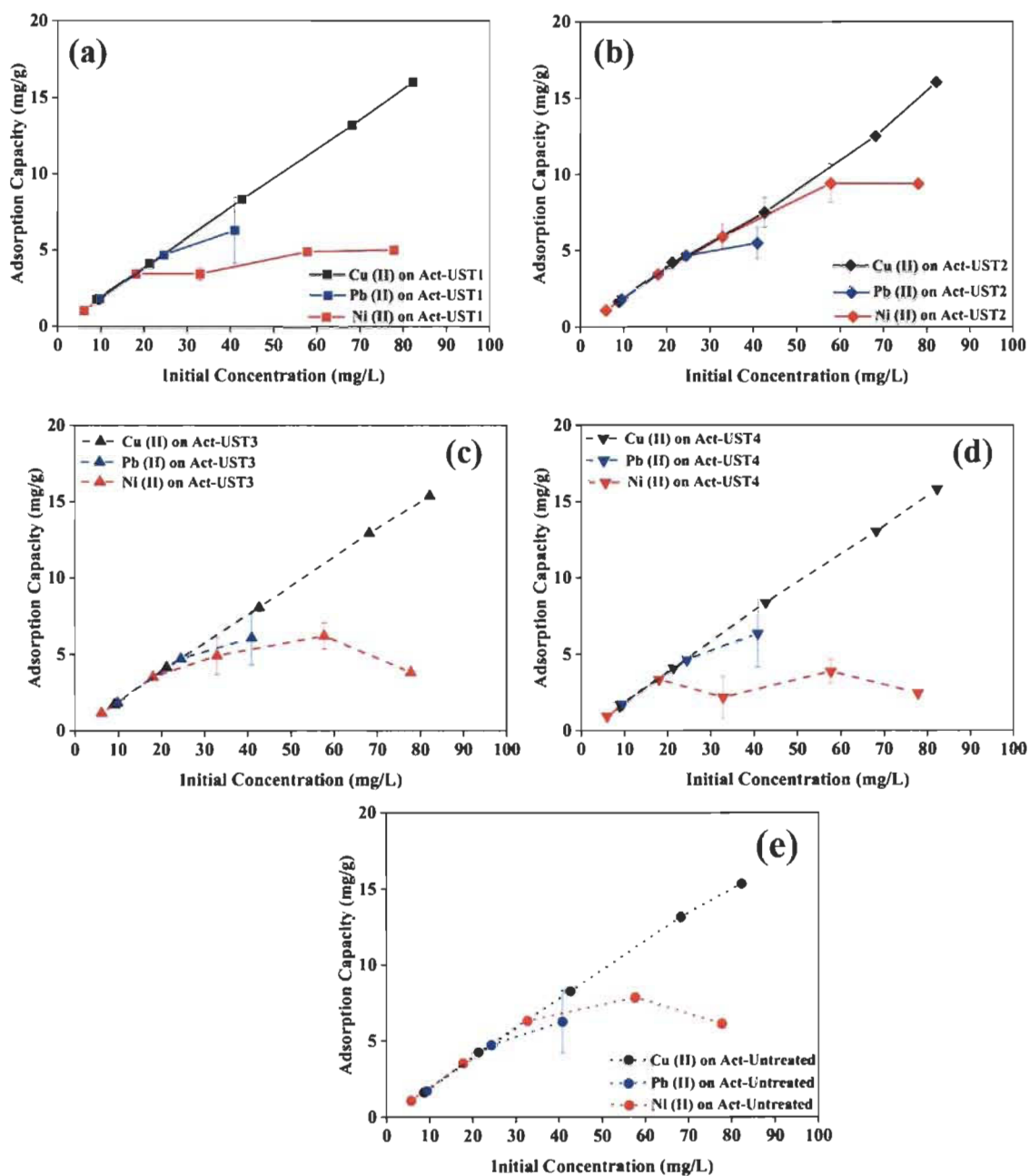


**Figure 6.3** Comparison of competitive metal adsorption for Cu (II), Pb (II) and Ni (II) onto: (a) Act-UST1 (40 kHz, 1000 W at 80 °C for 2 h), (b) Act-UST2 (40 kHz, 250 W at 20 °C for 1 h), (c) Act-UST3 (170 kHz, 1000 W at 80 °C for 2 h), (d) Act-UST4 (170 kHz, 250 W at 20 °C for 1 h), and (e) Act-Untreated

## 6.7 Conclusions

In this study, we have seen that alkali activation of ultrasound pre-treated softwood biochar has improved physical as well as metal adsorption properties. Higher frequency ultrasound

enhances the activation process, thus modifies surface of the biochar favouring the metal adsorption capacity. The ultrasound pre-treatment facilitated the accessibility of a heterogenous surface with wide opening of already existing pores and microchannels, and the alkali treatment improved the availability surface anchoring sites. The underlying mechanism was found to be chemisorption, expected to be ion exchange reactions resulting from the sodium ions present on the surface anchoring sites. The higher equilibrium adsorption capacities of Act-UST samples in comparison with other reported wood biochars show that the synthesized biochars can be an efficient candidate for heavy metal removal from wastewater. Isotherm and thermodynamic studies also suggest that the Act-UST samples have improved physicochemical properties. The better adsorption properties of ultrasound pre-treated biochars, especially higher frequency pre-treated samples showed that combination of frequency, power, temperature and exposure time influences the base modification on the material. The two-step activation of the biochars exhibited promising adsorption capacities in the mixed metal systems as well. The higher selectivity towards copper ions indicates that these materials can be potentially used to remove particular ions from a mix of metal-contaminated solution. This study encourages to make use of power ultrasound enhanced modifications on biochar with better physicochemical properties and aides the potential conversion of feedstock residues towards process control and design.

## **6.8 Acknowledgement**

The authors are sincerely thankful to all the members of I2E3 for their great support and help to conduct experiments. This work was financially supported by the Natural Sciences and Engineering Research Council of Canada (NSERC). The authors thanks Queen Elizabeth II Diamond Jubilee Scholarship for financial assistance.

## **6.9 References**

- [1] Al-Anber MA. Thermodynamics approach in the adsorption of heavy metals: INTECH Open Access Publisher, 2011. <https://doi.org/10.5772/21326>

- [2] Angın D, Köse TE, Selengil U. Production and characterization of activated carbon prepared from safflower seed cake biochar and its ability to absorb reactive dyestuff. *Appl. Surf. Sci.* 2013; 280: 705-710. <https://doi.org/10.1016/j.apsusc.2013.05.046>
- [3] Barakat M. New trends in removing heavy metals from industrial wastewater. *Arab. J Chem.* 2011; 4: 361-377. <https://doi.org/10.1016/j.arabjc.2010.07.019>
- [4] Batool F, Akbar J, Iqbal S, Noreen S, Bukhari SNA. Study of isothermal, kinetic, and thermodynamic parameters for adsorption of cadmium: an overview of linear and nonlinear approach and error analysis. *Bioinorganic chemistry and applications* 2018; 2018. <https://doi.org/10.1155/2018/3463724>
- [5] Chatterjee R, Sajjadi B, Mattern DL, Chen W-Y, Zubatiuk T, Leszczynska D. Ultrasound cavitation intensified amine functionalization: A feasible strategy for enhancing CO<sub>2</sub> capture capacity of biochar. *Fuel* 2018; 225: 287-298. <https://doi.org/10.1016/j.fuel.2018.03.145>
- [6] Chen X, Chen G, Chen L, Chen Y, Lehmann J, McBride MB. Adsorption of copper and zinc by biochars produced from pyrolysis of hardwood and corn straw in aqueous solution. *Bioresour. Technol.* 2011; 102: 8877-8884. <https://doi.org/10.1016/j.biortech.2011.06.078>
- [7] Han Y, Boateng AA, Qi PX, Lima IM, Chang J. Heavy metal and phenol adsorptive properties of biochars from pyrolyzed switchgrass and woody biomass in correlation with surface properties. *J. Environ. Manage.* 2013; 118: 196-204. <https://doi.org/10.1016/j.jenvman.2013.01.001>
- [8] Ince M, Ince OK. An overview of adsorption technique for heavy metal removal from water/wastewater: A critical review. *Int. J. Pure Appl. Sci* 2017; 3: 10-19. <https://doi.org/10.29132/ijpas.358199>
- [9] Inyang MI, Gao B, Yao Y, Xue Y, Zimmerman A, Mosa A. A review of biochar as a low-cost adsorbent for aqueous heavy metal removal. *Crit. Rev. Environ. Sci. Technol.* 2016; 46: 406-433. <https://doi.org/10.1080/10643389.2015.1096880>

- [10] Jiang S, Huang L, Nguyen TA, Ok YS, Rudolph V, Yang H. Copper and zinc adsorption by softwood and hardwood biochars under elevated sulphate-induced salinity and acidic pH conditions. *Chemosphere* 2016; 142: 64-71. <https://doi.org/10.1016/j.chemosphere.2015.06.079>
- [11] Kołodyńska D, Wnętrzak R, Leahy J, Hayes M, Kwapiński W, Hubicki Z. Kinetic and adsorptive characterization of biochar in metal ions removal. *Chem. Eng. J.* 2012; 197: 295-305. <https://doi.org/10.1016/j.cej.2012.05.025>
- [12] Lee C-R, Kim H-S, Jang I-H, Im J-H, Park N-G. Pseudo first-order adsorption kinetics of N719 dye on TiO<sub>2</sub> surface. *ACS applied materials & interfaces* 2011; 3: 1953-1957 <https://doi.org/10.1021/am2001696>
- [13] Li B, Yang L, Wang C, Zhang Q, Liu Q, Li Y. Adsorption of Cd (II) from aqueous solutions by rape straw biochar derived from different modification processes. *Chemosphere* 2017; 175: 332-340. <https://doi.org/10.1016/j.chemosphere.2017.02.061>
- [14] Li PH, Bruce RL, Hobday MD. A pseudo first order rate model for the adsorption of an organic adsorbate in aqueous solution. *Journal of Chemical Technology & Biotechnology: International Research in Process, Environmental & Clean Technology* 1999; 74: 55-59 [https://doi.org/10.1002/\(SICI\)1097-4660\(199901\)74:1<55::AID-JCTB984>3.0.CO;2-D](https://doi.org/10.1002/(SICI)1097-4660(199901)74:1<55::AID-JCTB984>3.0.CO;2-D)
- [15] Liu Z, Zhang F-S, Wu J. Characterization and application of chars produced from pinewood pyrolysis and hydrothermal treatment. *Fuel* 2010; 89: 510-514. <https://doi.org/10.1016/j.fuel.2009.08.042>
- [16] Loranger, É., Pombert, O., Drouadaine, V. Ultrasonic Pre-treatments of Wood Chips used in a conventional pyrolysis and their effect on bio-oil composition and calorimetry. 2016; SAMPE Conference Proceedings.
- [17] Mahdi Z, Yu QJ, El Hanandeh A. Competitive adsorption of heavy metal ions (Pb<sup>2+</sup>, Cu<sup>2+</sup>, and Ni<sup>2+</sup>) onto date seed biochar: batch and fixed bed experiments. *Sep. Sci. Technol.* 2019; 54: 888-901. <https://doi.org/10.1080/01496395.2018.1523192>

- [18] Masindi V, Muedi KL. Environmental contamination by heavy metals. *Heavy metals* 2018; 10: 115-132. <https://doi.org/10.5772/intechopen.76082>
- [19] Mohan D, Pittman Jr CU. Arsenic removal from water/wastewater using adsorbents—a critical review. *J. Hazard. Mater.* 2007; 142: 1-53. <https://doi.org/10.1016/j.jhazmat.2007.01.006>
- [20] Mohan D, Sarswat A, Ok YS, Pittman Jr CU. Organic and inorganic contaminants removal from water with biochar, a renewable, low cost and sustainable adsorbent—a critical review. *Bioresour. Technol.* 2014; 160: 191-202. <https://doi.org/10.1016/j.biortech.2014.01.120>
- [21] Peter A, Chabot B, Loranger E. Enhancing Surface Properties of Softwood Biochar by Ultrasound Assisted Slow Pyrolysis. 2019 IEEE International Ultrasonics Symposium (IUS). IEEE, 2019, pp. 2477-2480. <https://doi.org/10.1109/ULTSYM.2019.8925793>
- [22] Peter A, Chabot B, Loranger E. The influence of ultrasonic pre-treatments on metal adsorption properties of softwood-derived biochar. *Bioresour. Technol. Rep.* 2020; 11: 100445. <https://doi.org/10.1016/j.biteb.2020.100445>
- [23] Prapagdee S, Piyatiratitivorakul S, Petsom A. Physico-chemical activation on rice husk biochar for enhancing of cadmium removal from aqueous solution. *Asian J. Water Environ. Pollut.* 2016; 13: 27-34. <https://doi.org/10.3233/AJW-160004>
- [24] Prasad KMK, Raheem S. Evaluation of the quality of colour changes of complexometric indicators in the titration of copper (II) with EDTA by tristimulus colorimetry. *Microchimica Acta* 1993; 112: 63-69. <https://doi.org/10.1007/BF01243322>
- [25] Rudzinski W, Plazinski W. Kinetics of solute adsorption at solid/solution interfaces: a theoretical development of the empirical pseudo-first and pseudo-second order kinetic rate equations, based on applying the statistical rate theory of interfacial transport. *J Phys. Chem. B* 2006; 110: 16514-16525 <https://doi.org/10.1021/jp061779n>

- [26] Sajjadi B, Broome JW, Chen WY, Mattern DL, Egiebor NO, Hammer N. Urea functionalization of ultrasound-treated biochar: a feasible strategy for enhancing heavy metal adsorption capacity. *Ultrason. Sonochem.* 2019a; 51: 20-30. <https://doi.org/10.1016/j.ultsonch.2018.09.015>
- [27] Sajjadi B, Chen W-Y, Egiebor NO. A comprehensive review on physical activation of biochar for energy and environmental applications. *Rev. Chem. Eng.* 2019b; 35: 735-776. <https://doi.org/10.1515/revce-2017-0113>
- [28] Shen Z, Zhang Y, Jin F, Alessi DS, Zhang Y, Wang F. Comparison of nickel adsorption on biochars produced from mixed softwood and Miscanthus straw. *Environmental Science and Pollution Research* 2018; 25: 14626-14635. <https://doi.org/10.1007/s11356-018-1674-2>
- [29] Taheran M, Naghdi M, Brar SK, Knystautas EJ, Verma M, Ramirez AA. Adsorption study of environmentally relevant concentrations of chlortetracycline on pinewood biochar. *Sci. Total Environ.* 2016; 571: 772-777. <https://doi.org/10.1016/j.scitotenv.2016.07.050>
- [30] Tan X, Liu Y, Zeng G, Wang X, Hu X, Gu Y. Application of biochar for the removal of pollutants from aqueous solutions. *Chemosphere* 2015; 125: 70-85. <https://doi.org/10.1016/j.chemosphere.2014.12.058>
- [31] Tomeczyk A, Sokołowska Z, Boguta P. Biomass type effect on biochar surface characteristic and adsorption capacity relative to silver and copper. *Fuel* 2020; 278: 118168. <https://doi.org/10.1016/j.fuel.2020.118168>
- [32] Van Vinh N, Zafar M, Behera S, Park H-S. Arsenic (III) removal from aqueous solution by raw and zinc-loaded pine cone biochar: equilibrium, kinetics, and thermodynamics studies. *International journal of environmental science and technology* 2015; 12: 1283-1294. <https://doi.org/10.1007/s13762-014-0507-1>

- [33] Wang H, Gao B, Wang S, Fang J, Xue Y, Yang K. Removal of Pb (II), Cu (II), and Cd (II) from aqueous solutions by biochar derived from KMnO<sub>4</sub> treated hickory wood. *Bioresour. Technol.* 2015; 197: 356-362. <https://doi.org/10.1016/j.biortech.2015.08.132>
- [34] Wang S, Kwak J-H, Islam MS, Naeth MA, El-Din MG, Chang SX. Biochar surface complexation and Ni (II), Cu (II), and Cd (II) adsorption in aqueous solutions depend on feedstock type. *Sci. Total Environ.* 2020; 712: 136538. <https://doi.org/10.1016/j.scitotenv.2020.136538>

### **6.10 Highlights**

- Two-step activation of softwood biochars displayed negatively charged surface
- UST samples showed higher adsorption capacity after activation over untreated
- 170kHz ultrasound further promotes activation and better adsorption capacity
- The activated UST biochars showed selective adsorption in the order of Cu>Pb>Ni

## Chapter 7 – Scientific Article 4: Metal Impregnation on Ultrasound Pre-treated Wood Biochar

### 7.1 Preface

As evident from article 1 to 3, the ultrasonic pre-treatments have significantly influenced the heavy metal adsorption properties of the materials. These results motivated us to further explore the effect of ultrasonic pre-treatment assisted modifications on biochar surface. In parallel with the adsorption study on UST-biochars, this article deals with the ultrasonic pre-treatment effects on doped metalbiochars. The efficiency of lab-scale pyrolyser to produce biochar with better yield and physicochemical properties were studied as a continuation of results reported in article 1. Post and pre-pyrolysis impregnations were also performed to study the influence on pyrolysis product yields and homogenous spread of iron particles on biochars pre-treated under different ultrasonic conditions. This work was published in SN Applied Sciences (DOI: <https://doi.org/10.1007/s42452-021-04636-y>) entitled *Post and pre-pyrolysis effect on iron impregnation using ultrasound pre-treated softwood biochar for catalysis applications*.

#### **Author Details:**

Aneeshma Peter

Ph.D. Student, Sciences de l'énergie et des matériaux

I2E3 – Institut d'Innovations en Écomatériaux, Écoproduits et Écoénergies, à base de biomasse, Université du Québec à Trois-Rivières, P.O. Box 500, Trois-Rivières, Québec, Canada, G9A 5H7

Email: [Aneeshma.Peter@uqtr.ca](mailto:Aneeshma.Peter@uqtr.ca)

Eric Loranger, Ph.D.

Research director and corresponding author

I2E3 – Institut d’Innovations en Écomatériaux, Écoproduits et Écoénergies à base de biomasse, Université du Québec à Trois-Rivières, P.O. Box 500, Trois-Rivières, Québec, Canada, G9A 5H7

Email: [Eric.loranger1@uqtr.ca](mailto:Eric.loranger1@uqtr.ca)

Bruno Chabot, Ph.D.

Co-director and co-author

I2E3 – Institut d’Innovations en Écomatériaux, Écoproduits et Écoénergies à base de biomasse, Université du Québec à Trois-Rivières, P.O. Box 500, Trois-Rivières, Québec, Canada, G9A 5H7

Email: [Bruno.Chabot@uqtr.ca](mailto:Bruno.Chabot@uqtr.ca)

#### **Author Credits:**

**Aneeshma Peter:** Methodology, Validation, Investigation, Data curation, Formal analysis, Writing - original draft, Visualization

**Bruno Chabot:** Conceptualization, Project administration, Writing - review & editing

**Eric Loranger:** Conceptualization, Project administration, Supervision, Writing - review & editing, Funding acquisition

## **7.2 Résumé**

La pyrolyse lente est largement utilisée pour convertir la biomasse en une forme d'énergie utilisable. Les propriétés et la distribution des produits dérivés (biocharbon, gaz et biohuiles) de la pyrolyse dépendent de divers facteurs tels que les conditions de pyrolyse, les types de matières premières, les techniques de post et de prétraitement sur celle-ci. La pyrolyse assistée par prétraitement aux ultrasons est une méthodologie récemment étudiée pour améliorer les propriétés physicochimiques des produits dérivés. L'efficacité des prétraitements par ultrasons pour améliorer la production de biohuile à partir de la pyrolyse

a déjà été rapportée avec succès. Le biochar ou résidu solide issu de la pyrolyse, fait l'objet d'une attention considérable en raison de ses bonnes propriétés physicochimiques. Diverses techniques de modification ont été mises en œuvre sur les biochars pour améliorer davantage leurs propriétés. Le biochar provenant de bois prétraité par ultrasons a déjà démontré des propriétés de surface et d'adsorption efficaces. Toutefois, le biochar imprégné de fer est aussi intéressant, car il a potentiellement prouvé son efficacité en tant que catalyseur efficace à faible coût. Dans cette étude, en combinant les avantages du prétraitement par ultrasons et de l'imprégnation au fer, nous avons synthétisé une série de biochars imprégnés à partir de copeaux de bois résineux. Des méthodes de post-pyrolyse et de pré-pyrolyse utilisant un pyrolyseur à l'échelle du laboratoire ont été mises en œuvre pour comparer les rendements des produits de pyrolyse et l'effet du degré d'imprégnation. Les biochars modifiés ont été caractérisés en utilisant la spectroscopie infrarouge, la microscopie électronique à balayage, la spectroscopie de rayons X à dispersion d'énergie pour la composition atomique de surface et l'analyse thermogravimétrique. Les biochars dérivés de copeaux de bois prétraités aux ultrasons par post-pyrolyse (imprégnation de Fe sur des copeaux de bois prétraités aux ultrasons suivi d'une pyrolyse) ont démontré une meilleure distribution en produits de pyrolyse tels que le biochar et le biogaz. Ces biochars présentaient également une meilleure imprégnation des ions Fe en surface et une meilleure stabilité thermique. Les caractéristiques chimiques de ces biochars modifiés sont finalement intéressantes et peuvent en effet, être potentiellement utilisées comme substitut rentable pour diverses applications catalytiques.

### 7.3 Abstract

Slow pyrolysis is widely used to convert biomass into useable form of energy. Ultrasound pre-treatment assisted pyrolysis is a recently emerging methodology to improve the physicochemical properties of products derived. Biochar, the solid residues obtained from pyrolysis, is getting considerable attention because of its good physicochemical properties. Various modification techniques have been implemented on biochars to enhance their properties. Ultrasonic pre-treated wood biochar has showcased efficient surface and adsorption properties. Iron impregnated biochar is interesting as it has potentially proved the efficiency as an efficient low-cost catalyst. In this study, by combining the advantages of ultrasonic pre-treatment and iron impregnation, we have synthesized a series of

Fe-impregnated biochar from softwood chips. Pre- and post-pyrolysis methods using a lab-scale pyrolyser had been implemented to compare the pyrolysis product yields and degree of impregnation. Biochars derived from ultrasound pre-treated woodchips by post pyrolysis demonstrated better impregnation of Fe ions on surface with better distribution of pyrolysis products such as biochar and biogas. The surface functionality of all ultrasound pre-treated biochars remained the same. However, post-pyrolysed samples at high frequency ultrasound pre-treatment showed better thermal stability. The chemical characteristics of these modified biochars are interesting and can indeed be used as a cost-effective replacement for various catalytic applications.

**Keywords:** Softwood biochar, iron impregnation, slow pyrolysis, ultrasound pre-treatments, physicochemical properties

#### 7.4 Introduction

Efficient use of biomass into useable form of energy has always been a key concern by virtue of increasing energy demand, depletion of fossil fuel and global climate change [1-4]. Intense researches have been carried out globally to seek solutions for climate change by making use of renewable energy resources [5]. The province of Quebec in Canada, being rich in forest biomass availability, has engaged in adopting research policies to make use of the biomass products to address these challenges. Adequate techniques to process feedstock for better material quality and enhancing production methodologies to have potential materials for other applications are part of these venture. Slow pyrolysis, being a technique to convert biomass to different energy forms, has gained considerable attention because of its relative low-cost, efficiency and ease in processability [6]. The thermal decomposition of feedstocks under limited oxygen conditions result in forming liquid bio-oil, solid biochar, and non-condensable gas and are efficiently used for various applications. The properties of these products depend on several important parameters such as pyrolysis conditions, feedstock types, pre- and post-processing techniques on feedstocks [7-10].

Influence of power ultrasound treatments on pyrolysis and derived products have recently been explored. Power ultrasound or high intensity ultrasound make use of frequency range between 20 kHz and 1 MHz. The application of power ultrasound on biomass is based on

the concept of cavitation. Formation of microjets during the implosion of cavitation bubbles disrupts the solid surface which is in contact and provides a unique physicochemical environment to the materials and thus, influences the material properties [11]. Understanding the ability of ultrasound to promote chemical and thermal decomposition reactions during pyrolysis with better efficiency in terms of product yield and physicochemical properties will be a key step to introduce ultrasound of biomass processing at industrial level. In one of the interesting studies carried out by Cherpozat et al. [12], it was shown that ultrasound pre-treatments on softwood chips resulted in enhanced bio-oil yield. A series of two ultrasound frequencies (170 kHz for 0.5 h followed by 40 kHz for 1.5 h) raised the bio-oil yield by 12 percent compared to untreated wood samples. Recently, Hazrati and co-workers [13] have shown the ability of ultrasonic pre-treatments to enhance the physicochemical characteristics and environmental applicability of sludge-derived biochar. Few other studies have also revealed the influence of ultrasonic treatments on improving adsorption properties of biochar produced from pyrolysis [14-17].

The intrinsic nature of the biomass feedstock and the processing techniques used play an important role in determining the properties of the biochar. Consequently, modification of biochar surfaces is an interesting approach to improve their physicochemical properties. Though activation is considered to be one among the efficient modification methods on biochar, introducing different composites on to the carbon surface is getting considerable attention because of the easy processability and efficiency. The resulting composites introduce completely new active sites on the carbon surface which has enhanced physicochemical properties suitable for various applications [18]. It has been shown that biochar modified with Fe oxides provides a selective affinity towards heavy metals like Cr, Eu and As [19-21]. They are also efficient for removing anionic contaminants from aqueous solutions [22]. Biochar supported metal oxides have also been studied for catalytic activity [23-26]. They have been used as efficient catalysts for biomass hydrolysis, dehydration and biodiesel production due to its tailoring properties and large surface area. A study by Ren and co-workers [27] revealed that the corn stover biochar catalyst enhanced the syngas and improved the bio-oil quality in biomass pyrolysis. Few other reports investigated the effect of metal impregnated biochar as catalyst for biomass gasification and the effect of such materials in upgrading process of bio-oils [28-30]. Kastner et al. [31] reported that the iron

supported biochar could decompose toluene, a model tar compound, with linear increase in temperature and catalyst loading. They claimed that the inexpensive iron impregnated biochar catalysts could potentially be used to decompose tar molecules in syngas generated via biomass gasification. The catalytic activity of Fe-impregnated sugarcane biochar (FSB) for removing azo dye Orange G was investigated by Park et al. [32]. They have shown that the FSB was more economical, efficient, and recyclable than other conventional Fenton oxidation catalysts. Recently, Cao et al. [33], had proved the electrocatalytic activity of biochar made from iron enriched plants. Nejati et al. [34] has also investigated the upgradation of pyrolysis products using Fe based biochar as catalyst. They have stated that the energy recovery and process efficiency was achieved using biochar catalyst.

Metal impregnation experiments are generally carried out directly on the feedstock as a pre-treatment or on the biochar produced after the pyrolysis (post-treatment). The effect of these two processes on biochar can be varied. However, to our knowledge, no reports are available on the examination of the difference in biochar surface morphology caused by metal impregnation. In previous studies, we have shown that the surface morphology of biochar synthesized could be altered by ultrasonication [14,15]. The modification with metal oxides on these ultrasound pre-treated wood biochars could be more effective because of their exposed surface pores and microchannels. In this work, pre- and post- pyrolysis treatments on metal impregnated samples were carried out to understand the difference in characteristics of biochar-metal composites and pyrolysis product yield. The effect of ultrasound pre-treatment assisted metal impregnation on biochars were also explored. Finally, we hope that these engineered biochars will offer better properties and yield, opening up potential use for various catalytic applications.

## **7.5 Materials and Methods**

### **7.5.1 Biomass feedstock and ultrasound pre-treatments**

The feedstock used to produce biochar is a mix of softwood mainly including pine, fir, spruce and larch. They are processed woodchips supplied by a local Canadian pulp and paper mill. The woodchips were ground to 5 by 5 mm sized needles and subjected to different ultrasonic

pre-treatments. In our previous studies on ultrasonic pre-treated (UST) wood biochar, we have shown that the combination of frequency, power, bath temperature and exposure time significantly affects the surface morphology and properties of resulting biochar [15]. Hence, in this study we have used the maximum and minimum conditions of these parameters. Table 7.1 presents ultrasonic pre-treatment conditions performed. A 34 L Ultrasonic bath (model BT90 from Ultrasonic Power Corporation USA) is used to perform the pre-treatments in water. For each treatment, 200 g of wood chips were dipped into 4 L of deionized water in a weighed mesh bag, to ensure that the wood chips are completely submerged in water and homogeneously treated by ultrasound. The pre-treated woodchips were dried in oven at 105 °C for 48 h.

**Table 7.1** Ultrasonic pre-treatment conditions applied to wood chips

Sample	Frequency (kHz)	Power (W)	Temperature (°C)	Time (h)
Fe-UST1	40	1000	80	2
Fe-UST2	40	250	20	1
Fe-UST3	170	1000	80	2
Fe-UST4	170	250	20	1

### 7.5.2 Lab-scale slow pyrolysis set up

The pyrolysis was performed using the method previously reported by Loranger et al. [35]. A schematic diagram of the pyrolysis system is given in Figure 7.1. This laboratory scale system was originally developed for the production of bio-oil. The detailed experimental set-up is also described in the study of Cherpozat et al. [12], who have mainly investigated the effect of different ultrasonic pre-treatments on bio-oil yield. However, the effect on biochar yield and properties were not analysed. The heating rate was approximately 15 °C/min and the peak temperature for the pyrolysis was 560 °C. The reaction was held at this temperature for about 1 h. From the heating rate and residence time (1 to 1.5 h), the system belongs to slow-pyrolysis category. At least three trials were performed on each treatment to confirm the average yield of biochar and other pyrolysis products. The pyrolysis products were collected separately, and the biochar was cleaned from tar using acetone and then stored in plastic bags.

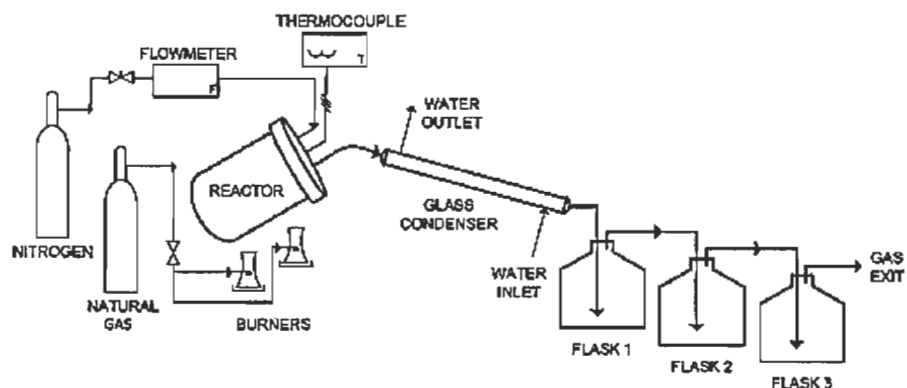


**Figure 7.1** Schematic representation of laboratory-scale pyrolysis set up to produce biochar

### 7.5.3 Metal impregnation

For metal impregnation, the method developed by Frišták et al. [19] was used. A 1:10 ratio (wt:V) of sample was mixed with a 200 mmols ferric chloride solution. The mixture was stirred for 12 h under moderate heating (50 °C) and then dried at 105 °C for 24 h. The dried composites were rinsed several times with deionized water in order to remove free ions on the surface and then dried overnight at 105 °C. Pre and post-pyrolysis methods were designated based on iron impregnation step. In the pre-pyrolysis technique, iron was impregnated on to the biochar sample obtained after pyrolysis. However, in post-pyrolysis, iron impregnation was carried out on the ultrasound pre-treated woodchips followed by pyrolysis (Figure 7.2).

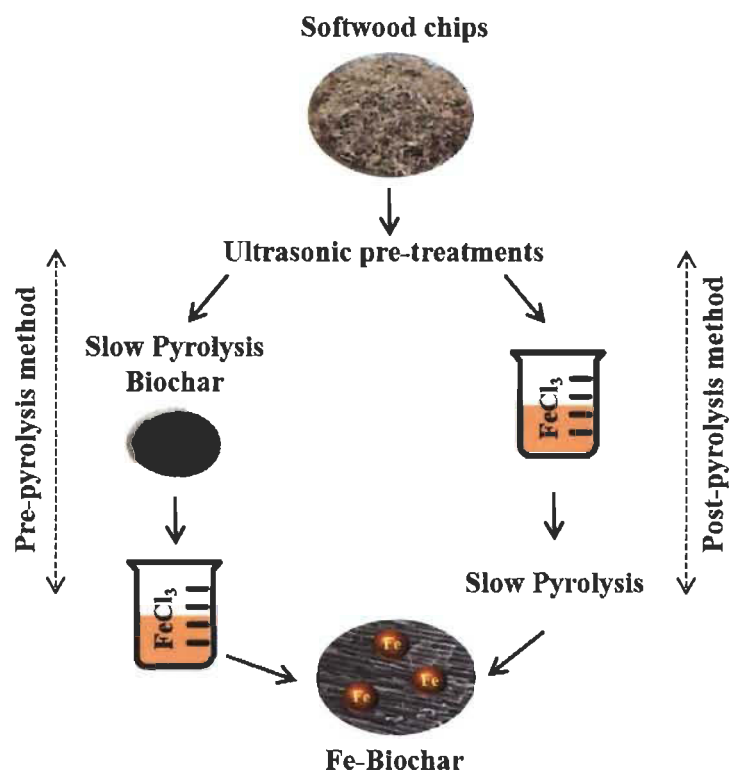


**Figure 7.2** Schematic representation of Fe-impregnation methods

#### 7.5.4 Surface and chemical characterisations

The surface functional groups were identified by infra-red spectroscopy (FTIR) using a Nicolet iS10 Smart iTR and KBr pellet. The reflection mode spectra were obtained in the range of 400-4000  $\text{cm}^{-1}$  for a minimum of 32 scans with 4  $\text{cm}^{-1}$  resolution. Scanning Electron Microscopy (SEM) (Hitachi SU1510) images of the materials were captured for surface morphology analysis. Energy Dispersive X-ray Spectroscopy (EDX) was obtained with an X-Max, Oxford instrument to verify the surface carbon and oxygen content. Thermogravimetric Analysis (TGA) was performed on a Perkin Elmer TGA 8000 Pyris series instrument. Under a flow of nitrogen (200 ml/min), the sample was heated from room temperature to 105 °C by ramping at 10 °C/min, and then heated to 800 °C.

## 7.6 Results and Discussion

### 7.6.1 Effect of iron impregnation on pyrolysis product yields

To study the influence of ultrasonic pre-treatment assisted iron impregnation on biochars, pyrolysis product yields were estimated (Figure 7.3). Fe-impregnation was done directly on the UST-woodchips, then subjected to pyrolysis (Post-pyrolysis) and the product yields were calculated and compared with corresponding non-impregnated sample yield. Figure 3a shows the product distribution of pyrolysis carried out on ultrasound pre-treated wood chips before Fe-impregnation. The percentage yield of biochar, aqueous phase obtained from condensation of gas, bio-oil, and biogas were compared to pyrolysis of a control feedstock (Untreated). The biochar and the liquid product yield (aqueous and bio-oil) was calculated directly from the initial and final weight difference of the containers. Biogas yield was calculated by mass balance (100- (biochar + aqueous + bio oil)). The UST-biochars exhibited the common trend which is dependent on pyrolysis temperature and reaction time. There was no significant change in yields with respect to ultrasonic pre-treatment conditions. However, a remarkable change in pyrolysis product yields were observed for post-pyrolysis method. As depicted in Figure 3b, the percentage yield of biochars increased significantly compared to the untreated sample. Concerning the related non-impregnated UST-biochars, this rise was more evident. Fe-UST1 has the maximum biochar yield among all with almost 33 percent increase compared to the corresponding non-impregnated sample (UST1). Despite an improvement in biochar yield, the bio-oil yield was dramatically decreased after Fe-impregnation. The pre-treated samples at 170 kHz (Fe-UST3 and Fe-UST4) had clearly lower yields compared to the untreated or non-impregnated UST-samples.

Dai et al. [29] have reported the same trend with bio oil. As explained in their study as well, the iron impregnated biochar formed during the pyrolysis itself act as a catalyst and facilitates the reforming or deoxygenation of pyrolysis vapors, forming the non-condensable gas. The primary reason for the increase in biogas percent during the post-pyrolysis method can be explained by this self-catalytic effect of iron impregnated biochars.

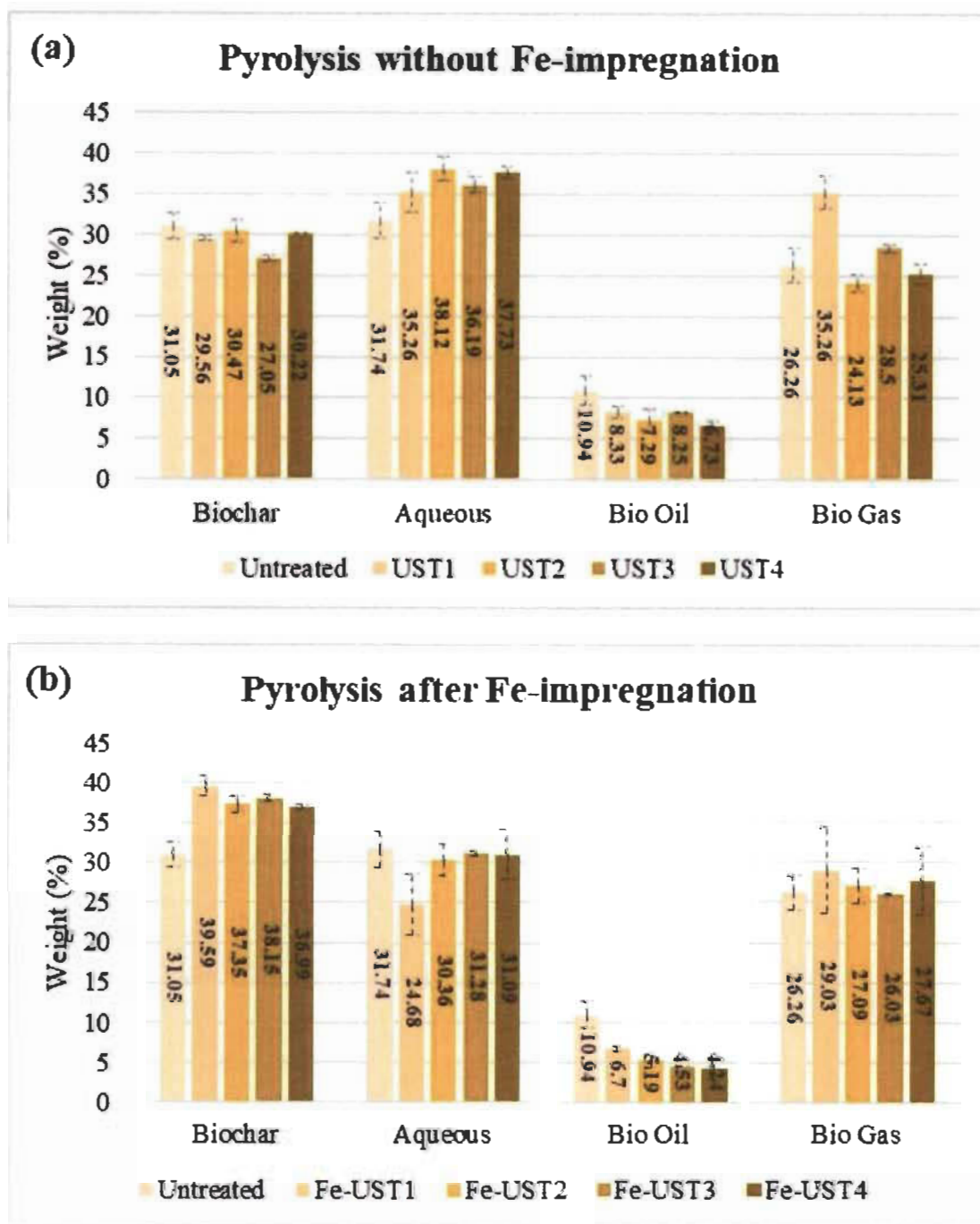


**Figure 7.3** Pyrolysis product distribution of pre and post-pyrolysis methods: (a) product yield for pyrolysis without Fe-Impregnation, (b) product yield for pyrolysis after Fe-impregnation

Similarly, Yaman et al. [28] have also described the presence of metal on biochar due to the impregnation methods that shifted the deoxygenation mechanism of the catalyst from

dehydration to decarbonylation and decarboxylation. They have reported a higher catalytic activity exhibited by Fe-impregnated SBA-15 with water, gas and solid product yields significantly enhanced.

These observations encouraged us to elucidate the efficiency of Fe-impregnated biochars for catalysis applications and how ultrasound pre-treatments could provide assistance to improve the impregnation on biochar surface.

## 7.6.2 Ultrasound pre-treatment and pyrolysis effect on Fe-impregnation

### 7.6.2.1 Effect of impregnation on biochar surface elemental composition

The surface elemental composition of modified biochars were analysed by EDX and the results are presented in Table 7.2. EDX gives total atomic percentage of elements found on the surface and the results excludes the contribution of hydrogen. Samples at 170 kHz (UST 3 and 4) showed comparatively higher atomic percentages than samples at 40 kHz (Fe-UST 1 and 2).

**Table 7.2** Atomic percent of different elements present on biochar surface

Sample	Pre-Pyrolysis			Post-Pyrolysis		
	C At%	O At%	Fe At%	C At%	O At%	Fe At%
Fe-UST1	87.9	10.5	1.1	95.4	3.3	1.3
Fe-UST2	89.1	10.0	0.5	91.7	7.1	0.7
Fe-UST3	90.6	7.0	1.4	88.8	8.7	1.5
Fe-UST4	89.1	9.5	1.0	90.8	7.3	1.5

However, the increase was marginal. Fe-UST2 displayed the lowest impregnation rate among all in both pre- and post-pyrolysis methods. With respect to the higher oxygen content in pre-pyrolysis samples, the impregnation of Fe-ions was expected to be higher in these samples. Interestingly, post-pyrolysed samples exhibited slightly better atomic percentage of iron on the surface. The quantity of iron impregnation on UST modified biochars was

better than those previously reported in the study by Dai et al. [29] in which they could achieve 0.15 percent of  $\text{Fe}^{3+}$  ions by using 0.2 mols of iron nitrate solution.

#### *7.6.2.2 Effect of impregnation on biochar surface morphology*

The morphology of the Fe-impregnated biochar samples prepared by pre- and post-pyrolysis was analyzed by SEM with magnification  $250\times$  (Figure 7.4). The images mainly showed the difference in structural characteristics at each ultrasonic pre-treatment level. In the case of pre-pyrolysis samples, the surface was more ruptured and heterogeneous with non-uniform channels and pores. This was more evident in the case of 40 kHz samples (Fe-UST1, Fe-UST2) and 170 kHz at high power (Fe-UST3). However, these alterations were less obvious in Fe-UST4 indicating that, at higher frequency and lower power, ultrasound pre-treatment did not really disturb the surface structure. For post-pyrolysed biochars, the microchannels and the layering were significantly altered, yet were consistent with the ultrasonic pre-treatments. Particularly, for low frequency samples (Fe-UST1 and Fe-UST2), the biochar surface seems to be more homogeneous and the microchannels were more polished compared to corresponding pre-pyrolysed samples. High frequency pre-treated samples (Fe-UST3 and Fe-UST4) were less affected and the surface was smooth. EDX mapping on localised surface indicated the homogenous spread of iron particles onto the surface. Post-pyrolysis samples demonstrated better distribution of Fe ions in comparison with pre-pyrolysis biochars. Among them, 170 kHz samples showed prominent distributions of Fe ions on the surface. The SEM and EDX results demonstrated the efficiency of ultrasonic pre-treatments to homogeneously impregnate iron particles on the material surface.

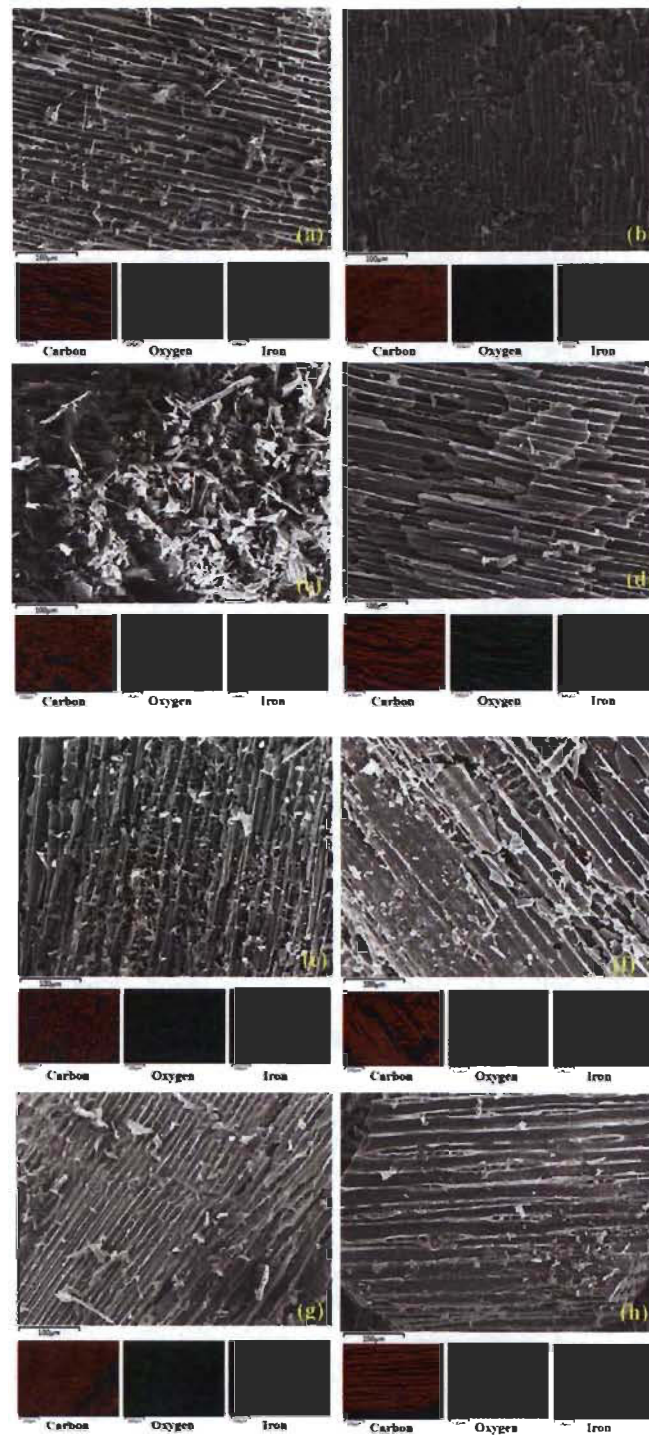


**Figure 7.4** Scanning Electron Microscope and EDX mapping images of different ultrasonic pre-treated samples: (a) and (b) Pre and post pyrolysis biochar of Fe- UST1 (c) and (d) Pre and post pyrolysis biochar of Fe- UST2 (e) and (f) Pre and post pyrolysis biochar of Fe- UST3 (g) and (h) Pre and post pyrolysis biochar of Fe- UST4

### 7.6.2.3 Effect of impregnation on biochar surface functional groups

To understand the influence of Fe-impregnation assisted by ultrasonic pre-treatment conditions on surface functionality of the biochar, infra-red spectra were analysed (Figure 7.5).

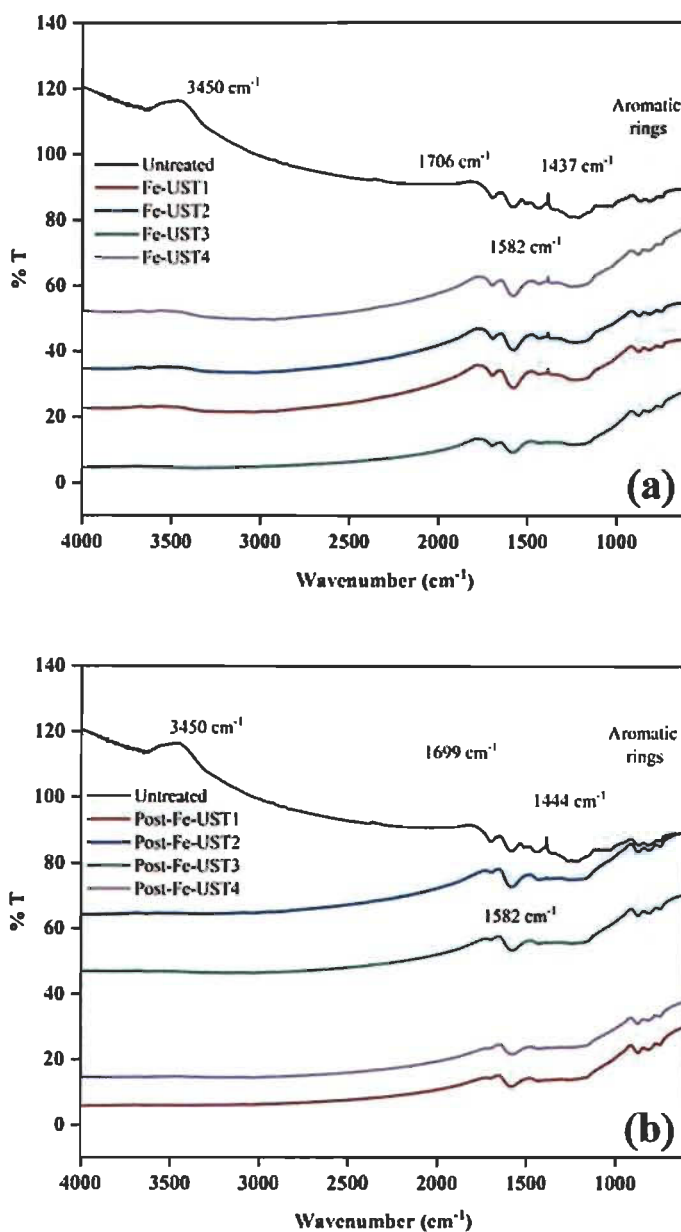


**Figure 7.5** Infrared spectra of Fe-impregnated biochars prepared from: (a) Pre-pyrolysis methods, (b) Post-pyrolysis method

The O-H vibration peak observed at  $3450\text{ cm}^{-1}$  disappeared after the impregnation experiments because of metal coordination with the functional group to form iron oxides. The main differences in FTIR spectra of unimpregnated and impregnated biochars were localized at wavelengths ranging from  $1750$  to  $1250\text{ cm}^{-1}$ . However, except for few intensity changes in bands, all the spectra were identical for every ultrasonic pre-treatment. At  $1700\text{ cm}^{-1}$ , C=O stretching vibrations of ketones and carboxylic acids were observed. Aromatic C-O stretching bands appeared at  $1440\text{ cm}^{-1}$ . A strong band at  $1582\text{ cm}^{-1}$  indicates the C=C and C=O stretching vibrations of aryl groups and this peak appeared to be more intense after Fe-impregnation.

These results provide a better understanding of the fact that the chemical composition of biochar is not affected by ultrasound pre-treatments, even after Fe-impregnation. The characteristic peaks were comparable with previously reported results for iron impregnated biochars [19,20,22].

#### ***7.6.2.4 Effect of iron impregnation on biochar thermal properties***

Thermal stability of all synthesized biochars were analysed using thermogravimetric analysis and Figure 7.6 represents comparative study between pre- and post-pyrolysis biochars. As evident from the graph, post-pyrolysed biochar samples exhibited significantly better thermal stability than untreated or corresponding pre-pyrolysed samples. The samples were stable up to around  $600\text{ }^{\circ}\text{C}$ . High frequency pre-treated samples had slightly improved thermal stability and low power sample (Post-Fe-UST4) possessed the highest stable temperature. This can be due to the strong chemical bond formation between biochar surface and impregnated Fe particles [20], which further enhanced by high frequency ultrasonication in low power condition. For the pre-pyrolysed biochars, major weight loss happened at around  $350\text{ }^{\circ}\text{C}$ , which is much lower than the post-pyrolysis samples. Ultrasonic pre-treatments had nominal influence on the thermal stability of Fe-impregnated biochars and the stability was less in comparison with the untreated biochar. High power pre-treated samples, irrespective of frequency, were the least stable biochars among all.

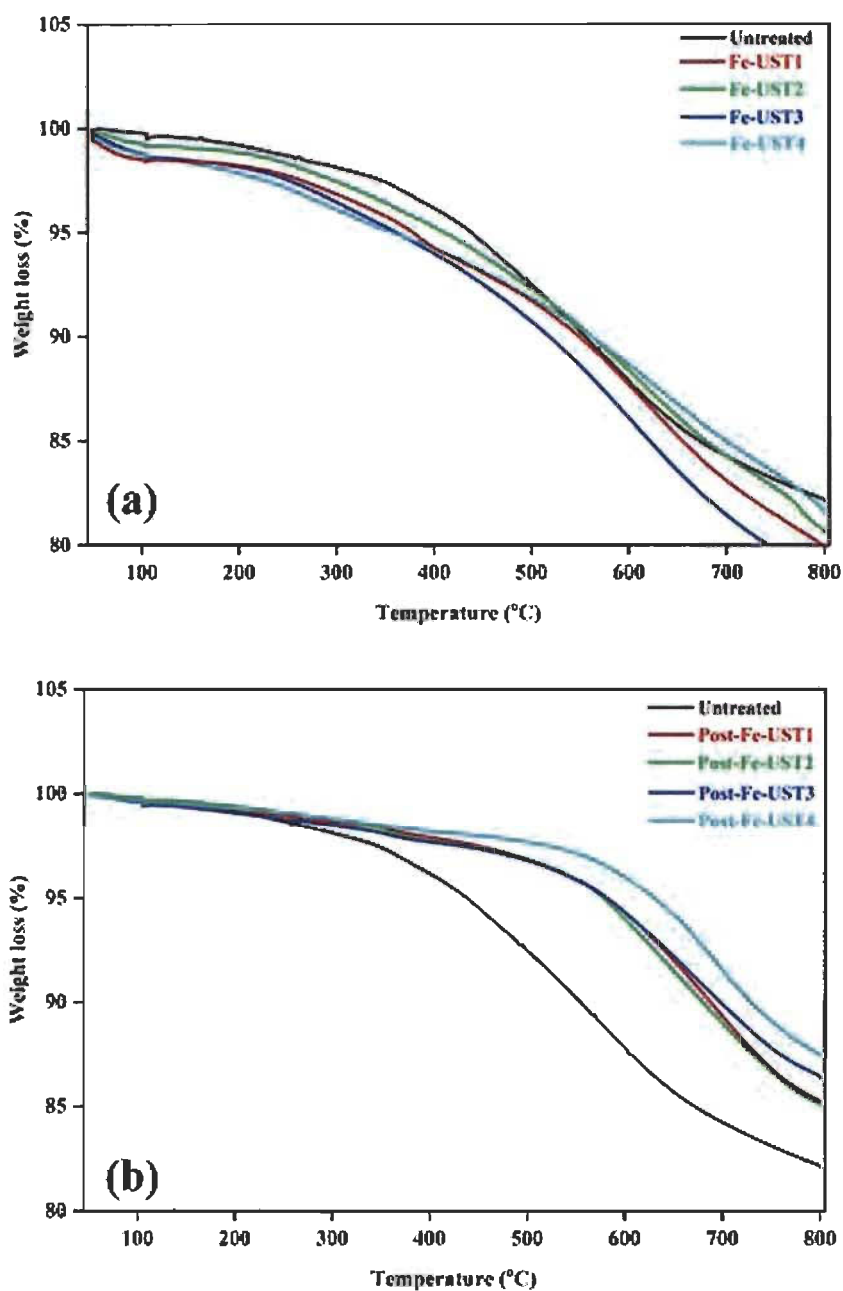


**Figure 7.6** Thermogravimetric analysis of Fe-impregnated biochars prepared using: (a) Pre-pyrolysis method, (b) Post-pyrolysis method

The chemical characteristic of biochar synthesized by pre- and post-pyrolysis method indicated that, even though the surface functionality remains the same with ultrasonic pre-treatments and iron impregnation, the thermal stability of the material was greatly influenced by the impregnation method and ultrasonic conditions. These results demonstrate

that, Fe-impregnation directly on biomass feedstock followed by pyrolysis provides biochar with higher yield, particle distribution on surface, and thermally much stable biochars. This low-cost, feasible methodology can be easily adapted in order to produce iron-based biochar catalysts to replace expensive and toxic metals like platinum, nickel etc.

## **7.7 Conclusions**

In this study, we have synthesized biochars modified with Fe ion particles using ultrasound assisted lab-scale slow pyrolysis. The lab-scale pyrolysis system could produce engineered biochars better yield exhibited after Fe-impregnation. post-pyrolysis method demonstrated better surface morphology with higher frequency samples and exhibited better impregnation results compared to low frequency samples. The surface functionality of all ultrasound pre-treated biochars remained the same in post and pre-pyrolysis method of impregnation. However, post-pyrolysed samples at high frequency ultrasound pre-treatment showed better thermal stability. These engineered biochars can be a potential, low-cost catalyst for various applications such as upgrading bio-oil, biodiesel production, hydrogen production, etc. Detailed investigations on bio-oil compositions produced with this technique and proof of catalytic activity of Fe-UST-biochars has yet to be done in order to examine potential applications.

## **7.8 Conflicts of interest**

The authors declare no competing interests.

## **7.9 Acknowledgement**

This project is funded by Natural Sciences and Engineering Research Council of Canada (NSERC). The authors are thankful to Queen Elizabeth II Diamond Jubilee Scholarship for other financial support and all the members of I2E3 for technical assistance during experiments.

## 7.10 References

- [1] Berndes G, Hoogwijk M, Van den Broek R (2003) The contribution of biomass in the future global energy supply: a review of 17 studies. *Biomass Bioenergy* 25 (1):1-28 [https://doi.org/10.1016/S0961-9534\(02\)00185-X](https://doi.org/10.1016/S0961-9534(02)00185-X)
- [2] Goyal H, Seal D, Saxena R (2008) Bio-fuels from thermochemical conversion of renewable resources: a review. *Renewable Sustainable Energy Rev.* 12 (2):504-517 <https://doi.org/10.1016/j.rser.2006.07.014>
- [3] Masnadi MS, Grace JR, Bi XT, Lim CJ, Ellis N (2015) From fossil fuels towards renewables: Inhibitory and catalytic effects on carbon thermochemical conversion during co-gasification of biomass with fossil fuels. *Appl Energy* 140:196-209 <https://doi.org/10.1016/j.apenergy.2014.12.006>
- [4] Gustavsson L, Börjesson P, Johansson B, Svaningsson P (1995) Reducing CO<sub>2</sub> emissions by substituting biomass for fossil fuels. *Energy* 20 (11):1097-1113 [https://doi.org/10.1016/0360-5442\(95\)00065-O](https://doi.org/10.1016/0360-5442(95)00065-O)
- [5] Gustavsson L, Holmberg J, Dornburg V, Sathre R, Eggers T, Mahapatra K, Marland G (2007) Using biomass for climate change mitigation and oil use reduction. *Energy Policy* 35 (11):5671-5691 <https://doi.org/10.1016/j.enpol.2007.05.023>
- [6] Kan T, Strezov V, Evans TJ (2016) Lignocellulosic biomass pyrolysis: A review of product properties and effects of pyrolysis parameters. *Renewable Sustainable Energy Rev.* 57:1126-1140 <https://doi.org/10.1016/j.rser.2015.12.185>
- [7] Mašek O, Budarin V, Gronnow M, Crombie K, Brownsort P, Fitzpatrick E, Hurst P (2013) Microwave and slow pyrolysis biochar—Comparison of physical and functional properties. *J Anal Appl Pyrolysis* 100:41-48 <https://doi.org/10.1016/j.jaap.2012.11.015>

- [8] Liaw S-S, Wang Z, Ndegwa P, Frear C, Ha S, Li C-Z, Garcia-Perez M (2012) Effect of pyrolysis temperature on the yield and properties of bio-oils obtained from the auger pyrolysis of Douglas Fir wood. *J Anal Appl Pyrolysis* 93:52-62 <https://doi.org/10.1016/j.jaap.2011.09.011>
- [9] Kloss S, Zehetner F, Dellantonio A, Hamid R, Ottner F, Liedtke V, Schwanninger M, Gerzabek MH, Soja G (2012) Characterization of slow pyrolysis biochars: effects of feedstocks and pyrolysis temperature on biochar properties. *J Environ Qual* 41 (4):990-1000 <https://doi.org/10.2134/jeq2011.0070>
- [10] Ahmad M, Lee SS, Dou X, Mohan D, Sung J-K, Yang JE, Ok YS (2012) Effects of pyrolysis temperature on soybean stover-and peanut shell-derived biochar properties and TCE adsorption in water. *Bioresour Technol* 118:536-544 <https://doi.org/10.1016/j.biortech.2012.05.042>
- [11] Martini S (2013) An overview of ultrasound. In: *Sonocrystallization of fats*. Springer, pp 7-16.
- [12] Cherpozat L, Loranger E, Daneault C (2017) Ultrasonic pretreatment effects on the bio-oil yield of a laboratory-scale slow wood pyrolysis. *J Anal Appl Pyrolysis* 126:31-38 <https://doi.org/10.1016/j.jaap.2017.06.027>
- [13] Hazrati S, Farahbakhsh M, Cerdà A, Heydarpoor G (2020) Functionalization of ultrasound enhanced sewage sludge-derived biochar: Physicochemical improvement and its effects on soil enzyme activities and heavy metals availability. *Chemosphere*:128767 <https://doi.org/10.1016/j.chemosphere.2020.128767>
- [14] Peter A, Chabot B, Loranger E Enhancing Surface Properties of Softwood Biochar by Ultrasound Assisted Slow Pyrolysis. In: *2019 IEEE International Ultrasonics Symposium (IUS)*, 2019. IEEE, pp 2477-2480 DOI: 10.1109/ULTSYM.2019.8925793

- [15] Peter A, Chabot B, Loranger E (2020) The influence of ultrasonic pre-treatments on metal adsorption properties of softwood-derived biochar. *Bioresour Technol Reports* 11 (September):100445. <https://doi.org/10.1016/j.biteb.2020.100445>
- [16] Sajjadi B, Broome JW, Chen WY, Mattern DL, Egiebor NO, Hammer N, Smith CL (2019) Urea functionalization of ultrasound-treated biochar: a feasible strategy for enhancing heavy metal adsorption capacity. *Ultrason Sonochem* 51:20-30 <https://doi.org/10.1016/j.ultsonch.2018.09.015>
- [17] Chatterjee R, Sajjadi B, Mattern DL, Chen W-Y, Zubatiuk T, Leszczynska D, Leszczynski J, Egiebor NO, Hammer N (2018) Ultrasound cavitation intensified amine functionalization: A feasible strategy for enhancing CO<sub>2</sub> capture capacity of biochar. *Fuel* 225:287-298 <https://doi.org/10.1016/j.fuel.2018.03.145>
- [18] Sizmur T, Fresno T, Akgül G, Frost H, Moreno-Jiménez E (2017) Biochar modification to enhance sorption of inorganics from water. *Bioresour Technol* 246:34-47 <https://doi.org/10.1016/j.biortech.2017.07.082>
- [19] Frišták V, Micháleková-Richveisová B, Víglášová E, Ďuriška L, Galamboš M, Moreno-Jiménez E, Pipíška M, Soja G (2017) Sorption separation of Eu and As from single-component systems by Fe-modified biochar: kinetic and equilibrium study. *J Iranian Chem Soc* 14 (3):521-530 DOI: 10.1007/s13738-016-1000-1
- [20] He R, Peng Z, Lyu H, Huang H, Nan Q, Tang J (2018) Synthesis and characterization of an iron-impregnated biochar for aqueous arsenic removal. *Sci Total Environ* 612:1177-1186 <https://doi.org/10.1016/j.scitotenv.2017.09.016>
- [21] Agrafioti E, Kalderis D, Diamadopoulos E (2014) Ca and Fe modified biochars as adsorbents of arsenic and chromium in aqueous solutions. *J Environ Manage* 146:444-450 <https://doi.org/10.1016/j.jenvman.2014.07.029>
- [22] Micháleková-Richveisová B, Frišták V, Pipíška M, Ďuriška L, Moreno-Jimenez E, Soja G (2017) Iron-impregnated biochars as effective phosphate sorption materials. *Environ Sci Pollut Res* 24 (1):463-475 DOI:10.1007/s11356-016-7820-9

- [23] Lee J, Kim K-H, Kwon EE (2017) Biochar as a catalyst. *Renewable Sustainable Energy Rev* 77:70-79 <https://doi.org/10.1016/j.rser.2017.04.002>
- [24] Xiong X, Iris K, Cao L, Tsang DC, Zhang S, Ok YS (2017) A review of biochar-based catalysts for chemical synthesis, biofuel production, and pollution control. *Bioresour Technol* 246:254-270 <https://doi.org/10.1016/j.biortech.2017.06.163>
- [25] Cao X, Sun S, Sun R (2017) Application of biochar-based catalysts in biomass upgrading: a review. *RSC Adv* 7 (77):48793-48805 DOI: 10.1039/C7RA09307A
- [26] Rubeena K, Reddy PHP, Laiju A, Nidheesh P (2018) Iron impregnated biochars as heterogeneous Fenton catalyst for the degradation of acid red 1 dye. *J Environ Manage* 226:320-328 <https://doi.org/10.1016/j.jenvman.2018.08.055>
- [27] Ren S, Lei H, Wang L, Bu Q, Chen S, Wu J (2014) Hydrocarbon and hydrogen-rich syngas production by biomass catalytic pyrolysis and bio-oil upgrading over biochar catalysts. *RSC Adv* 4 (21):10731-10737 DOI: 10.1039/C4RA00122B
- [28] Yaman E, Yargic AS, Ozbay N, Uzun BB, Kalogiannis KG, Stefanidis SD, Pachatouridou EP, Iliopoulou EF, Lappas AA (2018) Catalytic upgrading of pyrolysis vapours: Effect of catalyst support and metal type on phenolic content of bio-oil. *J Cleaner Prod* 185:52-61 <https://doi.org/10.1016/j.jclepro.2018.03.033>
- [29] Dai L, Zeng Z, Tian X, Jiang L, Yu Z, Wu Q, Wang Y, Liu Y, Ruan R (2019) Microwave-assisted catalytic pyrolysis of torrefied corn cob for phenol-rich bio-oil production over Fe modified bio-char catalyst. *J Anal Appl Pyrolysis* 143:104691 <https://doi.org/10.1016/j.jaap.2019.104691>
- [30] Nguyen HK, Pham VV, Do HT (2016) Preparation of Ni/biochar catalyst for hydrotreating of bio-oil from microalgae biomass. *Catal Lett* 146 (11):2381-2391 <https://doi.org/10.1007/s10562-016-1873-8>
- [31] Kastner JR, Mani S, Juneja A (2015) Catalytic decomposition of tar using iron supported biochar. *Fuel Process Technol* 130:31-37 <https://doi.org/10.1016/j.fuproc.2014.09.038>

- [32] Park J-H, Wang JJ, Xiao R, Tafti N, DeLaune RD, Seo D-C (2018) Degradation of Orange G by Fenton-like reaction with Fe-impregnated biochar catalyst. *Bioresour Technol* 249:368-376 <https://doi.org/10.1016/j.biortech.2017.10.030>
- [33] Cao X, Huang Y, Tang C, Wang J, Jonson D, Fang Y (2020) Preliminary study on the electrocatalytic performance of an iron biochar catalyst prepared from iron-enriched plants. *J. Environ. Sci.* 88:81-89 <https://doi.org/10.1016/j.jes.2019.08.004>
- [34] Nejati B, Adami P, Bozorg A, Tavasoli A, Mirzahosseini AH (2020) Catalytic pyrolysis and bio-products upgrading derived from *Chlorella vulgaris* over its biochar and activated biochar-supported Fe catalysts. *J Anal Appl Pyrolysis* 152:104799 <https://doi.org/10.1016/j.jaap.2020.104799>
- [35] Loranger É, Pombert O. and Drouadaine V. (2016) Ultrasonic pre-treatments of wood chips used in a conventional pyrolysis and their effect on bio-oil composition and calorimetry. SAMPE Conference Proceedings.

### 7.11 Highlights

- UST assisted Fe-impregnation showed homogenous spread of particles on surface
- Fe-impregnation followed by lab-scale pyrolysis exhibited better biochar yield
- Post-pyrolysed samples demonstrated better thermal stability
- Chemical characteristics were comparable with Fe-modified biochars from literature
- The modified biochars can be a low-cost replacement for biomass catalysts

## Chapter 8 – Conclusions and Future Perspectives

### 8.1 General conclusions

This research project was an effort to synthesize biochar using ultrasound pre-treated softwood biochar from a lab-scale pyrolyser, study its efficiency to remove toxic heavy metals from aqueous solution, and understand the influence of ultrasonic pre-treatments on different modifications on biochar surface. The detailed literature survey assisted in the understanding of the recent developments happening in biochar research related to heavy metal removal. It was also very helpful to show how power ultrasound techniques can provide a better assistance in order to improve material characteristics.

The main objective of scientific article 1 was to synthesize biochar from ultrasound pre-treated wood chips and his characterization to understand the physical and chemical effect of ultrasound on pyrolysis products yield and biochar structure. The low-cost, good quality biochar synthesized using lab-scale pyrolysis system showed a negatively charged surface at neutral and basic pH values, and a modified morphology from the ultrasonic pre-treatments. However, the chemical characteristics of biochar, including functional groups present on the surface, was not affected by ultrasound, even with is mechanical or sonochemical effect. Ultrasonic pre-treated samples also exhibited better equilibrium adsorption capacity for copper ions from water. The preliminary results obtained were encouraging to pursue more on the adsorption properties of these biochars. Thus, the detailed investigation on influence of ultrasonic pre-treatments on metal adsorption properties were carried out. Different combinations of ultrasound frequency, power, bath temperature and exposure time were employed to pre-treat post-consumer feedstock.

As reported in article 2, using copper as a model metal contaminant, adsorption kinetics, isotherm and thermodynamic properties were investigated for each ultrasonic pre-treatment conditions. It was interesting to see that the ultrasonic pre-treated wood biochar exhibited different adsorption behaviour than untreated sample. The equilibrium adsorption capacity of low frequency pre-treated samples was better in comparison with high frequency or

untreated biochars. However, the statistical studies showed that the combination of frequency with power, time and temperature equally contributed towards the enhancement of adsorption capacity of the material. The experimental data followed Langmuir isotherm for all UST-biochars, which describes a monolayer adsorption on a homogenous surface and thermodynamic parameters explaining an endothermic process of adsorption. Though the mechanical effect plays a vital role in adsorption capacity of these biochars, high frequency pre-treated samples exhibited better adsorption capacity per unit surface area ( $\text{mg}/\text{m}^2$ ). This motivated us to believe that activation or chemical modifications on these biochars is of further interest to investigate the ultrasonic pre-treatment effects on chemical modifications on biochar. This was the primary objective addressed in article 3.

Alkali activation of ultrasonic pre-treated wood biochar has been investigated to develop a cost-effective replacement of activated carbons for heavy metal removal from water. Ultrasound pre-treatment assisted biochars showed better adsorption capacity as compared to untreated biochar samples after activation using NaOH. The two-step activation of biochar resulted in highest equilibrium adsorption capacity for copper ions among the previously reported wood derived biochars. In contrast to the results from article 2, 170 kHz pre-treated sample exhibited highest equilibrium adsorption capacity which was almost 20 times higher than that of corresponding non-activated sample. The ultrasound pre-treatment facilitated the accessibility of a heterogeneous surface with wide opening of already existing pores and microchannels, and the alkali treatment improved the availability surface anchoring sites. The underlying mechanism was found to be chemisorption, expected to be ion exchange reactions resulting from the sodium ions present on the surface anchoring sites. The ultrasound pre-treated samples also displayed improved competitive adsorption behaviour towards copper ions in comparison with nickel or lead.

Motivated by the interesting results obtained for ultrasonic pre-treated softwood biochar, ultrasonic pre-treatment effects of iron impregnation were investigated as a side project. The influence of ultrasonic pre-treatments to modify the surface properties of biochar was proven from the first three scientific articles. Hence, the pre- and post- pyrolysis impregnation effects on ultrasound pre-treated biochars were investigated in article 4. UST assisted Fe-impregnation showed homogenous spread of particles on surface with chemical

characteristics comparable with previous reports on iron impregnation. Fe-impregnation followed by lab-scale pyrolysis exhibited better biochar yield and improved thermal stability. Thus, the modified biochars can be a low-cost replacement for biomass catalysts for various applications such as upgrading bio oil, biodiesel production, hydrogen production, etc.

The use of ultrasonic treatment in biomass to enhance the physicochemical properties gives the scientific world an insight to the potential use of power ultrasound in biomass processing. The enhanced adsorption properties of biochar we synthesized contribute to the development of an effective adsorbent based on cutting-edge technologies. This project is also a significant add up to the field of wastewater treatment, allowing an efficient removal of toxic metals. Influence of power ultrasound pre-treatment to enhance metal impregnations on material surface is also an additional benefit for biochars to be used as cost-effective catalysts. A decent number of publications we achieved from this project represent well our institution and the province of Quebec in the scientific community. This project can also help the authorities for the better management and processing of biomass feedstocks. We expect that the outcomes of this research will make a significant change in conventional methods of water recycling by providing improved properties of the materials used and enhance the water sustainability and environmental protection.

## **8.2 Future aspects**

The successful synthesis of ultrasound pre-treated softwood biochars with enhanced physicochemical properties and adsorption behaviour open up a variety of novel potential strategies that can be implemented on these engineered biochars. A few promising areas where the research can point out future perspectives are listed below:

- From scientific article II, we have seen that the low-frequency ultrasound pre-treatment has effectively modified surface morphology and the adsorption properties of these biochars were comparatively better than the untreated or high frequency pre-treated biochars. The mechanical effect of ultrasound was evident by these results and this effect could be further investigated by going down to even lower frequency regions. 25 kHz ultrasound pre-treatments could be implemented

by using the lab sonoreactor and the investigation on physicochemical properties would be interesting to explore.

- Article III and IV has demonstrated the efficiency of ultrasonic pre-treatments on enhancement of different modifications on material surface (chemical activation and iron impregnations). These findings are motivational to explore the effect of ultrasonic pre-treatments on organic functionalisation, modifications using nanocomposites and graphene oxide on biochar surface. The modified biochars could provide enhanced adsorption capacity and thus efficient removal of toxic contaminants from wastewater.
- The practical applications of biochars synthesized in this project could be achieved by evaluating the dynamic adsorption properties. Fixed-bed column studies could be performed to obtain breakthrough curves at different operating conditions varying the feed flow, feed concentration, pH and L/D ratio of packed bed. Parameters such as breakthrough time, saturation time, the bed adsorption capacity and the length of mass transfer zone could be evaluated to make use of ultrasound pre-treated biochars for real life application of industrial wastewater treatment.
- The detailed investigation on catalytic activity of Fe-impregnated biochars could be further explored. The analysis on composition of bio oil obtained from these studies can also be examined to understand the efficiency of Fe-impregnated biochars as catalyst for bio oil upgradation.

## **Appendix 1 – Supplementary Information of Article 2**

### **The influence of ultrasonic pre-treatments on metal adsorption properties of softwood-derived biochar**

Aneeshma Peter<sup>a</sup>, Bruno Chabot<sup>a</sup>, Eric Loranger<sup>a\*</sup>

<sup>a</sup> I2E3 – Institut d’Innovations en Écomatériaux, Écoproduits et Écoénergies, à base de biomasse, Université du Québec à Trois-Rivières, 3351, boul. des Forges, Trois-Rivières, Québec, Canada G8Z 4M3

\* Corresponding author:

Tel: +1 819 376-5011, poste 4518

Fax: +1 819 376-5148

E-mail address: [Eric.Loranger1@uqtr.ca](mailto:Eric.Loranger1@uqtr.ca)

## Supplementary Information

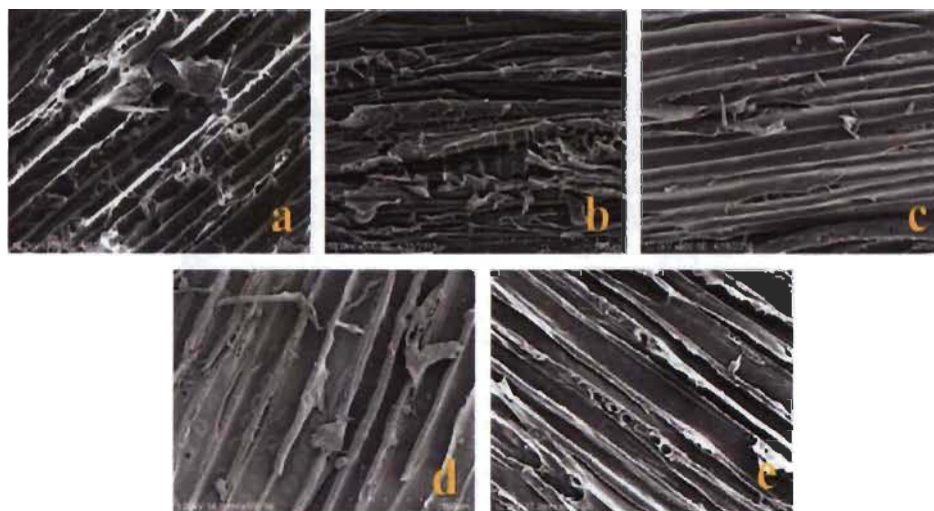


**Figure A1 S1** Scanning Electron Microscope images of different biochar samples (magnification 500x). (a) Untreated biochar, (b) UST-3 (40 kHz, 1000 W, 80 °C for 2 h), (c) UST-6 (40 kHz, 250 W, 20 °C for 1 h), (d) UST-11 (170 kHz, 1000 W, 80 °C for 2 h), (e) UST-14 (170 kHz, 250 W, 20 °C for 1 h)

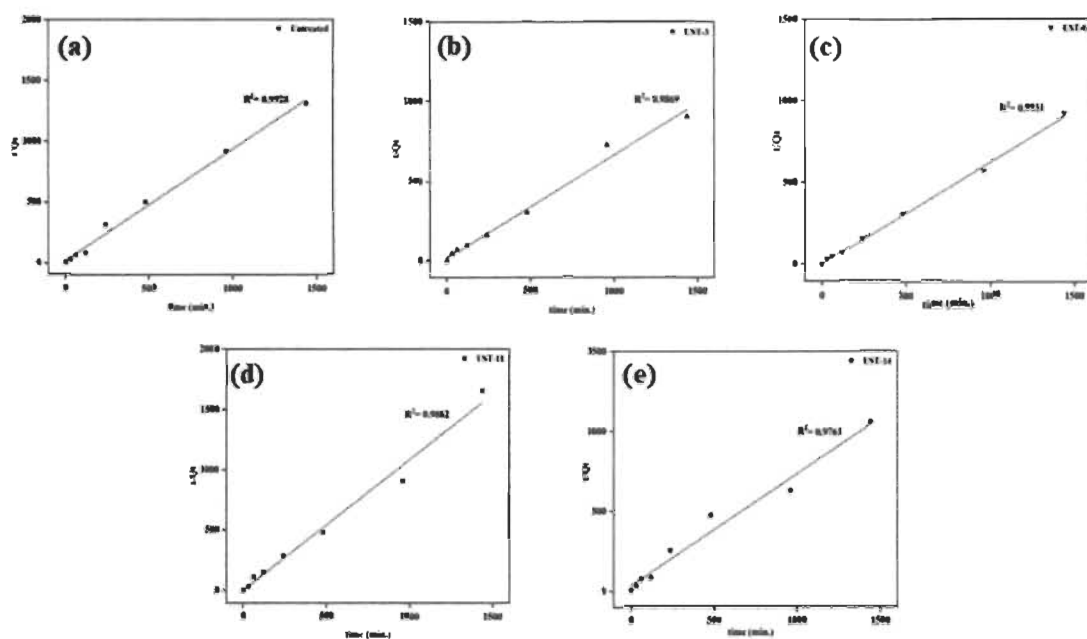


**Figure A1 S2** Linear Pseudo-second order kinetic models for: (a) Untreated biochar, (b) UST-3 (40 kHz, 1000 W, 80 °C for 2 h), (c) UST-6 (40 kHz, 250 W, 20 °C for 1 h), (d) UST-11 (170 kHz, 1000 W, 80 °C for 2 h), (e) UST-14 (170 kHz, 250 W, 20 °C for 1 h).

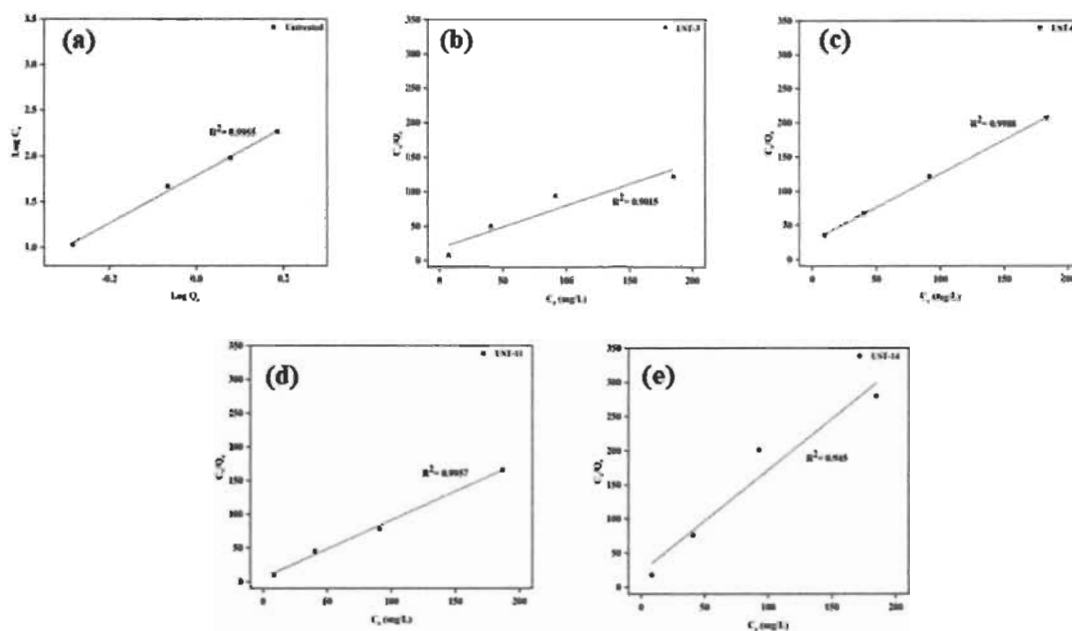


**Figure A1 S3** Best fit linear isotherm models for selected biochar samples: (a) Freundlich isotherm linear fitting for Untreated biochar, (b) Langmuir isotherm linear fitting for UST-3 (40 kHz, 1000 W, 80 °C for 2 h), (c) Langmuir isotherm linear fitting for UST-6 (40 kHz, 250 W, 20 °C for 1 h), (d) Langmuir isotherm linear fitting for UST-11 (170 kHz, 1000 W, 80 °C for 2 h), (e) Langmuir isotherm linear fitting for UST-14 (170 kHz, 250 W, 20 °C for 1 h).

## Appendix 2 – Supplementary Information of Article 3

### Enhanced activation of ultrasonic pre-treated softwood biochar for efficient heavy metal removal from water

Aneeshma Peter<sup>a</sup>, Bruno Chabot<sup>a</sup>, Eric Loranger<sup>a\*</sup>

<sup>a</sup> I2E3 – Institut d’Innovations en Écomatériaux, Écoproduits et Écoénergies, à base de biomasse, Université du Québec à Trois-Rivières, 3351, boul. des Forges, Trois-Rivières, Québec, Canada G8Z 4M3

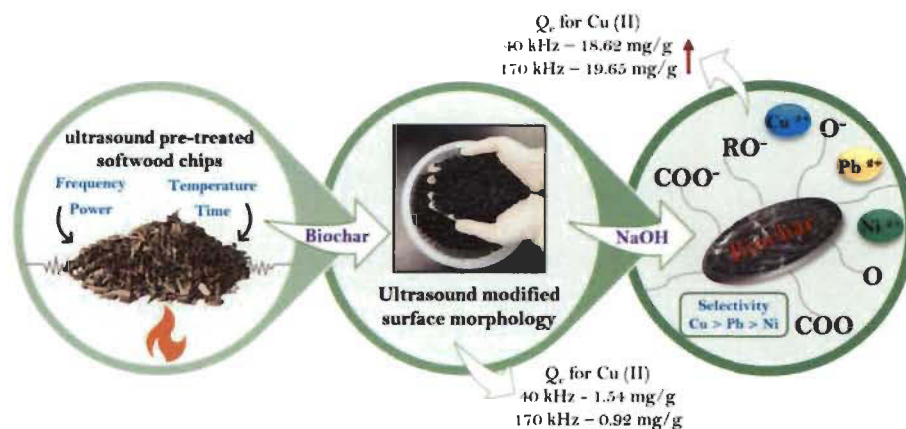
\* Corresponding author:

Tel: +1 819 376-5011, poste 4518

Fax: +1 819 376-5148

E-mail: [Eric.Loranger1@uqtr.ca](mailto:Eric.Loranger1@uqtr.ca)

#### Graphical Abstract



## Supplementary Information



Figure A2 S1 EDX mapping spectra of Act-Untreated

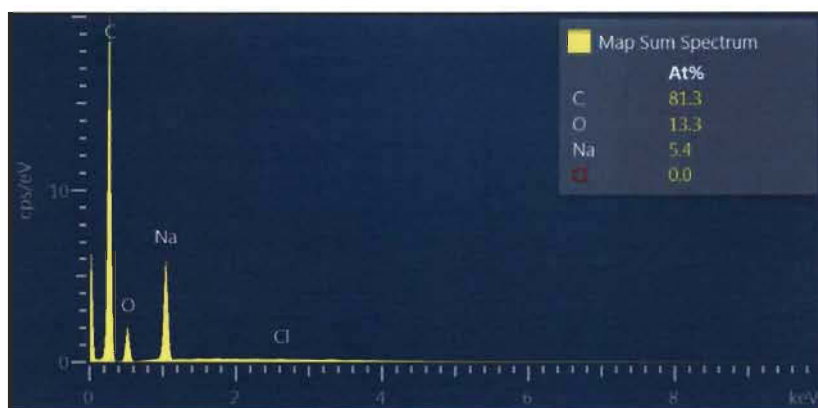


Figure A2 S2 EDX mapping spectra of Act-UST1 (40 kHz, 1000 W at 80 °C for 2 h)

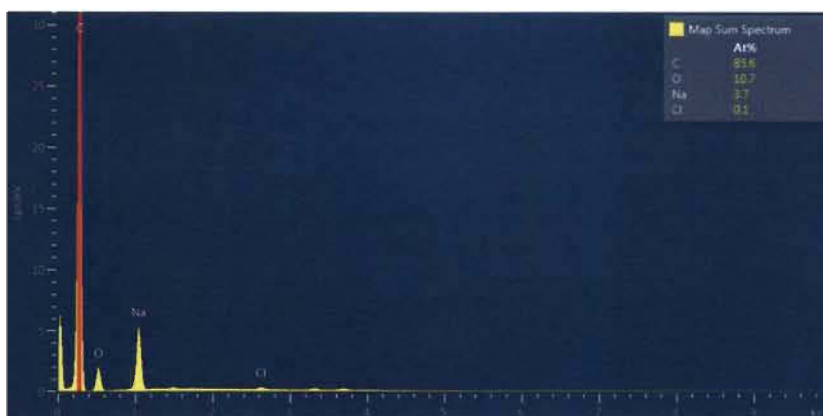
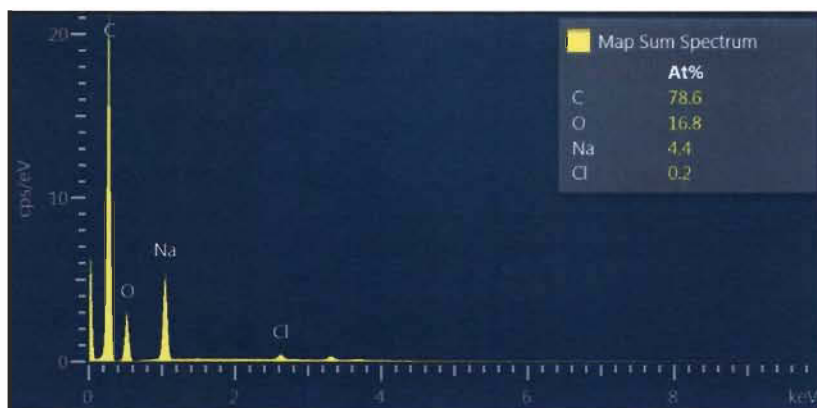
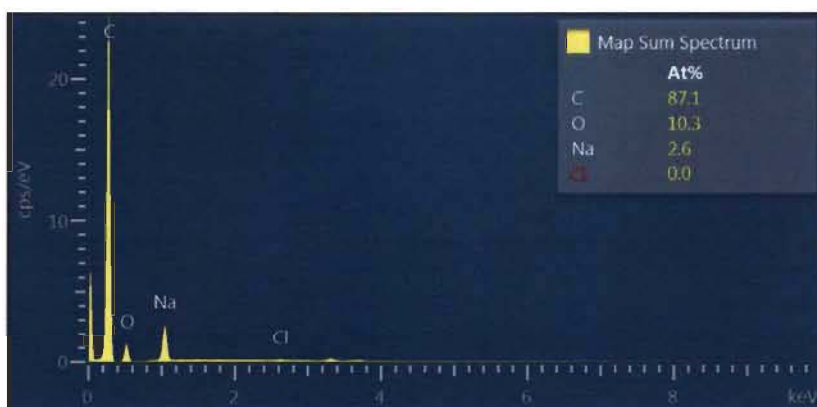


Figure A2 S3 EDX mapping spectra of Act-UST2 (40 kHz, 250 W at 20 °C for 1 h)



**Figure A2 S4** EDX mapping spectra of Act-UST3 (170 kHz, 1000 W at 80 °C for 2 h)



**Figure A2 S5** EDX mapping spectra of Act-UST4 (170 kHz, 250 W at 20 °C for 1 h)

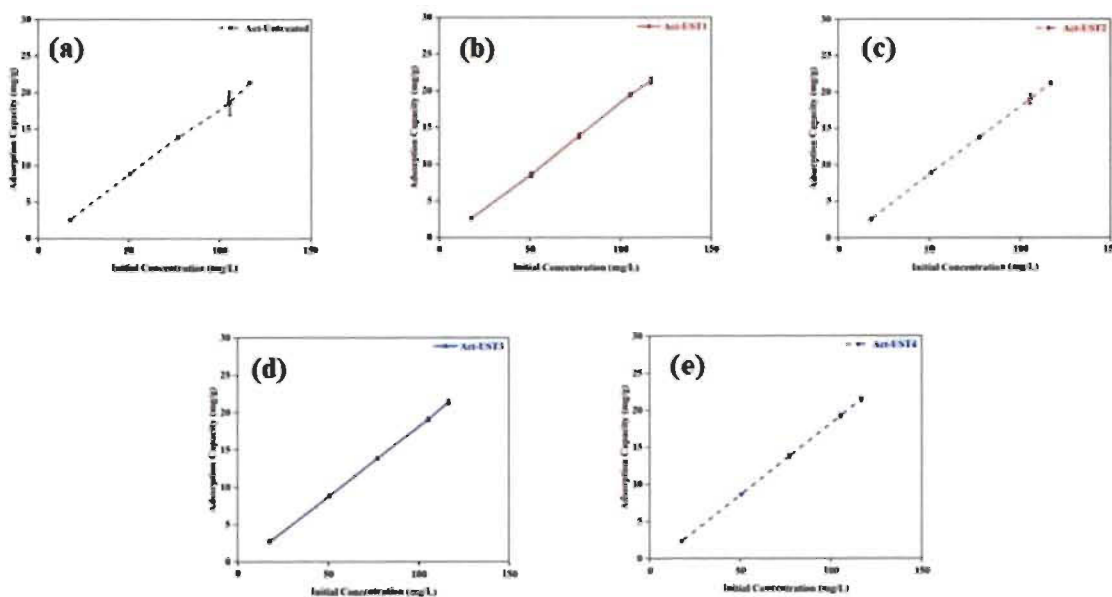


**Figure A2 S6** Change in adsorption capacity with initial metal concentration of: (a) Act-Untreated, (b) Act-UST1 (40 kHz, 1000 W at 80 °C for 2 h), (c) Act-UST2 (40 kHz, 250 W at 20 °C for 1 h), (d) Act-UST3 (170 kHz, 1000 W at 80 °C for 2 h), and (e) Act-UST4 (170 kHz, 250 W at 20 °C for 1 h)

**Table A2 S1** Competitive adsorption behaviour of biochar samples towards Cu (II), Ni (II) and Pb (II) ions

Metal/Sample	Initial Conc. (mg/L)	Act-Untreated	Act-UST1	Act-UST2	Act-UST3	Act-UST4
Cu (II)	9.06	1.69	1.78	1.79	1.77	1.72
	21.32	4.23	4.12	4.21	4.18	4.1
	42.635	8.27	8.30	7.55	8.06	8.39
	68.135	13.16	13.18	12.52	12.92	13.04
	82.22	15.34	16	16.04	15.37	15.81
Ni (II)	6.24	1.16	1.12	1.23	1.216	1.066
	18.25	3.6	3.49	3.56	3.56	3.43
	33.075	6.34	3.5	5.99	4.95	2.29
	57.885	7.85	4.93	9.44	6.23	3.94
	77.94	6.19	5.04	9.42	3.86	2.24
Pb (II)	9.77	1.79	1.86	1.92	1.89	1.82
	24.64	4.77	4.71	4.74	4.75	4.67
	41.01	6.29	6.31	5.56	6.10	6.40
	33.075	6.31	6.23	5.86	6.11	6.06
	33.68	5.67	6.29	6.35	5.71	5.99

## Chapter 9 – References

1. Mancosu, N.; Snyder, R. L.; Kyriakakis, G.; Spano, D., Water scarcity and future challenges for food production. *Water* 2015, 7 (3), 975-992.
2. Pengra, B., A Glass Half Empty: Regions at Risk Due to Groundwater Depletion. United Nations Environmental Program (UNEP) 2012.
3. Hassan, N., Ground Water Depletion Due To Water Mining–A Threat. *J. Environ. Sci. Comput. Sci. Eng. Technol.* 2016, 5 (2), 129-136.
4. Patterson, J. W., *Industrial wastewater treatment technology*. 1985.
5. Arceivala, S. J.; Asolekar, S. R., *Wastewater treatment for pollution control and reuse*. Tata McGraw-Hill Education: 2006.
6. Bhardwaj, R.; Gupta, A.; Garg, J., Evaluation of heavy metal contamination using environmetrics and indexing approach for River Yamuna, Delhi stretch, India. *Water Science* 2017, 31 (1), 52-66.
7. Briffa, J.; Sinagra, E.; Blundell, R., Heavy metal pollution in the environment and their toxicological effects on humans. *Heliyon* 2020, 6 (9), e04691.
8. Rajaganapathy, V.; Xavier, F.; Sreekumar, D.; Mandal, P., Heavy metal contamination in soil, water and fodder and their presence in livestock and products: a review. *J. Environ. Sci. Technol.* 2011, 4 (3), 234-249.
9. Dietrich, A. M.; Burlingame, G. A., Critical review and rethinking of USEPA secondary standards for maintaining organoleptic quality of drinking water. *Environ. Sci. Technol.* 2015, 49 (2), 708-720.
10. Barakat, M., New trends in removing heavy metals from industrial wastewater. *Arabian J. Chem.* 2011, 4 (4), 361-377.

11. Duruibe, J. O.; Ogwuegbu, M.; Egwurugwu, J., Heavy metal pollution and human biotoxic effects. *Int. J. Phys. Sci.* 2007, 2 (5), 112-118.
12. Environment, A. Environmental Case Study: 3 Historical Heavy Metal Disasters.
13. Fu, F.; Wang, Q., Removal of heavy metal ions from wastewaters: a review. *J. Environ. Manage.* 2011, 92 (3), 407-418.
14. Gunatilake, S., Methods of removing heavy metals from industrial wastewater. *Methods* 2015, 1 (1), 14.
15. Zhang, Y.; Duan, X., Chemical precipitation of heavy metals from wastewater by using the synthetical magnesium hydroxy carbonate. *Water Sci. Technol.* 2020, 81 (6), 1130-1136.
16. Deliyanni, E. A.; Kyzas, G. Z.; Triantafyllidis, K. S.; Matis, K. A., Activated carbons for the removal of heavy metal ions: A systematic review of recent literature focused on lead and arsenic ions. *Open Chemistry* 2015, 1 (open-issue).
17. Demirbas, A., Agricultural based activated carbons for the removal of dyes from aqueous solutions: a review. *J. Hazard. Mater.* 2009, 167 (1-3), 1-9.
18. Ince, M.; Ince, O. K., An overview of adsorption technique for heavy metal removal from water/wastewater: A critical review. *Int. J. Pure Appl. Sci* 2017, 3 (2), 10-19.
19. Tajar, A. F.; Kaghazchi, T.; Soleimani, M., Adsorption of cadmium from aqueous solutions on sulfurized activated carbon prepared from nut shells. *J. Hazard. Mater.* 2009, 165 (1-3), 1159-1164.
20. Mohan, D.; Singh, K. P., Single-and multi-component adsorption of cadmium and zinc using activated carbon derived from bagasse—an agricultural waste. *Water Res.* 2002, 36 (9), 2304-2318.
21. Bansal, R. C.; Goyal, M., Activated carbon adsorption. CRC press: 2005.

22. Saleem, J.; Shahid, U. B.; Hijab, M.; Mackey, H.; McKay, G., Production and applications of activated carbons as adsorbents from olive stones. *Biomass Convers. Biorefin.* 2019, 1-28.
23. Flèche, E. R. L. Quebec releases its Energy Policy 2030.
24. Prasad KMK; Raheem S. Evaluation of the quality of colour changes of complexometric indicators in the titration of copper (II) with EDTA by tristimulus colorimetry. *Microchimica Acta* 1993, 11, 63-69.
25. Manyà, J. J., Pyrolysis for biochar purposes: a review to establish current knowledge gaps and research needs. *Environ. Sci. Technol.* 2012, 46 (15), 7939-7954.
26. Oliveira, F. R.; Patel, A. K.; Jaisi, D. P.; Adhikari, S.; Lu, H.; Khanal, S. K., Environmental application of biochar: Current status and perspectives. *Bioresour. Technol.* 2017, 246, 110-122.
27. Tang, J.; Zhu, W.; Kookana, R.; Katayama, A., Characteristics of biochar and its application in remediation of contaminated soil. *J. Biosci. Bioeng.* 2013, 116 (6), 653-659.
28. Spokas, K. A.; Cantrell, K. B.; Novak, J. M.; Archer, D. W.; Ippolito, J. A.; Collins, H. P.; Boateng, A. A.; Lima, I. M.; Lamb, M. C.; McAloon, A. J., Biochar: a synthesis of its agronomic impact beyond carbon sequestration. *J. Environ. Qual.* 2012, 41 (4), 973-989.
29. Inyang, M. I.; Gao, B.; Yao, Y.; Xue, Y.; Zimmerman, A.; Mosa, A.; Pullammanappallil, P.; Ok, Y. S.; Cao, X., A review of biochar as a low-cost adsorbent for aqueous heavy metal removal. *Crit. Rev. Environ. Sci. Technol.* 2016, 46 (4), 406-433.
30. Tan, X.; Liu, Y.; Zeng, G.; Wang, X.; Hu, X.; Gu, Y.; Yang, Z., Application of biochar for the removal of pollutants from aqueous solutions. *Chemosphere* 2015, 125, 70-85.

31. Patra, J.; Panda, S.; Dhal, N., Biochar as a low-cost adsorbent for heavy metal removal: A review. *Int. J. Res. Biosciences* 2017, 6 (1), 1-7.
32. McLaughlin, H., *An Overview of the Current Biochar and Activated Carbon Markets: Biofuels Digest.* 2019.
33. Yu, K. L.; Lau, B. F.; Show, P. L.; Ong, H. C.; Ling, T. C.; Chen, W.-H.; Ng, E. P.; Chang, J.-S., Recent developments on algal biochar production and characterization. *Bioresour. Technol.* 2017, 246, 2-11.
34. Qian, K.; Kumar, A.; Zhang, H.; Bellmer, D.; Huhnke, R., Recent advances in utilization of biochar. *Renewable Sustainable Energy Rev.* 2015, 42, 1055-1064.
35. Kan, T.; Strezov, V.; Evans, T. J., Lignocellulosic biomass pyrolysis: A review of product properties and effects of pyrolysis parameters. *Renewable Sustainable Energy Rev.* 2016, 57, 1126-1140.
- 36.. Van Zwieten, L.; Kimber, S.; Morris, S.; Chan, K.; Downie, A.; Rust, J.; Joseph, S.; Cowie, A., Effects of biochar from slow pyrolysis of papermill waste on agronomic performance and soil fertility. *Plant Soil* 2010, 327 (1-2), 235-246.
37. Brewer, C. E.; Schmidt-Rohr, K.; Satrio, J. A.; Brown, R. C., Characterization of biochar from fast pyrolysis and gasification systems. *Environmental Progress & Sustainable Energy: An Official Publication of the American Institute of Chemical Engineers* 2009, 28 (3), 386-396.
38. Bridgwater, A., *Thermal biomass conversion and utilization: biomass information system.* Office for Official Publications of the European Communities: 1996.
39. Lehto, J.; Oasmaa, A.; Solantausta, Y.; Kytö, M.; Chiaramonti, D., Review of fuel oil quality and combustion of fast pyrolysis bio-oils from lignocellulosic biomass. *Applied Energy* 2014, 116, 178-190.
40. Scott, D. S.; Piskorz, J., The continuous flash pyrolysis of biomass. *Can. J. Chem. Eng.* 1984, 62 (3), 404-412.

41. Funke, A.; Ziegler, F., Hydrothermal carbonization of biomass: a summary and discussion of chemical mechanisms for process engineering. *Biofuels, Bioprod. Biorefin.* 2010, 4 (2), 160-177.
42. Zhu, X.; Liu, Y.; Qian, F.; Zhou, C.; Zhang, S.; Chen, J., Role of hydrochar properties on the porosity of hydrochar-based porous carbon for their sustainable application. *ACS Sustainable Chem. Eng.* 2015, 3 (5), 833-840.
43. Wang, T.; Zhai, Y.; Zhu, Y.; Li, C.; Zeng, G., A review of the hydrothermal carbonization of biomass waste for hydrochar formation: Process conditions, fundamentals, and physicochemical properties. *Renewable Sustainable Energy Rev.* 2018, 90, 223-247.
44. Shankar Tumuluru, J.; Sokhansanj, S.; Hess, J. R.; Wright, C. T.; Boardman, R. D., A review on biomass torrefaction process and product properties for energy applications. *Industrial Biotechnology* 2011, 7 (5), 384-401.
45. Chen, W.-H.; Hsu, H.-C.; Lu, K.-M.; Lee, W.-J.; Lin, T.-C., Thermal pretreatment of wood (Lauan) block by torrefaction and its influence on the properties of the biomass. *Energy* 2011, 36 (5), 3012-3021.
46. Kirubakaran, V.; Sivaramakrishnan, V.; Nalini, R.; Sekar, T.; Premalatha, M.; Subramanian, P., A review on gasification of biomass. *Renewable Sustainable Energy Rev.* 2009, 13 (1), 179-186.
47. É. Loranger, O. P. a. V. D., Ultrasonic pre-treatments of wood chips used in a conventional pyrolysis and their effect on bio-oil composition and calorimetry. *SAMPE Conference Proceedings*, 2016.
48. Cherpozat, L.; Loranger, E.; Daneault, C., Ultrasonic pretreatment effects on the bio-oil yield of a laboratory-scale slow wood pyrolysis. *J. Anal. Appl. Pyrolysis* 2017, 126, 31-38.

49. Pichon, L.; Loranger, E. In Preliminary study in using ultrasound as a post-treatment of pyrolytic bio-oils, 2019 IEEE International Ultrasonics Symposium (IUS), IEEE: 2019; pp 2439-2442.
50. Kloss, S.; Zehetner, F.; Dellantonio, A.; Hamid, R.; Ottner, F.; Liedtke, V.; Schwanninger, M.; Gerzabek, M. H.; Soja, G., Characterization of slow pyrolysis biochars: effects of feedstocks and pyrolysis temperature on biochar properties. *J. Environ. Qual.* 2012, 41 (4), 990-1000.
51. Li, S.; Harris, S.; Anandhi, A.; Chen, G., Predicting biochar properties and functions based on feedstock and pyrolysis temperature: A review and data syntheses. *J. Cleaner Prod.* 2019, 215, 890-902.
52. Kwak, J.-H.; Islam, M. S.; Wang, S.; Messele, S. A.; Naeth, M. A.; El-Din, M. G.; Chang, S. X., Biochar properties and lead (II) adsorption capacity depend on feedstock type, pyrolysis temperature, and steam activation. *Chemosphere* 2019, 231, 393-404.
53. Zhao, L.; Cao, X.; Mašek, O.; Zimmerman, A., Heterogeneity of biochar properties as a function of feedstock sources and production temperatures. *J. Hazard. Mater.* 2013, 256, 1-9.
54. Manyà, J. J.; Roca, F. X.; Perales, J. F., TGA study examining the effect of pressure and peak temperature on biochar yield during pyrolysis of two-phase olive mill waste. *J. Anal. Appl. Pyrolysis* 2013, 103, 86-95.
55. Kim, K. H.; Kim, J.-Y.; Cho, T.-S.; Choi, J. W., Influence of pyrolysis temperature on physicochemical properties of biochar obtained from the fast pyrolysis of pitch pine (*Pinus rigida*). *Bioresour. Technol.* 2012, 118, 158-162.
56. Satya Sai, P.; Krishnaiah, K., Development of the pore-size distribution in activated carbon produced from coconut shell char in a fluidized-bed reactor. *Ind. Eng. Chem. Res.* 2005, 44 (1), 51-60.

57. Skodras, G.; Diamantopoulou, I.; Zabaniotou, A.; Stavropoulos, G.; Sakellaropoulos, G., Enhanced mercury adsorption in activated carbons from biomass materials and waste tires. *Fuel Process. Technol.* 2007, 88 (8), 749-758.
58. Mukome, F. N.; Zhang, X.; Silva, L. C.; Six, J.; Parikh, S. J., Use of chemical and physical characteristics to investigate trends in biochar feedstocks. *J. Agric. Food Chem.* 2013, 61 (9), 2196-2204.
59. Gai, X.; Wang, H.; Liu, J.; Zhai, L.; Liu, S.; Ren, T.; Liu, H., Effects of feedstock and pyrolysis temperature on biochar adsorption of ammonium and nitrate. *PLoS One* 2014, 9 (12), e113888.
60. Jing, F.; Pan, M.; Chen, J., Kinetic and isothermal adsorption-desorption of PAEs on biochars: effect of biomass feedstock, pyrolysis temperature, and mechanism implication of desorption hysteresis. *Environ. Sci. Pollut. Res.* 2018, 25 (12), 11493-11504.
61. Xu, X.; Cao, X.; Zhao, L., Comparison of rice husk-and dairy manure-derived biochars for simultaneously removing heavy metals from aqueous solutions: role of mineral components in biochars. *Chemosphere* 2013, 92 (8), 955-961.
62. Xu, R.-k.; Xiao, S.-c.; Yuan, J.-h.; Zhao, A.-z., Adsorption of methyl violet from aqueous solutions by the biochars derived from crop residues. *Bioresour. Technol.* 2011, 102 (22), 10293-10298.
63. Mohan, D.; Sarswat, A.; Ok, Y. S.; Pittman Jr, C. U., Organic and inorganic contaminants removal from water with biochar, a renewable, low cost and sustainable adsorbent—a critical review. *Bioresour. Technol.* 2014, 160, 191-202.
64. Huggins, T. M.; Haeger, A.; Biffinger, J. C.; Ren, Z. J., Granular biochar compared with activated carbon for wastewater treatment and resource recovery. *Water Res.* 2016, 94, 225-232.

65. Xu, X.; Schierz, A.; Xu, N.; Cao, X., Comparison of the characteristics and mechanisms of Hg (II) sorption by biochars and activated carbon. *J. Colloid Interface Sci.* 2016, 463, 55-60.
66. Kołodyńska, D.; Krukowska, J.; Thomas, P., Comparison of sorption and desorption studies of heavy metal ions from biochar and commercial active carbon. *Chem. Eng. J.* 2017, 307, 353-363.
67. Park, J.-H.; Ok, Y. S.; Kim, S.-H.; Cho, J.-S.; Heo, J.-S.; Delaune, R. D.; Seo, D.-C., Competitive adsorption of heavy metals onto sesame straw biochar in aqueous solutions. *Chemosphere* 2016, 142, 77-83.
68. Zama, E. F.; Zhu, Y.-G.; Reid, B. J.; Sun, G.-X., The role of biochar properties in influencing the sorption and desorption of Pb (II), Cd (II) and As (III) in aqueous solution. *J. Cleaner Prod.* 2017, 148, 127-136.
69. Guilhen, S. N.; Mašek, O.; Ortiz, N.; Izidoro, J.; Fungaro, D., Pyrolytic temperature evaluation of macauba biochar for uranium adsorption from aqueous solutions. *Biomass Bioenergy* 2019, 122, 381-390.
70. Sattar, M. S.; Shakoor, M. B.; Ali, S.; Rizwan, M.; Niazi, N. K.; Jilani, A., Comparative efficiency of peanut shell and peanut shell biochar for removal of arsenic from water. *Environ. Sci. Pollut. Res.* 2019, 26 (18), 18624-18635.
71. Inyang, M.; Dickenson, E., The potential role of biochar in the removal of organic and microbial contaminants from potable and reuse water: a review. *Chemosphere* 2015, 134, 232-240.
72. Qiu, Y.; Zheng, Z.; Zhou, Z.; Sheng, G. D., Effectiveness and mechanisms of dye adsorption on a straw-based biochar. *Bioresour. Technol.* 2009, 100 (21), 5348-5351.
73. Yavari, S.; Malakahmad, A.; Sapari, N. B., Biochar efficiency in pesticides sorption as a function of production variables—a review. *Environ. Sci. Pollut. Res.* 2015, 22 (18), 13824-13841.

74. Lu, H.; Zhang, W.; Yang, Y.; Huang, X.; Wang, S.; Qiu, R., Relative distribution of  $Pb^{2+}$  sorption mechanisms by sludge-derived biochar. *Water Res.* 2012, 46 (3), 854-862.
75. Tong, X.-j.; Li, J.-y.; Yuan, J.-h.; Xu, R.-k., Adsorption of Cu (II) by biochars generated from three crop straws. *Chem. Eng. J.* 2011, 172 (2-3), 828-834.
76. Inyang, M.; Gao, B.; Ding, W.; Pullammanappallil, P.; Zimmerman, A. R.; Cao, X., Enhanced lead sorption by biochar derived from anaerobically digested sugarcane bagasse. *Sep. Sci. Technol.* 2011, 46 (12), 1950-1956.
77. Li, H.; Dong, X.; da Silva, E. B.; de Oliveira, L. M.; Chen, Y.; Ma, L. Q., Mechanisms of metal sorption by biochars: biochar characteristics and modifications. *Chemosphere* 2017, 178, 466-478.
78. Sizmur, T.; Fresno, T.; Akgül, G.; Frost, H.; Moreno-Jiménez, E., Biochar modification to enhance sorption of inorganics from water. *Bioresour. Technol.* 2017, 246, 34-47.
79. Cha, J. S.; Park, S. H.; Jung, S.-C.; Ryu, C.; Jeon, J.-K.; Shin, M.-C.; Park, Y.-K., Production and utilization of biochar: A review. *J. Ind. Eng. Chem.* 2016, 40, 1-15.
80. Sajjadi, B.; Chen, W.-Y.; Egiebor, N. O., A comprehensive review on physical activation of biochar for energy and environmental applications. *Rev. Chem. Eng.* 2019, 35 (6), 735-776.
81. Braghiroli, F. L.; Bouafif, H.; Neculita, C. M.; Koubaa, A., Activated biochar as an effective sorbent for organic and inorganic contaminants in water. *Water, Air, Soil Pollut.* 2018, 229 (7), 1-22.
82. Azargohar, R.; Dalai, A., Steam and KOH activation of biochar: Experimental and modeling studies. *Microporous Mesoporous Mater.* 2008, 110 (2-3), 413-421.
83. Marsh, H.; Reinoso, F. R., *Activated carbon*. Elsevier: 2006.

84. Jung, S.-H.; Kim, J.-S., Production of biochars by intermediate pyrolysis and activated carbons from oak by three activation methods using CO<sub>2</sub>. *J. Anal. Appl. Pyrolysis* 2014, 107, 116-122.
85. Lima, I. M.; Marshall, W. E., Granular activated carbons from broiler manure: physical, chemical and adsorptive properties. *Bioresour. Technol.* 2005, 96 (6), 699-706.
86. Shim, T.; Yoo, J.; Ryu, C.; Park, Y.-K.; Jung, J., Effect of steam activation of biochar produced from a giant Miscanthus on copper sorption and toxicity. *Bioresour. Technol.* 2015, 197, 85-90.
87. Lou, K.; Rajapaksha, A. U.; Ok, Y. S.; Chang, S. X., Pyrolysis temperature and steam activation effects on sorption of phosphate on pine sawdust biochars in aqueous solutions. *Chemical Speciation & Bioavailability* 2016, 28 (1-4), 42-50.
88. Dalai, A. K.; Azargohar, R., Production of activated carbon from biochar using chemical and physical activation: Mechanism and modeling. ACS Publications: 2007.
89. Jin, H.; Capareda, S.; Chang, Z.; Gao, J.; Xu, Y.; Zhang, J., Biochar pyrolytically produced from municipal solid wastes for aqueous As (V) removal: adsorption property and its improvement with KOH activation. *Bioresour. Technol.* 2014, 169, 622-629.
90. Jang, H. M.; Yoo, S.; Choi, Y.-K.; Park, S.; Kan, E., Adsorption isotherm, kinetic modeling and mechanism of tetracycline on Pinus taeda-derived activated biochar. *Bioresour. Technol.* 2018, 259, 24-31.
91. Zeng, H.; Zeng, H.; Zhang, H.; Shahab, A.; Zhang, K.; Lu, Y.; Nabi, I.; Naseem, F.; Ullah, H., Efficient adsorption of Cr (VI) from aqueous environments by phosphoric acid activated eucalyptus biochar. *J Cleaner Prod.* 2021, 286, 124964.
92. Herath, A.; Layne, C. A.; Perez, F.; Hassan, E. B.; Pittman Jr, C. U.; Mlsna, T. E., KOH-activated high surface area Douglas Fir biochar for adsorbing aqueous Cr (VI), Pb (II) and Cd (II). *Chemosphere* 2021, 269, 128409.

93. Prapagdee, S.; Piyatiratitivorakul, S.; Petsom, A., Physico-chemical activation on rice husk biochar for enhancing of cadmium removal from aqueous solution. *Asian J. Water Environ. Pollut.* 2016, 13 (1), 27-34.
94. Angın, D.; Köse, T. E.; Selengil, U., Production and characterization of activated carbon prepared from safflower seed cake biochar and its ability to absorb reactive dyestuff. *Appl. Surf. Sci.* 2013, 280, 705-710.
95. Acemioğlu, B., Removal of a reactive dye using NaOH-activated biochar prepared from peanut shell by pyrolysis process. *Int. J. Coal Prep. Util.* 2019, 1-23.
96. Taheran, M.; Naghdi, M.; Brar, S. K.; Knystautas, E. J.; Verma, M.; Ramirez, A. A.; Surampalli, R. Y.; Valéro, J. R., Adsorption study of environmentally relevant concentrations of chlortetracycline on pinewood biochar. *Sci. Total Environ.* 2016, 571, 772-777.
97. Braghiroli, F. L.; Bouafif, H.; Hamza, N.; Neculita, C. M.; Koubaa, A., Production, characterization, and potential of activated biochar as adsorbent for phenolic compounds from leachates in a lumber industry site. *Environ. Sci. Pollut. Res.* 2018, 25 (26), 26562-26575.
98. Micháleková-Richveisová, B.; Frišták, V.; Pipiška, M.; Ďuriška, L.; Moreno-Jimenez, E.; Soja, G., Iron-impregnated biochars as effective phosphate sorption materials. *Environ. Sci. Pollut. Res.* 2017, 24 (1), 463-475.
99. Braghiroli, F. L.; Bouafif, H.; Neculita, C. M.; Koubaa, A., Performance of physically and chemically activated biochars in copper removal from contaminated mine effluents. *Water, Air, Soil Pollut.* 2019, 230 (8), 1-14.
100. Li, R.; Wang, J. J.; Gaston, L. A.; Zhou, B.; Li, M.; Xiao, R.; Wang, Q.; Zhang, Z.; Huang, H.; Liang, W., An overview of carbothermal synthesis of metal-biochar composites for the removal of oxyanion contaminants from aqueous solution. *Carbon* 2018, 129, 674-687.

101. Lee, J.; Kim, K.-H.; Kwon, E. E., Biochar as a catalyst. *Renewable and Sustainable Energy Reviews* 2017, 77, 70-79.
102. Kastner, J. R.; Mani, S.; Juneja, A., Catalytic decomposition of tar using iron supported biochar. *Fuel Process. Technol.* 2015, 130, 31-37.
103. Yao, D.; Hu, Q.; Wang, D.; Yang, H.; Wu, C.; Wang, X.; Chen, H., Hydrogen production from biomass gasification using biochar as a catalyst/support. *Bioresour. Technol.* 2016, 216, 159-164.
104. Agrafioti, E.; Kalderis, D.; Diamadopoulos, E., Ca and Fe modified biochars as adsorbents of arsenic and chromium in aqueous solutions. *J. Environ. Manage.* 2014, 146, 444-450.
105. He, R.; Peng, Z.; Lyu, H.; Huang, H.; Nan, Q.; Tang, J., Synthesis and characterization of an iron-impregnated biochar for aqueous arsenic removal. *Sci. Total Environ.* 2018, 612, 1177-1186.
106. Frišták, V.; Michálekóvá-Richveisová, B.; Víglašová, E.; Ďuriška, L.; Galamboš, M.; Moreno-Jiménez, E.; Pipíška, M.; Soja, G., Sorption separation of Eu and As from single-component systems by Fe-modified biochar: kinetic and equilibrium study. *J. Iranian Chem. Soc.* 2017, 14 (3), 521-530.
107. Hasan, M. S.; Geza, M.; Vasquez, R.; Chilkoor, G.; Gadhamshetty, V., Enhanced heavy metal removal from synthetic stormwater using nanoscale zerovalent iron-modified biochar. *Water, Air, Soil Pollut.* 2020, 231 (5), 1-15.
108. Bao, D.; Li, Z.; Tang, R.; Wan, C.; Zhang, C.; Tan, X.; Liu, X., Metal-modified sludge-based biochar enhance catalytic capacity: Characteristics and mechanism. *J. Environ. Manage.* 2021, 284, 112113.
109. Tan, X.-f.; Liu, Y.-g.; Gu, Y.-l.; Xu, Y.; Zeng, G.-m.; Hu, X.-j.; Liu, S.-b.; Wang, X.; Liu, S.-m.; Li, J., Biochar-based nano-composites for the decontamination of wastewater: a review. *Bioresour. Technol.* 2016, 212, 318-333.

110. Zhang, M.; Gao, B.; Yao, Y.; Xue, Y.; Inyang, M., Synthesis, characterization, and environmental implications of graphene-coated biochar. *Sci. Total Environ.* 2012, 435, 567-572.
111. Genovese, M.; Jiang, J.; Lian, K.; Holm, N., High capacitive performance of exfoliated biochar nanosheets from biomass waste corn cob. *J. Mater. Chem. A* 2015, 3 (6), 2903-2913.
112. Rajapaksha, A. U.; Chen, S. S.; Tsang, D. C.; Zhang, M.; Vithanage, M.; Mandal, S.; Gao, B.; Bolan, N. S.; Ok, Y. S., Engineered/designer biochar for contaminant removal/immobilization from soil and water: potential and implication of biochar modification. *Chemosphere* 2016, 148, 276-291.
113. Wang, B.; Gao, B.; Fang, J., Recent advances in engineered biochar productions and applications. *Crit. Rev. Environ. Sci. Technol.* 2017, 47 (22), 2158-2207.
114. Zhang, H.; Xu, F.; Xue, J.; Chen, S.; Wang, J.; Yang, Y., Enhanced removal of heavy metal ions from aqueous solution using manganese dioxide-loaded biochar: Behavior and mechanism. *Sci. Rep.* 2020, 10 (1), 1-13.
115. Rangabhashiyam, S.; Balasubramanian, P., The potential of lignocellulosic biomass precursors for biochar production: performance, mechanism and wastewater application-a review. *Ind. Crops Prod.* 2019, 128, 405-423.
116. (FAO), F. a. A. O., Global Forest Resources Assessment. Wood volume and Woody biomass (Internet) 2000, (2).
117. Mohan, D.; Pittman Jr, C. U.; Steele, P. H., Pyrolysis of wood/biomass for bio-oil: a critical review. *Energy Fuels* 2006, 20 (3), 848-889.
118. Piskorz, J.; Radlein, D.; Scott, D. S., On the mechanism of the rapid pyrolysis of cellulose. *J. Anal. Appl. Pyrolysis* 1986, 9 (2), 121-137.
119. DeGROOT, W. F.; Pan, W.-P.; Rahman, M. D.; Richards, G. N., First chemical events in pyrolysis of wood. *J. Anal. Appl. Pyrolysis* 1988, 13 (3), 221-231.

120. Liu, Q.; Wang, S.; Zheng, Y.; Luo, Z.; Cen, K., Mechanism study of wood lignin pyrolysis by using TG–FTIR analysis. *J. Anal. Appl. Pyrolysis* 2008, 82 (1), 170-177.
121. Niazi, N. K.; Bibi, I.; Shahid, M.; Ok, Y. S.; Shaheen, S. M.; Rinklebe, J.; Wang, H.; Murtaza, B.; Islam, E.; Nawaz, M. F., Arsenic removal by Japanese oak wood biochar in aqueous solutions and well water: Investigating arsenic fate using integrated spectroscopic and microscopic techniques. *Sci. Total Environ.* 2018, 621, 1642-1651.
122. Kunhikrishnan, A.; Bibi, I.; Bolan, N.; Seshadri, B.; Choppala, G.; Niazi, N.; Kim, W.; Ok, Y.; Uchimiya, S.; Chang, S., Biochar for inorganic contaminant management in waste and wastewater. *Biochar: Production, Characterization and Applications*; CRC Press: Boca Raton, FL, USA 2015, 167-219.
123. Ding, Z.; Hu, X.; Wan, Y.; Wang, S.; Gao, B., Removal of lead, copper, cadmium, zinc, and nickel from aqueous solutions by alkali-modified biochar: Batch and column tests. *J Ind. Eng. Chem.* 2016, 33, 239-245.
124. Kim, J.-Y.; Oh, S.; Park, Y.-K., Overview of biochar production from preservative-treated wood with detailed analysis of biochar characteristics, heavy metals behaviors, and their ecotoxicity. *J. Hazard. Mater.* 2020, 384, 121356.
125. Wang, H.; Gao, B.; Wang, S.; Fang, J.; Xue, Y.; Yang, K., Removal of Pb (II), Cu (II), and Cd (II) from aqueous solutions by biochar derived from KMnO<sub>4</sub> treated hickory wood. *Bioresour. Technol.* 2015, 197, 356-362.
126. Kizito, S.; Wu, S.; Kirui, W. K.; Lei, M.; Lu, Q.; Bah, H.; Dong, R., Evaluation of slow pyrolyzed wood and rice husks biochar for adsorption of ammonium nitrogen from piggery manure anaerobic digestate slurry. *Sci. Total Environ.* 2015, 505, 102-112.
127. Singh, E.; Kumar, A.; Mishra, R.; You, S.; Singh, L.; Kumar, S.; Kumar, R., Pyrolysis of waste biomass and plastics for production of biochar and its use for removal of heavy metals from aqueous solution. *Bioresour. Technol.* 2021, 320, 124278.

128. Martini, S., An overview of ultrasound. In *Sonocrystallization of fats*, Springer: 2013; pp 7-16.
129. Robertson, V. J.; Baker, K. G., A review of therapeutic ultrasound: effectiveness studies. *Phys. Ther.* 2001, 81 (7), 1339-1350.
130. Ter Haar, G. R., High intensity focused ultrasound for the treatment of tumors. *Echocardiography* 2001, 18 (4), 317-322.
131. Frizzell, L., Biological Effects of Acoustic Cavitation, in *Ultrasound: Its Chemical, Physical and Biological Effects*, Suslick, KS (Ed.). 1988.
132. Marin, A.; Sun, H.; Husseini, G. A.; Pitt, W. G.; Christensen, D. A.; Rapoport, N. Y., Drug delivery in pluronic micelles: effect of high-frequency ultrasound on drug release from micelles and intracellular uptake. *J. Control. Release* 2002, 84 (1-2), 39-47.
133. Bianchi, S.; Martinoli, C.; Abdelwahab, I. F., High-frequency ultrasound examination of the wrist and hand. *Skeletal Radiol.* 1999, 28 (3), 121-129.
134. Dolatowski, Z. J.; Stadnik, J.; Stasiak, D., Applications of ultrasound in food technology. *Acta Scientiarum Polonorum Technologia Alimentaria* 2007, 6 (3), 88-99.
135. Zheng, L.; Sun, D.-W., Innovative applications of power ultrasound during food freezing processes—a review. *Trends Food Sci. Technol.* 2006, 17 (1), 16-23.
136. Ruecroft, G.; Hipkiss, D.; Ly, T.; Maxted, N.; Cains, P. W., Sonocrystallization: the use of ultrasound for improved industrial crystallization. *Organic Process Research & Development* 2005, 9 (6), 923-932.
137. Thornycroft, J. I.; Barnaby, S. W. In *Torpedo-boat destroyers (including appendix and plate at back of volume)*, Minutes of the Proceedings of the Institution of Civil Engineers, Thomas Telford-ICE Virtual Library: 1895; pp 51-69.
138. Rayleigh, L., On the pressure developed in a liquid during the collapse of a spherical cavity: *Philosophical Magazine Series* 6, 34, 94–98. 1917.

139. Richards, W. T.; Loomis, A. L., The chemical effects of high frequency sound waves I. A preliminary survey. *J. Am. Chem. Soc.* 1927, 49 (12), 3086-3100.
140. Yasui, K., Fundamentals of acoustic cavitation and sonochemistry. In *Theoretical and experimental sonochemistry involving inorganic systems*, Springer: 2010; pp 1-29.
141. Leong, T.; Ashokkumar, M.; Kentish, S., *The fundamentals of power ultrasound-A review*. 2011.
142. Fuchs, J., *Ultrasonics—Number and Size of Cavitation Bubbles*. Technical blog bringing cleaning technology to the next generation 2015.
143. Bussemaker, M. J.; Zhang, D., Effect of ultrasound on lignocellulosic biomass as a pretreatment for biorefinery and biofuel applications. *Ind. Eng. Chem. Res.* 2013, 52 (10), 3563-3580.
144. He, Z.; Wang, Z.; Zhao, Z.; Yi, S.; Mu, J.; Wang, X., Influence of ultrasound pretreatment on wood physiochemical structure. *Ultrason. Sonochem.* 2017, 34, 136-141.
145. Qiu, S.; Wang, Z.; He, Z.; Yi, S., The effect of ultrasound pretreatment on poplar wood dimensional stability. *BioResources* 2016, 11 (3), 7811-7821.
146. Wang, Z.; Qu, L.; Qian, J.; He, Z.; Yi, S., Effects of the ultrasound-assisted pretreatments using borax and sodium hydroxide on the physicochemical properties of Chinese fir. *Ultrason. Sonochem.* 2019, 50, 200-207.
147. Wang, Z.; He, Z.; Zhao, Z.; Yi, S.; Mu, J., Influence of ultrasound-assisted extraction on the pyrolysis characteristics and kinetic parameters of eucalyptus. *Ultrason. Sonochem.* 2017, 37, 47-55.
148. Paquin, M.; Loranger, É.; Hannaux, V.; Chabot, B.; Daneault, C., The use of Weissler method for scale-up a Kraft pulp oxidation by TEMPO-mediated system from a batch mode to a continuous flow-through sonoreactor. *Ultrason. Sonochem.* 2013, 20 (1), 103-108.

149. Loranger, E.; Paquin, M.; Daneault, C.; Chabot, B., Comparative study of sonochemical effects in an ultrasonic bath and in a large-scale flow-through sonoreactor. *Chem. Eng. J.* 2011, 178, 359-365.
150. Loranger, E.; Daneault, C.; Milot, G.; Cherab, L. E. In Investigation on using two types of sonoreactors for Kraft lignin fractionation, 2014 IEEE International Ultrasonics Symposium, IEEE: 2014; pp 943-946.
151. Cherpozat, L.; Loranger, E.; Daneault, C., Ultrasonic pretreatment of soft wood biomass prior to conventional pyrolysis: Scale-up effects and limitations. *Biomass Bioenergy* 2019, 124, 54-63.
152. Chatterjee, R.; Sajjadi, B.; Mattern, D. L.; Chen, W.-Y.; Zubatiuk, T.; Leszczynska, D.; Leszczynski, J.; Egiebor, N. O.; Hammer, N., Ultrasound cavitation intensified amine functionalization: A feasible strategy for enhancing CO<sub>2</sub> capture capacity of biochar. *Fuel* 2018, 225, 287-298.
153. Chatterjee, R.; Sajjadi, B.; Chen, W.-Y.; Mattern, D. L.; Egiebor, N. O.; Hammer, N.; Raman, V., Low frequency ultrasound enhanced dual amination of biochar: a nitrogen-enriched sorbent for CO<sub>2</sub> capture. *Energy Fuels* 2019, 33 (3), 2366-2380.
154. Sajjadi, B.; Broome, J. W.; Chen, W. Y.; Mattern, D. L.; Egiebor, N. O.; Hammer, N.; Smith, C. L., Urea functionalization of ultrasound-treated biochar: a feasible strategy for enhancing heavy metal adsorption capacity. *Ultrason. Sonochem.* 2019, 51, 20-30.
155. Sajjadi, B.; Shrestha, R. M.; Chen, W.-Y.; Mattern, D. L.; Hammer, N.; Raman, V.; Dorris, A., Double-layer magnetized/functionalized biochar composite: Role of microporous structure for heavy metal removals. *J Water Process Eng.* 2021, 39, 101677.
156. Wang, C.; Wang, H.; Cao, Y., Pb (II) sorption by biochar derived from *Cinnamomum camphora* and its improvement with ultrasound-assisted alkali activation. *Colloids Surf. Physicochem. Eng. Aspects* 2018, 556, 177-184.

157. Hazrati, S.; Farahbakhsh, M.; Cerdà, A.; Heydarpoor, G., Functionalization of ultrasound enhanced sewage sludge-derived biochar: Physicochemical improvement and its effects on soil enzyme activities and heavy metals availability. *Chemosphere* 2020, 128767.
158. Wang, T.; Li, G.; Yang, K.; Zhang, X.; Wang, K.; Cai, J.; Zheng, J., Enhanced ammonium removal on biochar from a new forestry waste by ultrasonic activation: Characteristics, mechanisms and evaluation. *Sci. Total Environ.* 2021, 778, 146295.
159. Lim, J.-L.; Okada, M., Regeneration of granular activated carbon using ultrasound. *Ultrason. Sonochem.* 2005, 12 (4), 277-282.
160. Breitbach, M.; Bathen, D.; Schmidt-Traub, H., Effect of ultrasound on adsorption and desorption processes. *Ind. Eng. Chem. Res.* 2003, 42 (22), 5635-5646.
161. Yamaguchi, T.; Nomura, M.; Matsuoka, T.; Koda, S., Effects of frequency and power of ultrasound on the size reduction of liposome. *Chem. Phys. Lipids* 2009, 160 (1), 58-62.
162. Yao, Y.; Pan, Y.; Liu, S., Power ultrasound and its applications: A state-of-the-art review. *Ultrason. Sonochem.* 2020, 62, 104722.
163. Režek Jambrak, A.; Lelas, V.; Herceg, Z.; Badanjak, M.; Batur, V.; Muža, M., Advantages and disadvantages of high power ultrasound application in the dairy industry. *Mljekarstvo: časopis za unaprjeđenje proizvodnje i prerade mlijeka* 2009, 59 (4), 267-281.
164. Dubinin, M., Fundamentals of the theory of adsorption in micropores of carbon adsorbents: characteristics of their adsorption properties and microporous structures. *Carbon* 1989, 27 (3), 457-467.
165. Chiou, C. T., Partition and adsorption of organic contaminants in environmental systems. John Wiley & Sons: 2003.

166. Al-Anber, M. A., Thermodynamics approach in the adsorption of heavy metals. INTECH Open Access Publisher: 2011.
167. Lagergren, S. K., About the theory of so-called adsorption of soluble substances. *Sven. Vetenskapsakad. Handlingar* 1898, 24, 1-39.
168. Ys, H.; McKay, G.; Ys, H.; McKay, G., Pseudo-second order model for sorption processes. *Process Biochem.* 1999, 34 (5), 451-465.
169. Simonin, J.-P., On the comparison of pseudo-first order and pseudo-second order rate laws in the modeling of adsorption kinetics. *Chem. Eng. J.* 2016, 300, 254-263.
170. Wu, F.-C.; Tseng, R.-L.; Juang, R.-S., Initial behavior of intraparticle diffusion model used in the description of adsorption kinetics. *Chem. Eng. J.* 2009, 153 (1-3), 1-8.
171. Aharoni, C.; Tompkins, F., Kinetics of adsorption and desorption and the Elovich equation. In *Advances in catalysis*, Elsevier: 1970; Vol. 21, pp 1-49.
172. Langmuir, I., The adsorption of gases on plane surfaces of glass, mica and platinum. *J. Am. Chem. Soc.* 1918, 40 (9), 1361-1403.
173. Hall, K. R.; Eagleton, L. C.; Acrivos, A.; Vermeulen, T., Pore-and solid-diffusion kinetics in fixed-bed adsorption under constant-pattern conditions. *Industrial & engineering chemistry fundamentals* 1966, 5 (2), 212-223.
174. Freundlich, H., Over the adsorption in solution. *J. Phys. Chem* 1906, 57 (385471), 1100-1107.
175. Dubinin, M., The potential theory of adsorption of gases and vapors for adsorbents with energetically nonuniform surfaces. *Chem. Rev.* 1960, 60 (2), 235-241.
176. Redlich, O.; Peterson, D. L., A useful adsorption isotherm. *J. Phys. Chem.* 1959, 63 (6), 1024-1024.
177. Temkin, M.; Pyzhev, V., Recent modifications to Langmuir isotherms. 1940.

178. Harkins, W. D.; Jura, G., The decrease ( $\pi$ ) of free surface energy ( $\gamma$ ) as a basis for the development of equations for adsorption isotherms; and the existence of two condensed phases in films on solids. *J. Chem. Phys.* 1944, 12 (3), 112-113.
179. Brunauer, S.; Emmett, P. H.; Teller, E., Adsorption of gases in multimolecular layers. *J. Am. Chem. Soc.* 1938, 60 (2), 309-319.
180. Kecili, R.; Hussain, C. M., Mechanism of Adsorption on Nanomaterials. In *Nanomaterials in Chromatography*, Elsevier: 2018; pp 89-115.